Interpenetrating Polymer Networks with Polyurethane and Methacrylate-based Polymers

by

Samantha Amelia Bird

A dissertation submitted to the Graduate Faculty of
Auburn University
in partial fulfillment of the
requirements for the Degree of
Doctor of Philosophy

Auburn, Alabama
August 3, 2013

Keywords: interpenetrating polymer networks, polyurethane, poly(methyl methacrylate), fracture toughness, transparency

Approved by

Maria L. Auad, Chair, Associate Professor of Polymer and Fiber Engineering
Peter Schwartz, Professor of Polymer and Fiber Engineering
Gwynedd Thomas, Associate Professor of Polymer and Fiber Engineering
Hareesh Tippur, Professor of Mechanical Engineering

Abstract

Interpenetrating polymer networks (IPNs) were synthesized with polyurethane (PU) and methacrylate-based polymers in order to create a transparent device with high toughness for potential applications in high-impact scenarios. This research consisted of four parts with the first involving successful synthesis of an IPN based on PU and poly(methyl methacrylate) (PMMA). Aspects studied included the following: aliphatic versus aromatic isocyanates in the PU phase, the presence of an inhibitor in the PMMA phase (sequential versus simultaneous reactions), curing profiles, and ratios of PU:PMMA. Samples which included an aliphatic isocyanate, PU content around 80 wt%, and a sequential polymerization demonstrated the best material properties, ultimately due to increased phase compatibility between PU and PMMA.

Further analysis on the IPNs involved manipulating the PU network to enhance polymer compatibility and material properties. One approach involved using diols of different molecular weight in the PU phase. Both the PU and the IPN networks' morphologies were consequently affected. Increasing the chain length also increased the molecular weight between cross-links and decreased cross-link density. Fracture toughness did improve with an upper limit in the molecular weight of the diol.

Another method in altering the PU network consisted of changing the diol:triol ratio. In other words, the ratio of the linear chain to the cross-linking agent of the PU phase was varied. Morphological changes did take place, which in turn affected material properties, but the results were not as pronounced as when the molecular weight of the diol was increased.

The last approach was, to some extent, different than the other methods in the creation of IPNs. Instead of synthesizing a full-IPN, where only physical cross-links existed between the polymer networks, a graft-IPN was synthesized with physical and chemical cross-links connecting PU and PMMA. This was accomplished by replacing the PMMA phase with a copolymer of bisphenol A glycidyl methacrylate (BisGMA) and triethylene glycol dimethacrylate (TRI-EDMA). The ability of the hydroxyl groups in BisGMA to react with the isocyanate groups in PU allowed cross-link points to exist between the two phases. Increased compatibility resulted, but further analysis is needed to reduce the brittleness of the materials.

Acknowledgments

This research would not have been possible without the help of many individuals and parties, and for that, I would like to extend my thanks for their many contributions and constant assistance.

The first group of individuals that I would like to thank is my family, which includes my parents Bonnie and Garry Bird as well as my younger brother, Brian. From the very start, they took great effort to ensure that I would excel in academics and in everyday life. Not only have they always pushed me to work harder and to achieve more, but they have also been a major support through the tough times with their love, words of encouragement, and faith that I could accomplish this much.

I would like to thank my committee members, Dr. Maria L. Auad, Dr. Hareesh Tippur, Dr. Peter Schwartz, and Dr. Gwynedd Thomas, for taking the time to help with this project. Thank you also to Dr. Maobing Tu, my University Reader, for taking the time to read about my research.

I especially want to thank Dr. Maria L. Auad for her guidance throughout this entire research. Since working with her starting my junior year as an undergraduate, she has taught me a wealth of knowledge about the field and has helped me grow not only as a professional, but also as an individual. She has watched me struggle with problems in and out of school, but she has always offered her advice and guidance to see me through.

Furthermore, I would like to thank Dr. Hareesh Tippur and his research group members, Kailash Jajam and Bala Meenakshi Sundaram, for not only providing mechanical testing vital to this research, but also taking the time to teach me aspects of the test methods.

Additionally, I would like to thank the members in Dr. Auad's research group as well as the undergraduate student workers that have helped me over the years. These individuals include Tara Jones, Cihan Uzunpinar, Buket Demir, Bernal Sibaja, Ricardo Ballestero, Charles Blackwell, and Andrea Alexander. Tara, who was kind enough to let me live with her for at least a year, was not only a role model, but she was also a good friend and an inspiration. Charles and Andrea, the undergraduate workers, were a great help in the lab; besides providing an extra hand with making and testing samples, they also lent an ear to my frustrations and anxiety. Thanks also to Dan Clary who worked with Dr. Auad for a summer and who, after I started my graduate studies, provided the reins for me to progress the research.

The Department of Polymer and Fiber Engineering also deserves acknowledgment. I appreciate the ability to use the equipment and facilities, as well as the friendships and lessons learned from the staff and faculty members.

I want to also thank the Defense Threat Reduction Agency and the United States Department of the Army for providing the funds necessary for this research to be conducted.

Finally, I particularly want to thank my fiancé, Christopher John Ward, for everything he has done for me. Our friendship began when we undergraduates, and over time, our love for each other has grown. These last few years finishing graduate school have given us many challenges and obstacles to overcome, but together we have come so far, and we will finish together. Chris still amazes me with how much he was able to stand by me through my problems while also going through his own dilemmas with his studies and research. Thank you so much

for believing in me and making sure I did not give up, for taking the time to always lend a helping hand, and for being a wonderful best friend.

Table of Contents

List of Tables

List of Figures

List of Abbreviations

IPN	Interpenetrating polymer network
PU	Polyurethane
PMMA	Poly(methyl methacrylate)
PTMG	Poly(tetramethylene ether) glycol
TRIOL	1,1,1-trimethylolpropane
DCH	1,6-diisocyanatohexane
TDI	Tolylene-2,4-diisocyanate
DD	Dibutyltin dilaurate
MMA	Methyl methacrylate
TRIM	Trimethylolpropane trimethacrylate
AIBN	Azobisisobutyronitrile
EA	Ethyl acetate
BisGMA	Bisphenol A glycidyl methacrylate
TRI-EDMA	Triethylene glycol dimethacrylate
BPO	Benzoyl peroxide
THF	Tetrahydrofuran
DSC	Differential scanning calorimetry
DMA	Dynamic mechanical analysis
UV-vis	UV-visible spectrophotometry

SEM	Scanning electron microscopy
TEM	Transmission electron microscopy
T_g	Glass transition temperature
T_m	Melting temperature
T_c	Crystallization temperature
T_{cc}	Cold crystallization temperature
K_{Ic}	Quasi-static crack initiation toughness

CHAPTER I

INTRODUCTION

Introduction

Humans need just a few basic necessities to survive, and among these, protection is greatly desired. While shelter and clothing may have been enough to shield people from the harsh elements in the past, a much higher degree of shielding is needed today. With the advancement of technology, the requirement for appropriate protection, especially transparent devices, has risen. In everyday civil applications, transparent, durable, and impact-absorbing equipment is used, such as in eye goggles for chemical splashes and flying debris [1], windshields for automotives [2], and windows for bank tellers [3], jewelry cases [4], and artwork [5]. Bullet-resistant glass, sometimes referred to as bullet-proof glass, also cover historical documents, such as the Declaration of Independence [6, 7]. Even important individuals, such as the President of the United States, are often shielded by bullet-resistant glass when making appearances in public [8]. Transparent, protective glass is not only used in civil applications, but also in the military.

Fighter jets and helicopters can travel at extremely high speeds, and if any birds or debris is present, a strong canopy is required to keep the pilot and passengers safe [9]. In riots, shields are often needed to protect a police force from any projectile that may be fired or launched [10]. These are just some examples of where a transparent, high-impact absorbing material would be

greatly needed to keep individuals safe. With advanced munitions and firepower being created every year, conventional materials will not be able to satisfy necessary requirements. The National Institute of Justice (NIJ), part of the U.S. Department of Justice, currently has standards for ballistic protection (NIJ Standard 0108.01), which can be seen in Table I-1 [11]. Devices comprised of any material should be able to meet these standards for protection against ballistics.

Table I-1. NIJ standards for ballistic-protective materials

Armor Type	Test Ammunition	Nominal Bullet Mass
I	22 Long Rifle High Velocity	2.6 gram
	Lead	40 grain
	38 Special	10.2 gram
	Round Nose Lead	158 grain
II-A	357 Magnum	10.2 gram
	Jacketed Soft Point	158 grain
	9 mm	8.0 gram
	Full Metal Jacket	124 grain
II	357 Magnum	10.2 gram
	Jacketed Soft Point	158 grain
	9 mm	8.0 gram
	Full Metal Jacket	124 grain
III-A	44 Magnum	15.55 gram
	Lead Semi-Wadcutter Gas Checked	240 grain
	9 mm	8.0 gram
	Full Metal Jacket	124 grain
III	7.62 mm	9.7 gram
	308 Winchester Full Metal Jacket	150 grain
IV	30-06	10.8 gram
	Armor Piercing	166 grain

Transparent, Impact-Resistant Glass

In order to make advancements in transparent, protective materials, it is important to study what has been attempted in the past and to take note on why these devices would not be suitable for today's hazards. One conventional, clear material that has been produced for many years by both man and natural phenomena is glass. It has been suggested that glass originated in the Middle East thousands of years ago and did not initially appear colorless. This material was used for pottery glazing, jewelry, and mirrors. Through trade and experimentation, the various methods of producing and using glass spread around the world and evolved over time, especially during the Industrial Revolution, to what is seen today [12, 13].

Glass material today is an amorphous substance that usually consists of silica, calcium oxide, and sodium oxide [14]. Glass windows and similar objects easily break when dropped or when struck with a sufficient amount of force. Because of the lack of a uniform, atomic arrangement, glass will tend to break into irregular fragments upon fracturing [14]. These fragments become sharp shards that can be extremely dangerous; thus, other methods for obtaining transparent materials without this dilemma have been investigated.

In today's market, tempered and laminated glass will often be found in place of conventional glass. Tempered glass, sometimes referred to as safety glass, is chemically and thermally treated during manufacturing. This type of glass is more than four times stronger than normal window glass, and the way it breaks is also another advantage. Instead of breaking into sharp shards, the

glass breaks into many small pieces that do not have jagged edges. Tempered glass is commonly found in automotive windows, shower doors, and some home windows [15].

Laminated glass, mainly known as bullet-proof glass, can be commonly found in automobile windshields and in devices during combat and high security situations. It first became popular as airplanes and jets began reaching extremely high speeds, where windshields were sometimes broken by birds. Therefore, this type of glass especially proved to be invaluable during military flight [16]. The reason for laminated glass's frequent use can be attributed to how it is constructed and its resulting properties. This glass consists of a "sandwich" of various materials, such as tempered glass layered with three to five plastic sheets [17], which are bonded together with heat and pressure [18]. A diagram of this type of glass can be seen in Figure I-1.

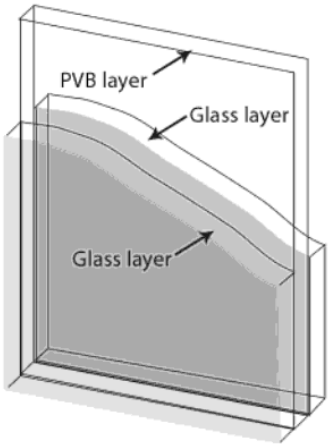

Figure I-1. Diagram of laminated glass [18]

Because repeatedly harsh blows are needed in order to break through the plastic layers, this transparent material is capable of withstanding handheld weapons, including guns, bricks, and hammers [19]. Unfortunately, after a sufficient amount of impacts, the glass is not completely

transparent in that “spider web” cracks form, impeding anyone from being able to easily look through. Thus, while this kind of glass may last longer than conventional glass and tempered glass, it still has its limitations. These limitations in the material properties are the motivation for many research groups to find better alternatives. Some have even turned to investigating transparent, ceramic armor.

Transparent, Impact-Resistant Ceramics

Some individuals have begun looking into other methods for creating a clear, protective material by using crystalline ceramics. These materials have a high elastic modulus, strength, and high wear resistance, which enable them to withstand damage from high impacts [20]. It has been found that transparent, crystalline ceramics can be thinner and lighter as well as be used as a substitute for laminated glass [13]. In fact, the United States Army Research Laboratory (ARL) discovered that these materials can exhibit a higher performance over laminated glass. Some ceramics that are popular in current studies include magnesium aluminate spinel ($MgAl_2O_4$), aluminum oxynitride spinel (AION), and single crystal aluminum oxide, also known as sapphire, (Al_2O_3) [21, 22]. Although ceramics have demonstrated improvements in material properties when compared to the different types of glasses mentioned earlier, their commercial availability, costs, and difficulty in manufacturing are still major obstacles to overcome before everyday application is feasible [21].

Transparent, Impact-Resistant Polymeric Materials

Polymers are a relatively new type of material when compared to glass and ceramics. While polymers are present even in human bodies, experimentation with these macromolecules only began a couple of centuries ago [23]. Researchers were initially interested in the chemical modification of cellulose, but it was not until the 20th century that Leo Baekeland invented the first completely synthetic plastic, Bakelite [24]. Since that time, polymers have been utilized in a wide range of structures, forms, and applications.

It has been discovered that polymers can be very effective when used as transparent, impact-absorbing materials. As mentioned earlier, plastics have been used in conjunction with glass in the structure of laminated glass to create a more impact-absorbing material. Polymers used in laminated glass, such as polyvinyl butyral (PVB), as well as polycarbonate (PC) [15, 16, 18], have increasingly found their way into the field of protective materials. Furthermore, some transparent, protective materials are completely made of polymers.

When discussing transparent, protective materials made of polymers, there are generally two main kinds of plastics: acrylates and polycarbonates (PC). Some brand names for acrylates, or acrylic plastics, include Plexiglas® and Acrylite®, and brand names for PC include Lexan® and Tuffak®, among others. Out of the two, PC is more commonly included in transparent armor structures [21, 22].

Polycarbonate

PC is a thermoplastic and can be available in thicknesses up to half an inch [25]. This material can also be up to 17% stronger than acrylics and be three times lighter than acrylics and six times lighter than glass [26]. While PC is more flexible than acrylics, and is therefore more impact-resistant, this material is much more expensive and susceptible to UV degradation and scratches when used alone [25, 27]. Despite some drawbacks, PC has been very useful in many applications. For example, the most recognized PC called Lexan, which was created by General Electric lab technician Daniel Fox in 1953, was used in "bubble helmets," worn by Neil Armstrong and Buzz Aldrin during their moonwalk in 1969 [28]. Other applications include hard hats, riot shields, automotive bumpers, and housings for power tools. Additionally, different polymers may be blended with PC to give flame retardency and UV-resistance [29]. Figure I-2 shows the structure of polycarbonate. The –OCOO– chain with the benzene rings provide the optical transparency, rigidity, and toughness, even at high temperatures, that make this polymer so popular [29].

.

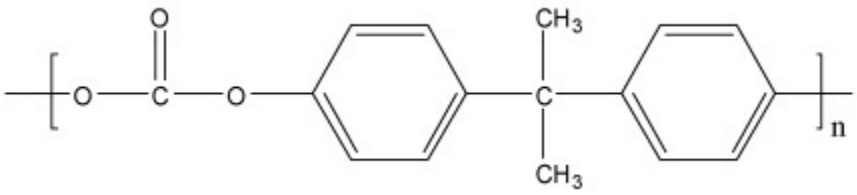

Figure I-2. Chemical structure PC [30]

Poly(methyl methacrylate)

The thermoplastic that most closely resembles glass's transparency and resistance to weathering is poly(methyl methacrylate) (PMMA), also called acrylic [29]. This material was first

synthesized in 1902 by German chemist Röhm and later patented as Plexiglas® by Rohm and Haas Company in 1928 [31, 32]. The first major application of PMMA occurred during World War II, where it was used for the cockpit canopies of fighter aircraft [24, 29]. This material is stiff, hard, and easy to polish, but it is also sensitive to stress concentrations and is more fragile and easier to scratch than glass. Some of these disadvantages can be overcome by blending other polymers with PMMA or by applying a coating. Other applications of PMMA include windows, advertisement signs, tool handles, bone cement, large aquariums, dentures, prosthetic devices, and safety spectacles [29, 31-33].

The synthesis of PMMA takes place through a fairly simple radical polymerization. Basically, methyl methacrylate (MMA) monomers are joined together by adding an initiator. When heat is applied, the initiator forms radicals to start the PMMA chains growing [33]. Figure I-3 shows a MMA monomer and its subsequent PMMA chain after initiation.

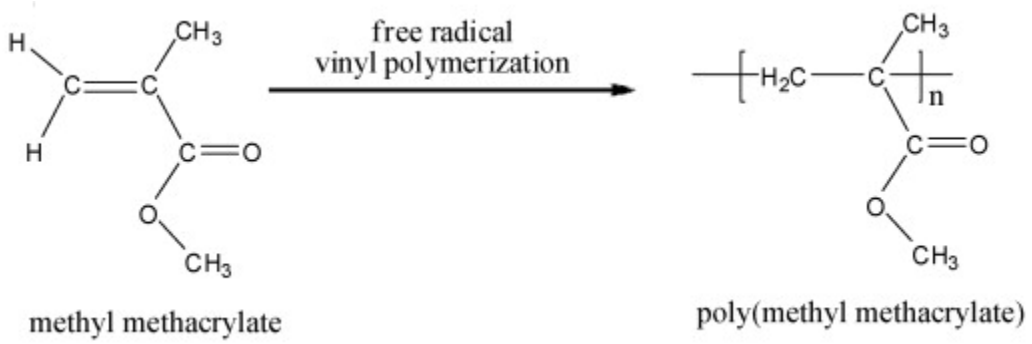

Figure I-3. Polymerization reaction of PMMA [30]

As discussed earlier, there are some problematic aspects of using pure poly(methyl methacrylate), and so it is not uncommon for PMMA to be blended with other polymers to fulfill requirements for certain applications. As an example, many researchers are currently looking

into different methods to improve the toughness and impact-resistance of PMMA by adding other components. Blends of PMMA and polyvinyl chloride (PVC) can offer good toughness, impact resistance, and durability at different temperatures [34]. Bernini et al. have investigated blending ethylene-co-vinylacetate (EVA) with PMMA, and their results showed that transparency was retained while excellent impact behavior was achieved, on par with commercially available ultra-tough PMMA [35]. Cangialosi et al. have investigated synthesizing MMA with rubber by an induced in-situ polymerization through the use of an electron beam, in the hopes of creating a blend with better compatibility between the two phases [36].

Other components that have been blended and studied with PMMA for increasing toughness, conductivity, and other properties include polystyrene (PS) [37], high density polyethylene (HDPE) [38], cellulose acetate hydrogen phthalate (CAP) [39], poly(vinylidene fluoride) (PVDF) [40, 41], polyvinylmethylether [42], as well as many others.

Despite acrylics having a higher stiffness than PC and lower cost ($1.70/kg-$2.40/kg for PMMA versus $3.80/kg-$4.30/kg for PC [29]), these materials are prone to cracking and splitting more easily [27]. These materials have still been used in many applications that require transparency and protection. For instance, Acrylite, manufactured by CYRO Industries, is utilized in museum displays, framing, optical displays, aircraft glazing, spectator protection at hockey rinks, and bullet-resistant applications [43]. Differences in the mechanical properties between PMMA and PC can be seen in Table I-2.

Table I-2. Mechanical properties of PMMA and PC [44]

Property	Units		Conditions	PMMA		Conditions	PC
Tensile Modulus	MPa		- 23°C, air 37°C, water	3,100 3,180 2,700		ASTM: D638, D759, D1708	2,380
Tensile Strength	MPa		-	48-76		at yield at ultimate	62.1 65.5
Flexural Modulus	MPa		-	2,900-3,100		-	2,340
Flexural Strength	MPa		n/a	n/a		-	93.1
Impact Strength	J/m		notched	16-27		izod, notched	850

Although both PC and PMMA have been very effective in certain scenarios and have shown improvement in the protection of individuals, each has their limitations and disadvantages when used individually.

Polyurethane

Another material that has been extensively studied is polyurethane (PU). The first group of researchers to study PU was Otto Bayer and his coworkers at I. G. Farbenindustrie in Germany in 1937, where their original focus was duplicating or improving synthetic polyamide fibers [45]. During this time, Bayer proposed using diisocyanates and diols for synthesizing macromolecules. The first PU that became commercially available was based on hexamethylene diisocyanate and butanediol. This material resulted in properties similar to polyamide fibers; in fact, this type of PU is still used for fibers and brushes today [46]. However, industrial scale production did not start until the 1940's to 1950's [45, 46]. Since these experiments, PU has been used in a wide array of applications, and their use in transparent impact-absorbing materials has become increasingly popular.

Polyurethanes are formed through a condensation, or polyaddition, reaction with polyols and isocyanates. Because there are many different isocyanates and hydroxyl-containing compounds, such as diols and triols, that are available, the structure and morphology of a PU can vary. Catalysts used in the formation of PU also have an effect on the final material morphology and properties. These chemicals are generally used for increasing the rate of reaction, affecting the reactions between isocyanate groups with hydroxyl groups or water, as well as completing all reactions so that a properly cured polymer can be achieved. For instance, it is commonly known that catalysts consisting of an organotin compound are effective for reactions between isocyanates and hydroxyl groups while tertiary amines are effective for isocyanates and water to form a foaming reaction [47]. Other factors, such as the reaction conditions, can also affect the type of PU that is formed.

However, what all polyurethanes have in common is a urethane group. The chemical structure of a urethane group can be seen in Figure I-4.

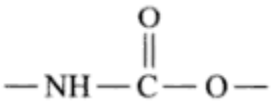

Figure I-4. Chemical structure of a urethane group [46]

Due to the possibility of synthesizing PU in a number of different ways, many properties can be obtained. The ability to tailor this polymer for specific characteristics is what makes PU so popular for a variety of uses [46]. Some applications for PUs include coatings, adhesives, elastomers, fibers, and foams [45].

Studies with polyurethane as a transparent, protective material have also been in recent development. Research in the 1970s demonstrated promising results for PU as a potential armor material; however, sufficient optical properties were lacking. Since then, Simula Technologies has improved PU's optical characteristics [21, 22]. Ballistic evaluations also showed that PU outperformed both PMMA and PC when equal amounts of weight of each sample were compared [21].

PU is generally a flexible polymer, and sometimes a more rigid material is required for high-impact situations. Perhaps the answer to creating a more durable and cheaper transparent material lies in combining polymers at the molecular level to create a synergistic system taking advantage of each individual phase.

Interpenetrating Polymer Networks

Over time, the use of traditional, tempered, and laminated glass for use in protection has been found to be insufficient for the safety of individuals. As weaponry advances, both in ballistics and in chemical warfare, ceramic protection as well as acrylics and PC will not be enough. Combining multiple materials in newer ways may be a possible solution for creating an affordable, transparent material capable of withstanding high-impacts and remaining intact for multiple uses.

The field of polymers is known for its wide range in chemical, mechanical, thermal, and optical properties, along with many others characteristics. Polymeric materials can be rigid or elastic, in

the structure of a foam, a dense solid, or a fiber, and some can even conduct electricity. These macromolecules can further be enhanced with different side groups on the carbon backbone chain, making their uses even more expansive. The possibilities for these unique macromolecules are continuously evolving.

Mixtures and Combinations of Polymeric Materials

One technique many researchers have employed over the years when studying polymers is combining multiple polymers instead of trying to synthesize a completely new monomer to meet desired characteristics. As an alternative to spending resources and expenses for creating new materials, mixtures of polymers can save time and effort in finding solutions to needs that may require immediate attention [48]. Additionally, using multiple polymers together simultaneously can offer a much larger spectrum of characteristics, versus using a single polymer, which can be tailored for a specific application.

Numerous ways exist in order to combine several polymers into one general material. The most common methods of mixing polymers together and creating multi-component systems can be seen in Figure I-5.

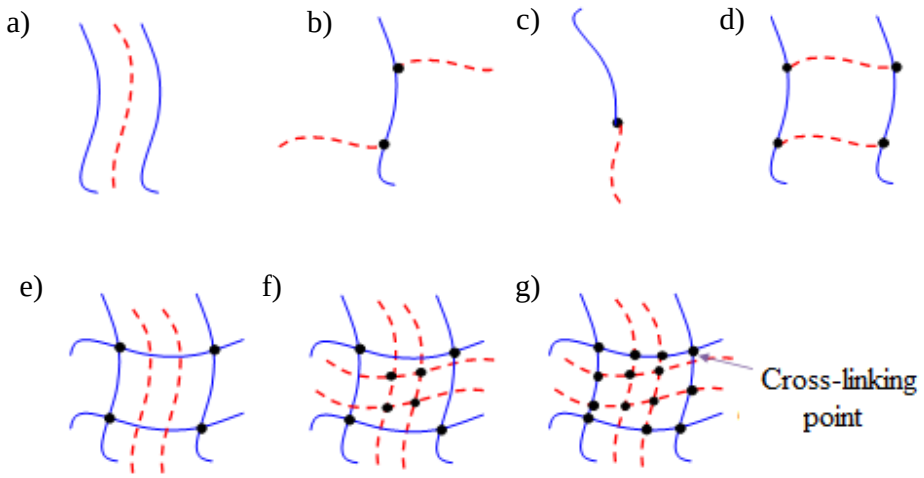

Figure I-5. Common multi-component polymer systems include a) blends, b) graft copolymers, c) block copolymers, d) AB cross-linked copolymers, e) semi-IPNs, f) full-IPNs, and g) graft-IPNs

Figure I-5-a illustrates a frequent method to combine polymers, which is to physically and mechanically mix several polymer systems together, such as in a solution or as a latex in an emulsion polymerization [49-51].

A graft copolymer is shown in Figure I-5-b, where polymer chains are randomly connected to another polymer chain's backbone structure, similar to a side chain. In order to make this kind of mixture, a polymer, a polymerizable monomer, and an initiator, which serves to make active sites on either component, are required [49, 51, 52].

Unlike the graft copolymer, a block copolymer, shown in Figure I-5-c, contains two different kinds of chains that are connected end-to-end. The carbon backbone is shared, but the constituents differ, making one long macromolecule with segmented sections [49, 51]. Besides linear copolymers, there are also star-block and radial-block copolymers [53].

Figure I-5-d shows an AB cross-linked copolymer, where a network is formed with at least two different polymer chains that are chemically bonded together at multiple points [49, 51]. These are similar to graft-copolymers, but instead of having loose chains, a cross-linked network is created.

Another way of combining polymers can be seen in Figures I-5-e, I-5-f, and I-5-g; these are known as interpenetrating polymers networks (IPNs) [49]. Polymer blends are usually totally immiscible or partially miscible, but combining polymers in an IPN, where physical constraints are present, can help overcome this obstacle [54]. In other words, polymers that would normally experience phase separation when mixed together can become more compatible when used in an IPN formation [55]. An IPN basically consists of at least one polymer network that is cross-linked in the immediate presence of one or more polymers [49]. The polymer systems do not necessarily have to be chemically bonded to each other; similar to a blend, these chains are simply held amongst each other through physical entanglements.

Figure I-5-e shows what is referred to as a semi-IPN, and in this material, only one polymer is cross-linked, and all other networks are either linear or branched [49, 51], or in the form of a graft-copolymer [56].

What is principally studied in this research is a full-IPN, shown in Figure I-5-f, where all polymers present are cross-linked, but not to each other [49, 51]. For this type of system, homogeneity is strongly favored at the microstructure level. Some heterogeneity may exist at the

nanoscale since some chains of one kind of polymer can be adjacent to each other, thus creating a separate nanophase [57].

Finally, Figure I-5-g shows another system that has also been investigated in this research, a graft-IPN. This system can be thought of as a combination between a graft copolymer and an IPN. In addition to the networks being physically entangled with one another, there also exist certain points where the networks are chemically bonded to each other [49, 51]. In other words, both physical and chemical cross-links are present between the different polymer phases.

Although the unique class of IPNs is extensively studied today, these systems are a relatively new area of interest. Jonas Aylsworth, the chief chemist of Thomas Edison, is accredited for being the first individual to create an IPN. At the time, Edison was developing phonograph records by switching currently used materials to phenol-formaldehyde. Unfortunately, the records became too brittle for use. Aylsworth added rubber and sulfur to this compound and vulcanized the resin to make durable and tougher records [49, 51].

It was not until the 1960s when the term "interpenetrating polymer network" was coined by Millar when he started working on these systems [49, 51]. Millar studied homo-IPNs, that is, IPNs with networks of the same polymer. For his work, the homo-IPNs consisted of polystyrene cross-linked with divinyl benzene. Homo-IPN systems such as these are sometimes referred to as Millar-IPNs today [58]. Since that time, many other researchers have explored the creation and behavior of IPNs, providing a better understanding of the properties behind these materials. A summary of the historical development of IPNs and copolymers can be seen in Table I-3.

Table I-3. Development of IPNs and other multi-component polymeric materials [59]

Event	Investigator	Year
IPN Structure	Aylsworth	1914
Macromolecular Hypothesis	Staudinger	1920
Graft Copolymers	Ostromislensky	1927
Block Copolymers	Dunn and Melville	1952
Homo-IPNs	Millar	1960
AB Cross-linked Copolymers	Bamford, Dyson, and Eastmond	1967
Sequential IPNs	Sperling and Friedman	1969
Latex Interpenetrating Elastomer Networks (IENs)	Frisch, Klempner, and Frisch	1969
Simultaneous IPNs	Sperling and Arnts	1971
Thermoplastic IPNs	Davison and Gergen	1977

IPNs have been found to offer significant improvement in physical properties, such as increased toughness, thermal stability, creep resistance, and elastic modulus through their cross-links [60]. Further growth in the knowledge of IPNs has also increased the number of applications and uses. IPN materials are often utilized in adhesives, coatings, elastomers, medical applications, and many other devices [61].

Categories of Interpenetrating Polymer Networks

Just as polymers can be mixed together in a variety of blends and copolymer forms, there are also several structures in which IPNs can be synthesized. For instance, gradient IPNs exhibit gradual changes in compositions or degrees of cross-linking throughout the material. An example could be that one particular polymer system is more prevalent on one side while another polymer is more prevalent on the other side of the whole material; in the middle of the material, an equal amount of both polymer systems is present [49, 51]. Some researchers have

synthesized gradient IPNs to create materials with a hard exterior, a soft interior, and an intermediate zone consisting of a gradient composition. These materials were found to be useful for noise and vibration damping [62].

Another type of an interpenetrating polymer network is a latex IPN, sometimes also referred to as an interpenetrating elastomeric network (IEN). These materials are created in the form of latexes, usually with a core-shell structure, where film formation and cross-linking then occur [49, 51]. Generally, the morphology of these IPNs depends on how the polymerization process takes place. If both monomers are added and polymerized at the same time, the particles will be more uniform. If one monomer is polymerized first and forms a latex, a homogeneous network can form, depending on how quickly the monomer diffuses into the latex system. On the other hand, the monomer may react near the surface of the latex particle, creating a core-shell morphology [63].

Other examples of interpenetrating polymer networks include thermoplastic IPNs where the networks are not chemically bonded or cross-linked to each other and only physical entanglements exist. Additionally, at elevated temperatures, it is possible for these IPNs to flow [49, 51]. These materials behave as IPNs at their intended use temperature, but when they are exposed to higher temperatures, they behave as thermoplastics, hence the name thermoplastic IPNs. These types of IPNs can be even further classified as either thermoplastic apparent IPNs, where the networks are physically cross-linked, or thermoplastic semi-IPNs, where one network is physically cross-linked and the other network is chemically cross-linked [64].

One way to classify IPNs is through the sequence of reactions that take place during curing. There are two categories for this, sequential polymerization and simultaneous polymerization, which can be seen in Figure I-6.

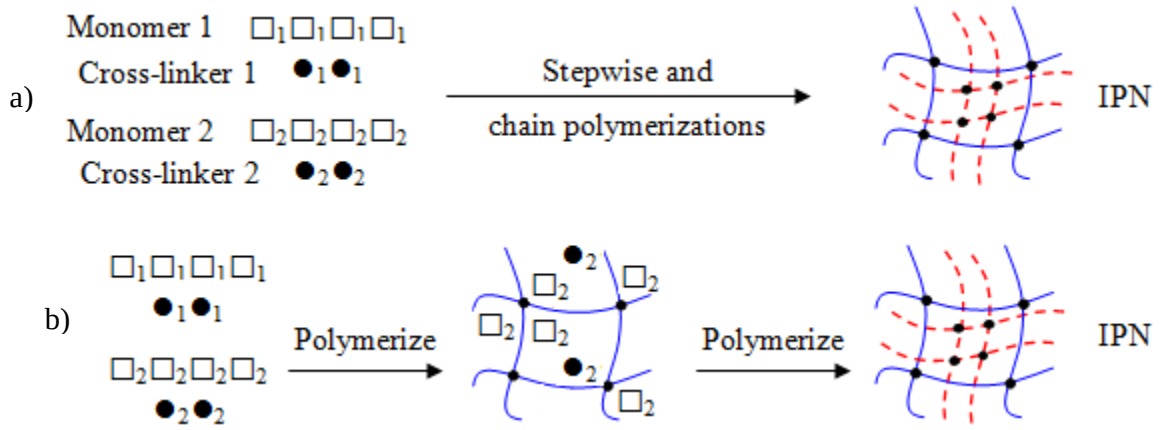

Figure I-6. Syntheses of a) simultaneous IPNs and b) sequential IPNs [49, 51]

With sequential IPNs, the polymers present in the mixture do not all synthesize at the same time. Thus, one polymer synthesizes and cross-links into a network while at the same time being swollen by the monomers and constituents of the other polymer [49, 51, 65]. The first polymer that synthesizes is often considered the "continuous phase," and the second polymer is merely a network that fills in the holes of the first polymeric network [49, 51].

With simultaneous IPNs, all polymer systems synthesize concurrently with no interfering reactions occurring between them. For instance, one monomer should react by a radical polymerization, and the other polymer system should react through a condensation or polyaddition reaction [66]. Because of this, kinetic differences may be present with each system which would not quite allow complete coinciding syntheses with the different polymers present

in the mixture. However, these IPN systems are still considered simultaneous since the onset of polymerization occurred at the same time for every polymer present [49, 51].

As can be seen, there are several methods of combining polymeric networks together. Even IPNs can be classified into many different forms. The benefits of using this technique of uniting materials that are usually immiscible with each other can have great benefits. For instance, in order to create a windshield-like device capable of remaining rigid and intact after experiencing repeated, harsh impacts from ballistics, some researchers have investigated methods of toughening plastics through the addition of a rubbery material into a polymeric matrix [67-69]. Generally, these materials have the morphology of a continuous, highly stiff phase, with a large number of dispersed elastomeric domains.

Additionally, some research groups have attempted creating IPNs using various forms of PMMA and PU [70-77]. Incorporating PMMA and PU into one synergistic material and combining the aspects of rubber-toughened plastics with IPNs could broaden the possibilities on the material properties necessary for high impact-absorbing windshield-like applications, with better phase compatibility between the networks.

Research Objectives

Noted before, combining an elastomeric material with PMMA has been attempted by some researchers in the past. However, little research has been performed on combining PMMA and

PU in an interpenetrating polymer network and analyzing different aspects important in improving the impact-resistance while maintaining transparency.

Thus, the purpose of this research was to incorporate PMMA and other acrylates with PU into an IPN system with the capabilities of enduring high impacts, while remaining durable, transparent, and useful in real applications. With the transparency and rigidity of PMMA and other similar acrylates, along with PU's elastomeric behavior and toughness, it was hypothesized that there existed a possibility in creating such an ideal, synergistic structure. In this study, several techniques were explored, such as the initial reaction parameters, the use of different constituents in the PMMA and PU systems which included changing the IPN networks, as well as the effect of changing the interaction between the phases. Full-, semi-, graft-, simultaneous, and sequential IPNs were all explored, and their subsequent effects were investigated. Successful studies with these multi-component, homogeneous systems may prove to be the next revolutionary step in transparent, defensive devices for both civilian and military applications.

CHAPTER II

INTERPENETRATING POLYMER NETWORKS WITH POLYURETHANE AND POLY(METHYL METHACRYLATE)

Introduction

In order to have a successful interpenetrating polymer network (IPN), there are many factors to consider. One of the most important parameters to investigate is the phase compatibility, and resulting morphology, between the polymer networks. Kinetic (reaction rate) and thermodynamic (Gibbs free energy) differences can play a major role in how much the components in an IPN will phase separate [78, 79]. Structural aspects, such as cross-link density, also contribute to the degree of phase separation in an IPN [80]. In a sequential IPN, for example, if the phase that synthesizes first is too heavily cross-linked, there may be insufficient space for the second polymer to synthesize and interweave in the first polymer network, thus creating a material not in the form of an IPN. In a simultaneous IPN, if even just one network is too cross-linked, it may reject the other polymer phase, and two phases will synthesize at the same time apart from each other [81]. The morphology of the IPNs greatly influence how the final material properties will be affected [82]. Thus, any phase separation will ultimately be reflected in subsequent characteristics, such as transparency, thermo-mechanical properties, and structural stability.

Finding the perfect balance between all the constituent components in the polymer networks presents a challenge. Polyurethane, as mentioned before, does not have just one single structure, such as polyethylene or polypropylene. Instead, the morphology of this polymer depends on the starting reactants as well as the reaction conditions. For instance, the major reactants used to synthesize PU include isocyanates and compounds with active hydrogen atoms, such as diamines, alcohols, polyhydroxyl compounds, fatty acids, and oligomers. Even other reactants that do not have active hydrogen atoms, such as N,N-dimethylformamide (DMF), acid anhydrides, and compounds with double bonds, can also be used. With these chemicals, the isomeric properties, molecular weight, among other aspects, influence the final structure and properties of PU [83]. Thus, creating a polymer compatible with PMMA in an IPN poses an even greater obstacle.

This portion of the research focused on finding an effective and efficient method for creating an IPN material consisting of PU and PMMA with minimal phase separation, a high degree of optical transparency, stiffness, and toughness properties. An important goal was to also achieve comparable mechanical performance to impact-resistant glass or similar materials. In this work, both simultaneous and sequential full-IPNs were developed. The sequential IPNs involved PU reacting first at one temperature, and then PMMA reacting in situ at a higher, subsequent temperature during curing. Parameters also investigated were ratios of PMMA to PU, effects of different curing profiles, and the use of two kinds of isocyanates in the PU phase. The phase morphology and final thermal and mechanical properties of the various IPNs were then evaluated.

Materials and Methods

Materials

For the PU phase, two types of polyols were utilized: 1,1,1-tris(hydroxymethyl) propane (TRIOL) from Acros Organics (U.S.) and poly(tetramethylene ether) glycol (PTMG) with an average molecular weight of 650g/mol from Sigma Aldrich (U.S.). The triol and the diol were melted and mixed together beforehand to ensure an equal dispersion. This PTMG/TRIOL mixture was melted in an oven while a strong vacuum was pulled to remove any residual moisture present. Also used in the PU phase were two different isocyanates, used separately for comparison: 1,6-diisocyanatohexane 99+% (DCH) from Acros Organics (U.S.) and tolylene-2,4-diisocyanate 95% (TDI) from Sigma Aldrich (U.S.). Dibutyltin dilaurate, 98% (DD), distributed by Pfaltz & Bauer (U.S.), was used as catalyst, and ethyl acetate was used as an analogue to dilute the DD.

The PMMA phase included methyl methacrylate, 99% stabilized (MMA) from Acros Organics (U.S.). Two versions of MMA were explored in order to study the effects of the polymerization on the final material properties. The first version was simply the MMA used as received where an inhibitor, 10-20ppm hydroquinone monomethyl ether (MEHQ), was present. Another version of the MMA monomer was prepared where the inhibitor was removed manually through distillation. Before use, both types of monomers were dried with molecular sieves to remove any water content present in the liquids. Trimethylolpropane trimethacrylate (TRIM) from Sigma Aldrich (U.S.), another methacrylate monomer, was used as a cross-linker so that PMMA would form a three-dimensional network required for an IPN. 2,2’-azobis(2-methylpropionitrile), 98%

(AIBN), also from Sigma Aldrich (U.S.), was used as an initiator with ethyl acetate as an analogue.

The following ratios were used for the reactants: PTMG to TRIOL (5.3:1.1 by mass), PTMG/TRIOL to DCH/TDI (1.8571:1 by mass), PTMG/TRIOL to DD (1g:15.3846µL), PMMA to TRIM (95:5 by mass), and 1.3mL of AIBN (with ethyl acetate as an analogue) for every 123.5g of MMA.

Methods

Synthesis of all IPN materials was carried out in a one-step bulk polymerization with no solvent, where all reactants were mixed together at room temperature conditions. The PMMA precursor was prepared by mixing one of the MMA monomers, TRIM, and AIBN. The PU precursor was prepared by mixing the PTMG/TRIOL mixture with DCH or TDI. After these precursors were thoroughly mixed separately, they were combined, followed by further mixing and the addition of DD to catalyze the PU phase. After a final mixing of the IPN precursor, samples were placed in an oven at 60°C for 24 hours and then another 24 hours at 80°C.

For this particular study, one parameter that was investigated was the effect of different heat treatments on the IPNs. Some IPN samples remained in the oven an additional 2 hours at 120°C for post-curing. The additional curing resulted in a yellow discoloration in the samples, thus decreasing transparency. Although this did not affect the thermo-mechanical properties, it was decided that further studies with post-curing would not be included.

As discussed earlier, the use of two different types of MMA monomer, one with an inhibitor and one without, were explored. The procedure for synthesizing an IPN remained exactly the same, regardless of which monomer was used during the experiment. It was found that the inhibitor did not delay the time until synthesis began; instead, the inhibitor simply changed the temperature needed to cure the PMMA phase.

IPNs of the following ratios (PMMA:PU) were prepared: 80:20, 70:30, 60:40, 50:50, and 40:60. With each of these ratios, the inclusion of either TDI or DCH and an MMA monomer with or without an inhibitor alternated so that a spectrum of IPNs could be analyzed.

Techniques

Dynamic, strain-controlled 3-point bending tests were performed on a TA Instruments RSAIII Dynamic Mechanical Analyzer (DMA) so that information on the thermo-mechanical properties of the IPNs could be obtained. The following testing parameters were used: frequency of 1.0Hz, initial temperature between 25°-30°C (or lower temperature for liquid nitrogen), final temperature of 200°C, ramp rate of 5°C/min, and a strain of 0.1%.

Thermal properties were analyzed using a TA Instruments Q2000 Modulated Differential Scanning Calorimeter (DSC). The following procedure was used to analyze the samples: equilibrate at -80°C, modulate ± 1.00°C every 60 seconds, isothermal for 5 minutes, ramp 10.00°C/min to 250°C, ramp 10.00°C/min to -80°C, equilibrate at -80°C, isothermal for 5 minutes, ramp 10.00°C/min to 250°C, ramp 10.00°C/min to -80°C. After testing the samples, no

thermal peaks, such as the glass transition temperature, could be observed. Therefore, thermal transitions were reported using DMA.

The transparency of the IPNs was also measured using a UV-visible 2450 Spectrophotometer from Shimadzu Scientific Instruments, where ambient air was used as a standard.

Two electron microscopes were utilized to study the morphology of the IPNs: a Zeiss EVO 50 Variable Pressure Scanning Electron Microscope (SEM) with Digital Imaging and EDS (with the IPNs sputter-coated with an EMS 550X Auto Sputter Coating Device with a carbon coating attachment) and a Zeiss EM 10C 10CR Transmission Electron Microscope (TEM).

All SEM and TEM samples were broken after being immersed in liquid nitrogen for at least a minute or two. This method was used to ensure that the phase morphology of the sample was not distorted had the temperature increased and reached the glass transition temperature (T_g) during breaking at ambient temperatures.

Before observing the IPN samples under the TEM, the materials were first stained using osmium tetroxide (OsO_4). Samples were first cut into small wedges and were allowed to sit in the dye for at least 48 hours. Once a sufficient amount of OsO_4 had penetrated through the materials, the specimens were microtomed. During the staining process, it was discovered that pure PU absorbed the dye, appearing black, and the pure PMMA sample did not absorb the dye, therefore remaining clear and unstained. This difference in appearance between the PMMA and the PU enabled the distinction of the two phases when observed under the microscope. Study of the

morphology, domains, and phase separation processes for the IPN systems became possible. The method of staining the IPNs has also been used by many other research groups for studying their own IPN systems [75, 76, 84].

Quasi-static fracture analysis was performed using the ASTM D5045 testing standard for characterizing the toughness of the IPNs in terms of the critical-stress intensity factor, K_{Ic}, also known as the crack initiation toughness. Preparation of these materials involved machining the cured IPN sheets into rectangular coupons with the dimensions 80mm x 20mm x 8mm. Following this, an edge notch of 6mm in length was cut into each sample, and the notch tip was sharpened with a razor blade. These single edge notched bend (SENB) samples were then loaded in a displacement control mode with a testing speed of 0.25mm/min. Figure II-1 shows how the samples were prepared for such a test.

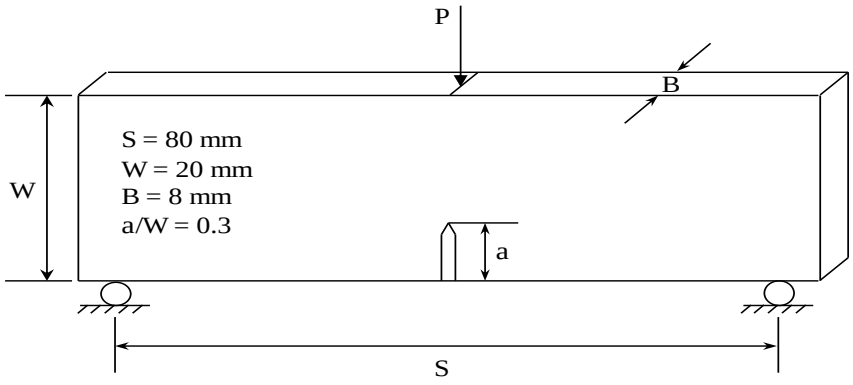

Figure II-1. Experimental setup for quasi-static fracture analysis

Load vs. deflection data was recorded until crack initiation and during stable crack growth, if any, occurred. K_{Ic} values were calculated using the load (P) at crack initiation. For each type of IPN, at least three sets of tests were performed. The mode-I stress intensity factor for a SENB

specimen loaded in a 3-point bending test, using linear elastic fracture mechanics, is given by the following equations [85]:

$$f\left(\frac{a}{W}\right) = \frac{3\frac{S}{W}\sqrt{\frac{a}{W}}}{2\left(1+2\frac{a}{W}\right)\left(1-\frac{a}{W}\right)^{3/2}}\left[1.99 - \frac{a}{W}\left(1-\frac{a}{W}\right)\left\{2.15 - 3.93\left(\frac{a}{W}\right) + 2.7\left(\frac{a}{W}\right)^2\right\}\right] \qquad \text{Equation II-1}$$

$$K_{Ic} = Pf\left(\frac{a}{W}\right)/B\sqrt{W} \qquad \text{Equation II-2}$$

For these equations, 'P' is the load at fracture, 'S' is the span, 'B' is the thickness, 'W' is the width, and 'a' is the crack length of the material.

Results and Discussion

Network Morphology

The final phase morphology of the IPN as well as its two polymer components showed a great dependence on both the reactants and the reaction conditions. TEM photos are shown in Figure II-1 of specimens that were cut from stained IPNs samples that contained 80:20 (PMMA:PU) with different isocyanates, DCH (Figures II-2-a and II-2-c) and TDI (Figures II-2-b and II-2-d), and MMA monomers either with an inhibitor present (Figures II-2-a and II-2-b) or without (Figures II-2-c and II-2-d). Also included in Figure II-2-e is a TEM photo of pure PMMA. Since the PU phase absorbed the dye, thus appearing as a dark grey, and the PMMA remained unstained, appearing as clear domains, it was possible to compare the different phase morphologies of each kind of sample.

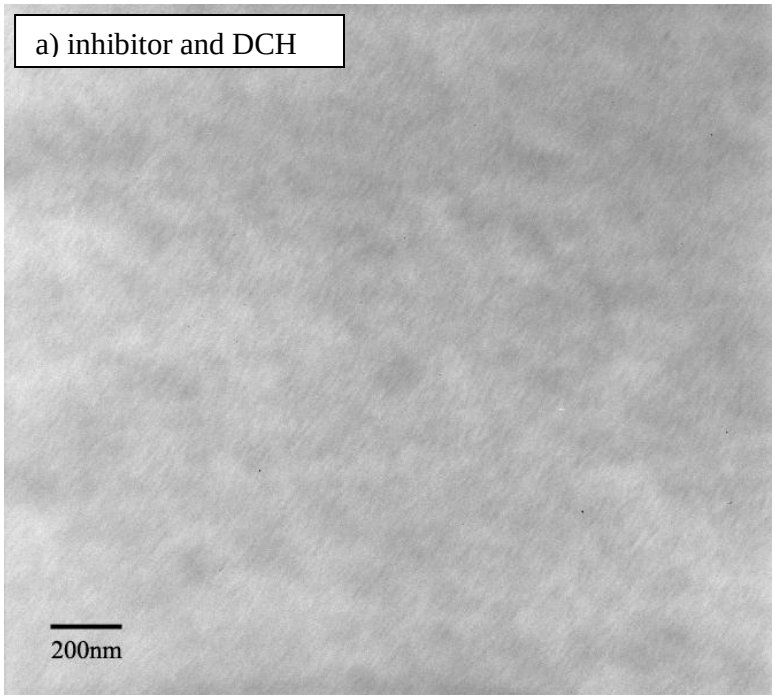
a) inhibitor and DCH
200nm

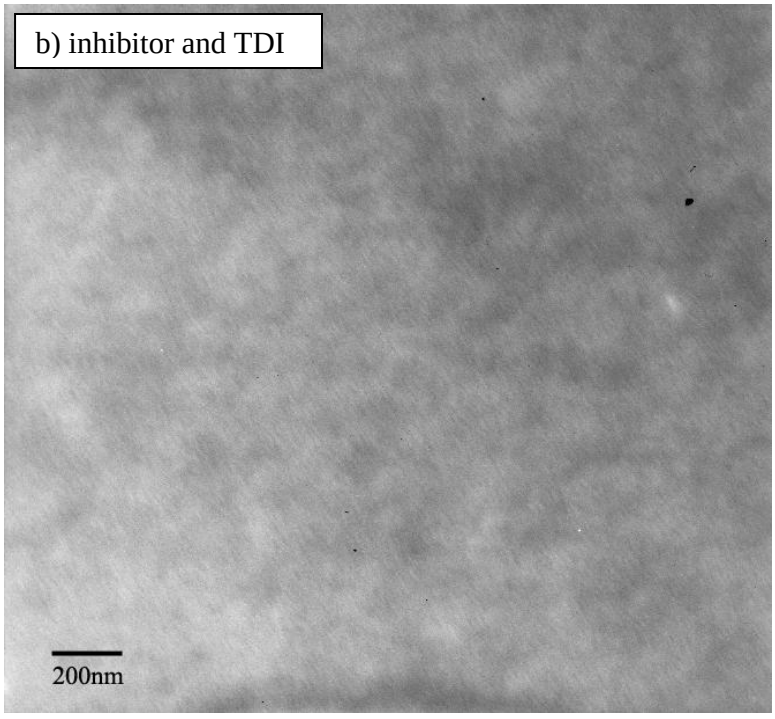
b) inhibitor and TDI
200nm

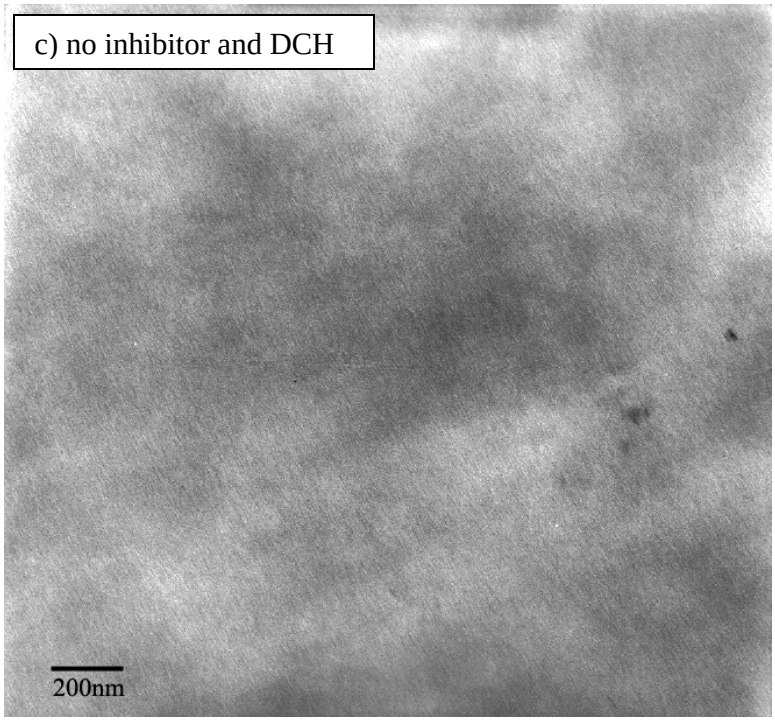
c) no inhibitor and DCH
200nm

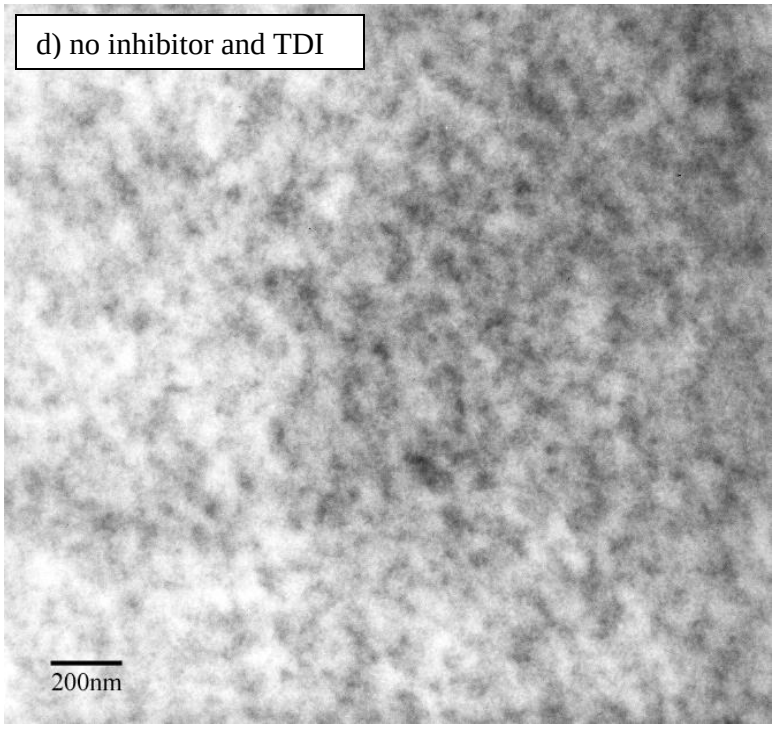
d) no inhibitor and TDI
200nm

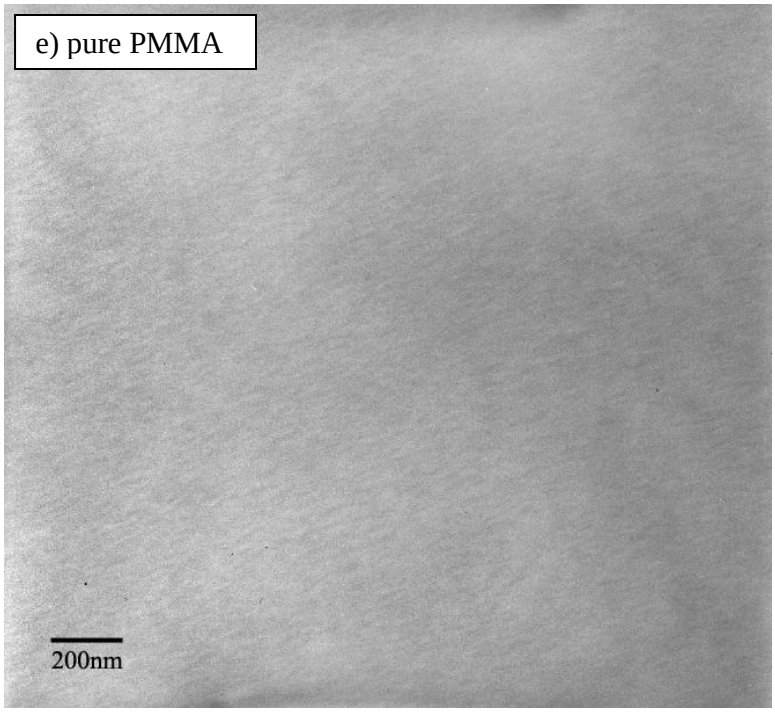

Figure II-2. TEM photos of IPNs with 80 wt% PMMA with a) an inhibitor and DCH, b) an inhibitor and TDI, c) no inhibitor and DCH, d) no inhibitor and TDI, and e) pure PMMA with inhibitor

For Figures II-2-a and II-2-b, a fine dispersion of both polymer components was evident throughout each sample. This correlated to interpenetration of the two polymers among each other, a requirement for synthesizing an IPN. The grey and white domains were not localized, and although they did not have a defined shape, they appeared to be rather spherical. This observation also indicated that the interpenetration process was produced at the molecular level.

On the other hand, by observing the images in Figures II-2-c and II-2-d, which included the MMA monomer with no inhibitor, it appears that using this particular monomer produced considerable changes in the final morphology of the IPN, especially the sample in Figure II-2-d. White and grey domains were localized in different areas within the IPN, suggesting that this

sample exhibited phase separation at the molecular level, possibly due to incompatibility of the growing species during the polymerization process.

For the samples that contained an MMA monomer with the inhibitor present, curing of these samples resulted in a sequential IPN, where one polymer synthesized first, followed by the synthesis of the other polymer phase [68, 77]. In this case, the PU network developed first at 60°C, while concurrently being swelled by the PMMA constituents, and then when the curing temperature was raised to 80°C, the PMMA network synthesized in situ. Thus, the continuous phase of the IPN was the PU network, and this was filled with PMMA domains. These samples also appeared to have minimal phase separation.

Babkina and his research group suggests that when IPNs are formed by a sequential polymerization, this reaction creates a considerable amount of topological engagements between the two networks, facilitating compatibility between the polymer components [86]. Thus, formation of the PU phase before the PMMA phase played a significant role in the development of the PMMA network and the final morphology of the entire IPN. Since the PU was the continuous phase, the size of the PMMA regions were governed by how "loosely or tightly" the PU network cross-linked. A PU network with very spacious areas within its network will permit larger regions of PMMA phases to form. Alternatively, a denser PU network will allow smaller, but an increased number of PMMA domains to fill the porous regions within the PU phase.

One side experiment that was part of this study was the creation of an IPN with 90 wt% PMMA and 10 wt% PU. No IPN was successfully synthesized using this ratio due to the formation of a

substantial phase separation. It is believed that the excessive amount of PMMA precursor prevented the PU phase to efficiently create a continuous network capable of holding the PMMA phase during synthesis. Therefore, the phases did not form interlocked networks with each other, the PU phase synthesized in a localized area, and the PMMA phase synthesized at a higher temperature in another localized area. This created a completely phase separated material, incapable of being considered an IPN.

As mentioned earlier, another approach was taken for synthesizing the PMMA phase. The use of an MMA monomer without an inhibitor created a simultaneous IPN where both the PU and the PMMA phase polymerized concurrently, at the same temperature. In other words, with the absence of an inhibitor in the PMMA phase, a simultaneous IPN was created. Apparently, differences in the kinetic and thermodynamic behavior between the two polymer phases played a fundamental role in creating phase separation in the IPN. During curing, it was found that gelation of the PU phase within the first 24 hours of curing at 60°C was vital for the PMMA phase to form a network interwoven with the PU network. Allowing the two phases to react at the same time did not allow the PU phase to form a continuous network to hold the PMMA precursor, but instead, forced both networks to form networks completely independent of each other.

Some researchers have looked into reaching a better compatibility between PU and PMMA when used together to form IPNs. One method that has successfully been attempted is the application of a higher pressure than that of ambient conditions during curing. Lee et al. described that using a high pressure during synthesis of the IPNs made the two components more compatible, thereby

decreasing domain sizes of the two phases [76]. Using such approaches may allow better compatibility between other polymers when used in IPNs.

Optical Characteristics

Transparency analysis was performed on approximately 3.5mm thick IPN samples consisting of 80:20 (PMMA:PU). UV-visible spectra of the analysis can be seen in Figure II-3. It is should be noted that the actual values of the samples should be higher since the laser from the UV-vis device was reflected from the two surfaces of the IPN samples, upon entering and leaving. Additionally, the results will be slightly altered due to the difference in refractive indices between the samples and air.

The results indicate that samples including either DCH or TDI present similar transmittance values at approximately 82%. Other results have shown that all IPNs with varying amounts of PMMA and PU from 40 wt% to 80 wt% PMMA content also had high transmittance values ranging from 75% to 90%.

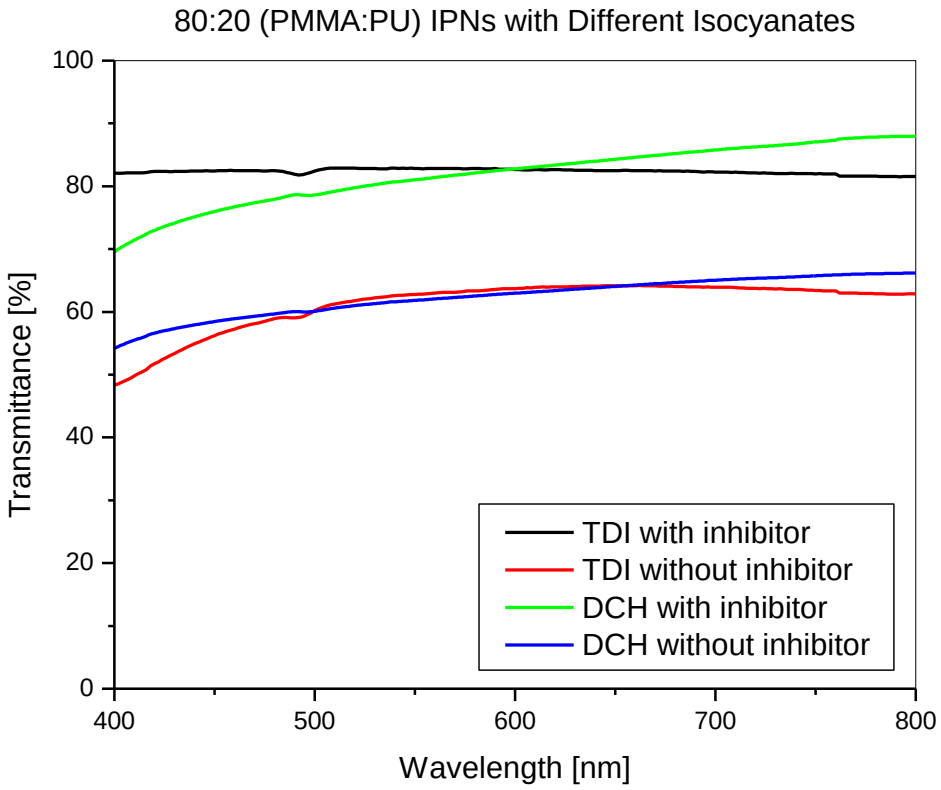

Figure II-3. UV-visible results showing IPNs consisting of 80 wt% PMMA and 20 wt% PU with different isocyanates

Upon visual inspection of the IPNs that were synthesized, samples containing the aliphatic diisocyanate, DCH, produced clear materials. Conversely, samples with the aromatic diisocyanate, TDI, resulted in materials with a dark yellow-orange discoloration. Other researchers have noted that with their PU systems, having a benzene ring present, such as in TDI, contributes to a drastic change in color. Rosu et al. reported that the yellowing effect is produced through UV-radiation, or more precisely, by photo-oxidation in the backbone chain through the aromatic ring. This ultimately leads to the degradation of PU, affecting the clarity and color of the material's surface [87].

Figure II-3 also shows samples with or without an inhibitor present in the MMA phase. Samples that did not have an inhibitor, also considered the simultaneous IPNs, displayed less transparency than those that did include an inhibitor, the sequential IPNs. The simultaneous IPNs displayed transparency values between 40% and 70% while the sequential IPNs had values that ranged from 70% to 90%. This phenomenon can be explained from the discussion earlier on the final morphology of the IPNs based on the reaction conditions. Phase separation not only appeared at the molecular level when studied under the electron microscope, but just by looking at the samples with the naked eye, it was easy to distinguish which samples had phase separation and which ones did not.

Thermo-mechanical Characteristics

Another characteristic that was studied was the thermo-mechanical properties of the IPNs. The most prominent effect that was noted was due to the different ratios of PMMA:PU. Figures II-4 and II-5 show the storage modulus, E', and tan δ of the DCH-based IPNs, as a function of temperature.

Samples containing increasing amounts of PMMA exhibited a higher stiffness than those with lower amounts of PMMA. This was expected since having more of the rigid phase present would increase the rigidity of the overall IPN. The IPN consisting of 80:20 (PMMA:PU) showed a storage modulus close to 2GPa at approximately 30°C, while samples with 60 wt% and 50 wt% showed lower values, due to the presence of more PU.

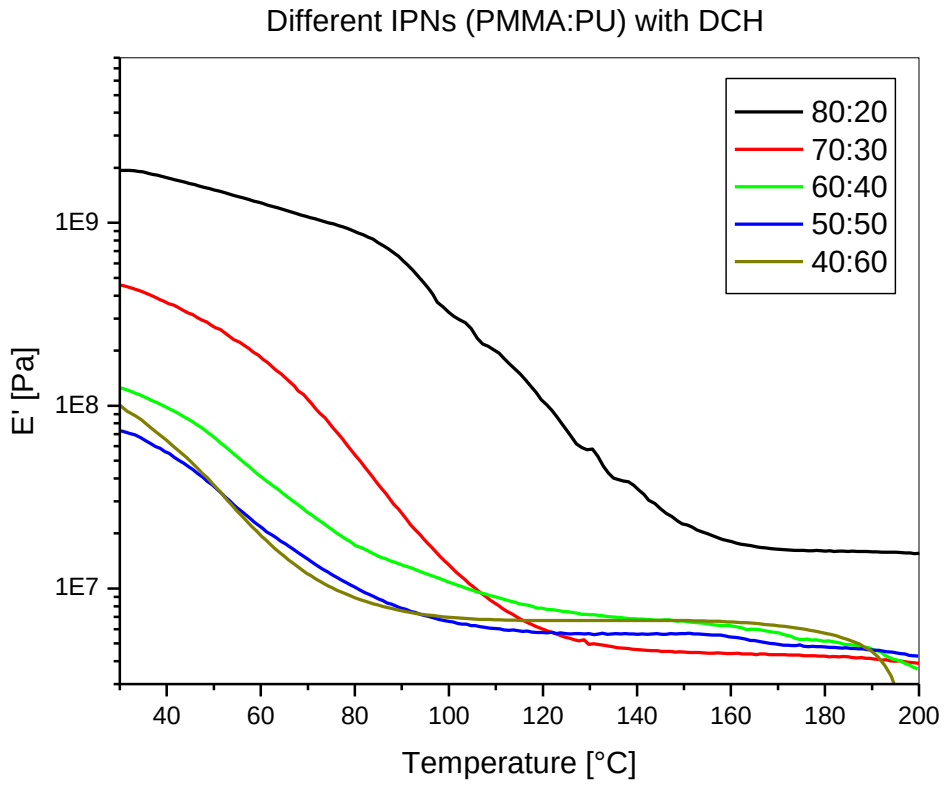

Figure II-4. DMA results showing change in E' for IPNs with various amounts of PMMA to PU content with DCH

The tan δ curves of the IPNs also demonstrated how changing the ratios of PMMA:PU would have profound effects on the thermo-mechanical properties. A maximum peak in each curve shows the glass transition temperature, T_g, which indicates the temperature where the IPN network transitions from the glassy state to the rubbery state. Looking at Figure II-5, with increasing amounts of PMMA, the peak became sharper and clearer. On the other hand, increasing the amount of PU resulted in broader peaks of the tan δ curve. This phenomenon suggests that several relaxation mechanisms may be present in the IPNs which could possibly be associated with the molecular domains when similar amounts of the two phases were used.

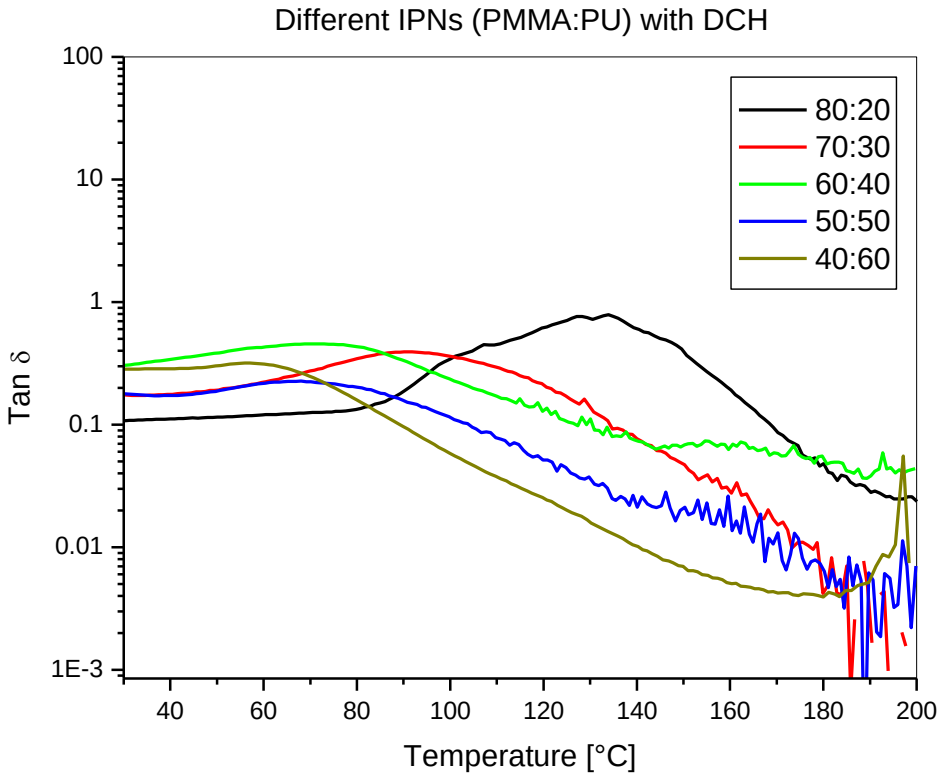

Figure II-5. DMA results showing change in tan δ for IPNs with various amounts of PMMA to PU content with DCH

Other features to note are the locations of the peaks for each IPN as well as each curve only having one peak and not two. When more PMMA was present in an IPN, the tan δ peak shifted more to the right, at higher temperatures. With increasing amounts of PU, the peak shifted to the left. This is due to the T_g's of the pure constituents. PMMA has a high T_g, and PU has a lower T_g, and having a mixture of the two would result in peaks between these two pure phases. IPNs consisting more of PU will shift the T_g even more to a lower temperature. Additionally, since only one peak is present in each curve, it is understood that intermolecular mixing was achieved

with minimal phase separation. If phase separation had occurred, two distinct phases would be seen by two different tan δ peaks, corresponding to each phase.

Both types of IPNs with DCH or TDI were compared, and the results in Table II-1 summarize the thermo-mechanical values for these samples as well as pure PMMA. Using different isocyanates in the PU phase also showed major changes in the thermo-mechanical properties. Table II-1 shows that IPNs with DCH had a much higher stiffness than samples containing TDI. This may have been due to the open conformation from DCH's aliphatic structure, which allowed a more open structure in the formation of the PU chains. Alternatively, TDI may have formed a less uniform structure with some incompatibilities in the network.

Similar thermo-mechanical results were found in the research conducted by Yang et al. when studying different isocyanates in the production of shape memory polymers [88]. Mishra et al. also compared aliphatic and aromatic PU samples, and they concluded that the better proximity of the aliphatic polyurethane can form a strong network that can ultimately generate large domains, which are responsible for the improvement in the thermo-mechanical behavior [89].

Table II-1. IPNs with an inhibitor, and their respective wt% of PMMA and storage modulus at 50°C; T_g's were obtained from the maximum in tan δ curves

Sample	wt% PMMA	E' [Pa] at 50°C	T_g [°C]
PMMA [24**]**	100%	$3.43 \pm 0.05 \times 10^9$	106.00
IPN with DCH	80%	$1.25 \pm 0.36 \times 10^9$	125.10 ± 7.63
	70%	$0.23 \pm 0.06 \times 10^9$	93.87 ± 4.15
	60%	$0.06 \pm 0.01 \times 10^9$	70.60 ± 0.34
	50%	$0.03 \pm 0.01 \times 10^9$	62.90 ± 3.55

IPN with TDI	80%	$0.22 \pm 0.02 \times 10^9$	111.27 ± 1.60
	70%	$0.12 \pm 0.03 \times 10^9$	70.62 ± 7.78
	60%	$0.10 \pm 0.01 \times 10^9$	63.00 ± 1.25
	50%	2.82×10^6	24.76

As mentioned before, another parameter investigated for the synthesis of these IPNs was the use of an inhibitor, making the polymerization either simultaneous if it was not included, or sequential if it was included. Differences when either one was used can also be seen, not only in the morphology, but also in the thermo-mechanical behavior. Figure II-6 shows a graph comparing the tan δ curves of 70:30 (PMMA:PU) IPN samples with either DCH or TDI, and with either an inhibitor present or not present.

Test results reveal that there were two peaks in the tan δ curves for samples that did not contain an inhibitor, and there was only one peak for samples that did have an inhibitor. Regardless if DCH or TDI was used, not having an inhibitor present, or having a simultaneous polymerization, resulted in phase separation, as seen with two distinct T_g's in the tan δ curves. This correlates to what was observed in the TEM photos; phase separation could be seen at the molecular level when clear domains of each phase were formed. This phase separation at the molecular level had major effects on the thermo-mechanical behavior. If complete integration of the two polymer systems was achieved, the TEM photo would show smaller domains and a higher dispersion of the phases, and the tan δ curve would only have one peak, such as those samples that had an inhibitor and sequential polymerization.

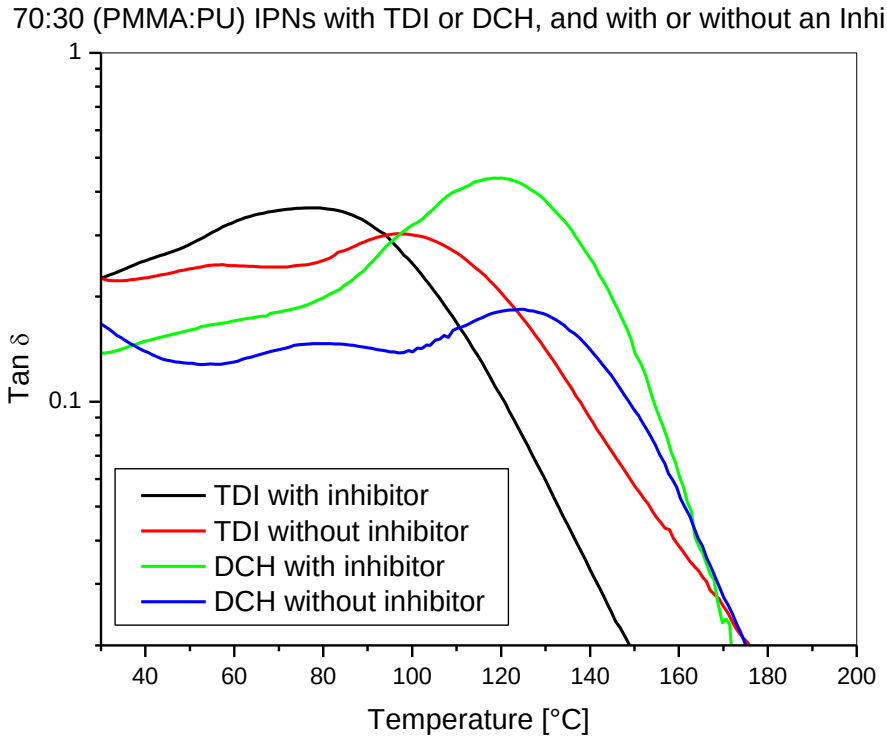

Figure II-6. Plots of tan δ versus temperature for IPNs with 70 wt% PMMA and 30 wt% PU content with DCH or TDI

A summary of the number of peaks observed in the tan δ curves and whether phase separation was observed in the IPNs can be seen in Table II-2.

Table II-2. Summary of number of peaks shown in tan delta curves and the appearance of phase separation for IPNs with TDI or DCH and with or without an inhibitor present

Sample	# of Peaks	Phase Separation
TDI with inhibitor	1	No
TDI without inhibitor	2	Yes
DCH with inhibitor	1	No
DCH without inhibitor	2	Yes

Fracture Properties

Figure II-7 shows the quasi-static crack initiation toughness behavior, also known as the fracture toughness or K_{Ic}, and Table II-3 summarizes the results for IPNs with DCH and an inhibitor present. These results were obtained from Dr. Hareesh Tippur's research group in the Department of Mechanical Engineering at Auburn University, Alabama. Note that different ratios of PMMA:PU from the experimental procedure are provided in this graph. These additional samples were prepared by Dr. Tippur's team.

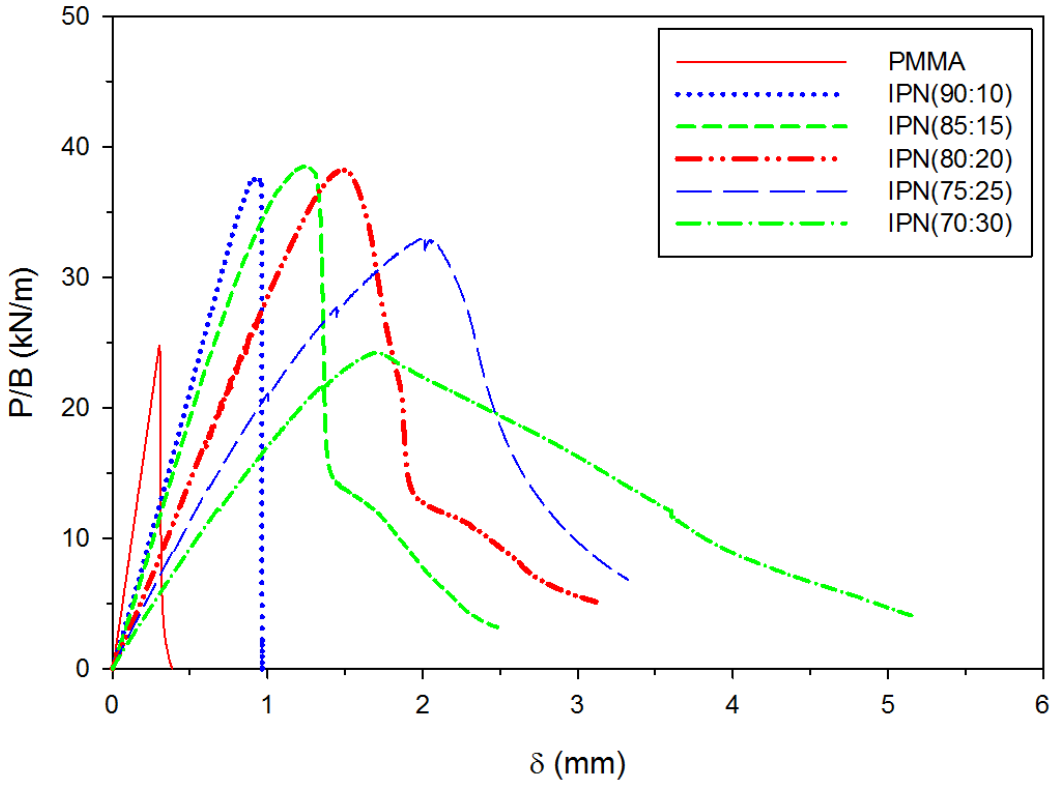

Figure II-7. Quasi-static fracture response (K_{Ic}) for various IPNs with an inhibitor and DCH

According to the graph above, pure PMMA exhibited extreme brittleness since very little strain was reached before failure. This type of behavior in PMMA has been reported before, and it is among the reasons why PMMA is not an ideal material for impact-resistant applications. Upon

further study of the graph, the IPNs seemed to exhibit brittle failure due to the sudden decrease in P/B when strain reached between 1-2mm. The sudden fall in the curve indicates that there was no plastic deformation present, and a brittle fracture took place.

Table II-3. Quasi-static fracture response (K_{Ic}) for various IPNs with an inhibitor and DCH

IPN (PMMA:PU)	Quasi-static fracture toughness K_{Ic} [MPa $m^{1/2}$]
100:0	1.12 ± 0.04
90:10	1.69 ± 0.09
85:15	1.73 ± 0.05
75:25	1.49 ± 0.06
70:30	1.08 ± 0.05

Looking at Table II-3, it appears the IPNs had approximately a 60% improvement in K_{Ic} when compared to pure PMMA. Furthermore, looking at the trends in K_{Ic} values, it appears that with increasing PU content, an optimum PMMA:PU ratio may exist where the K_{Ic} is highest.

Surface Morphology

In addition to studying the fracture mechanics, the morphology of fractured IPNs at the microscale was also investigated. Mentioned before, samples were broken after being immersed in liquid nitrogen in order to create brittle failure and to avoid breaking the samples above their glass transition temperatures where the morphology could have been altered. SEM photos taken of these broken samples' surfaces can be seen in Figure II-8. Different PMMA:PU ratios are included as well as a broken commercial PMMA sample.

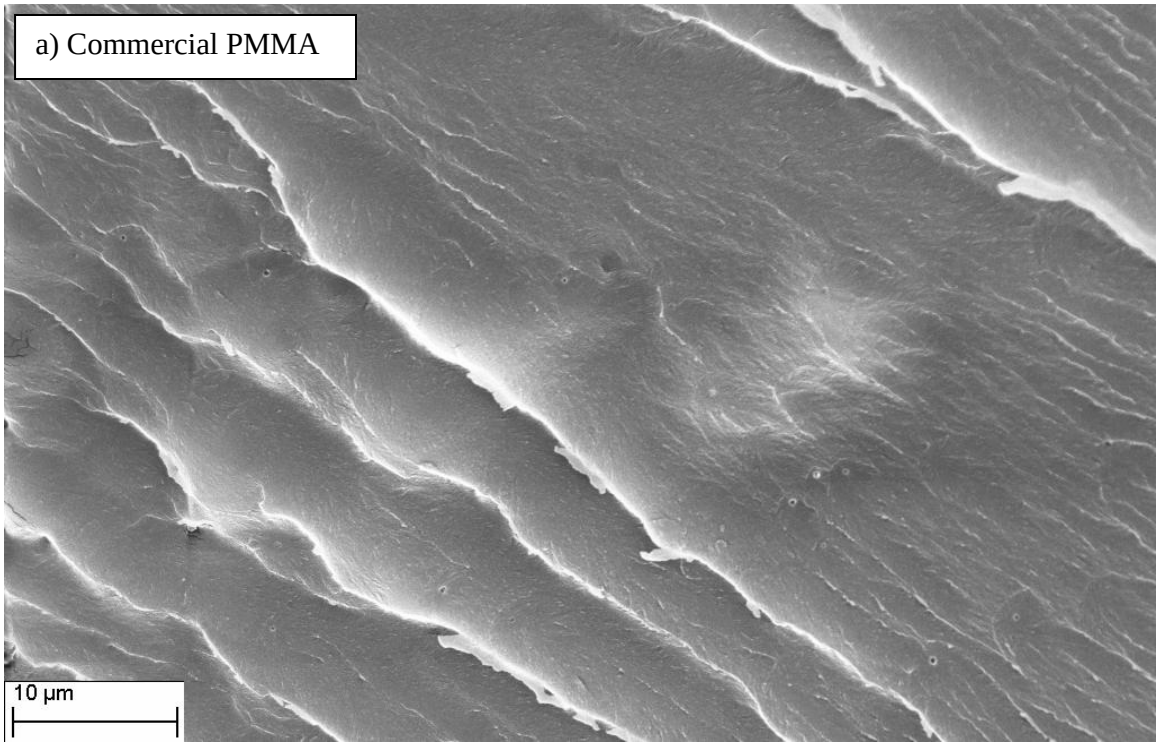
a) Commercial PMMA
10 µm

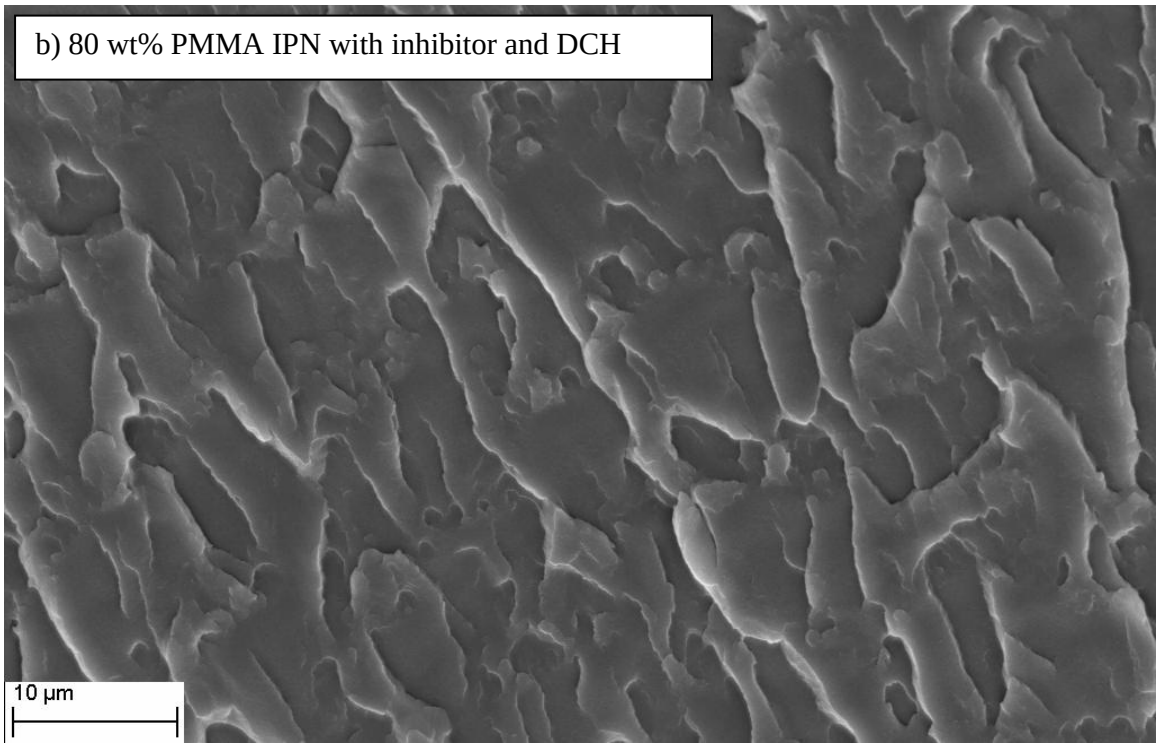
b) 80 wt% PMMA IPN with inhibitor and DCH
10 µm

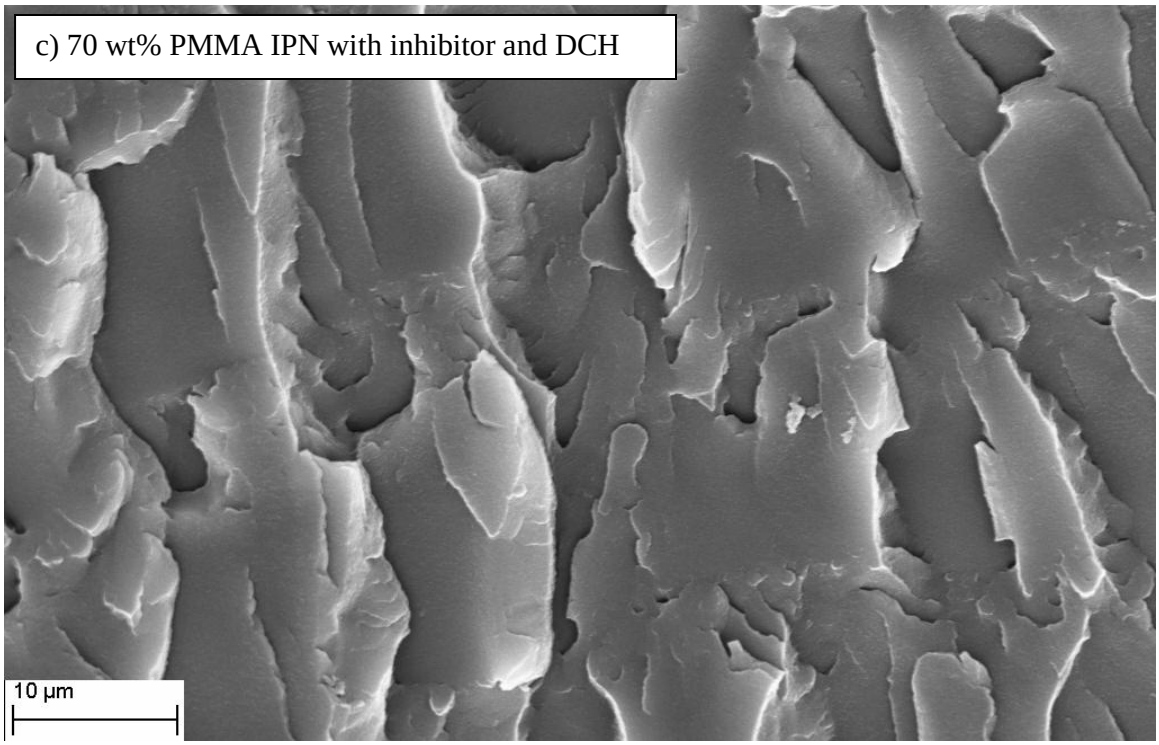
c) 70 wt% PMMA IPN with inhibitor and DCH
10 µm

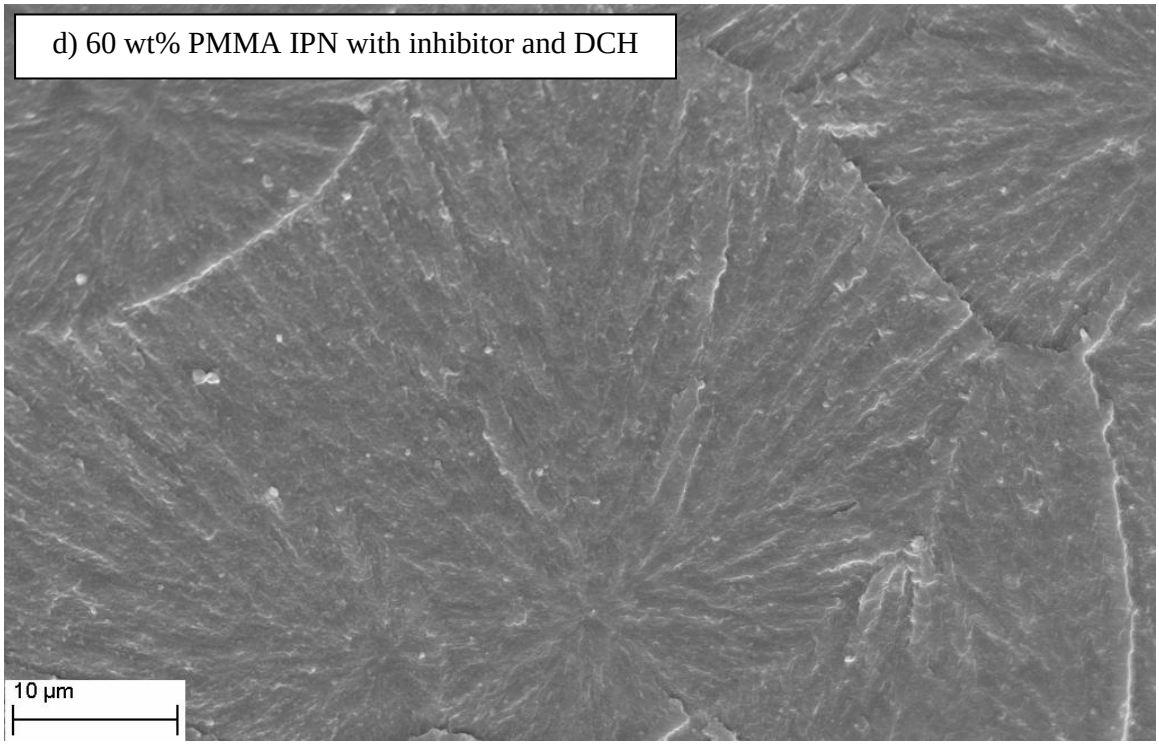
d) 60 wt% PMMA IPN with inhibitor and DCH
10 µm

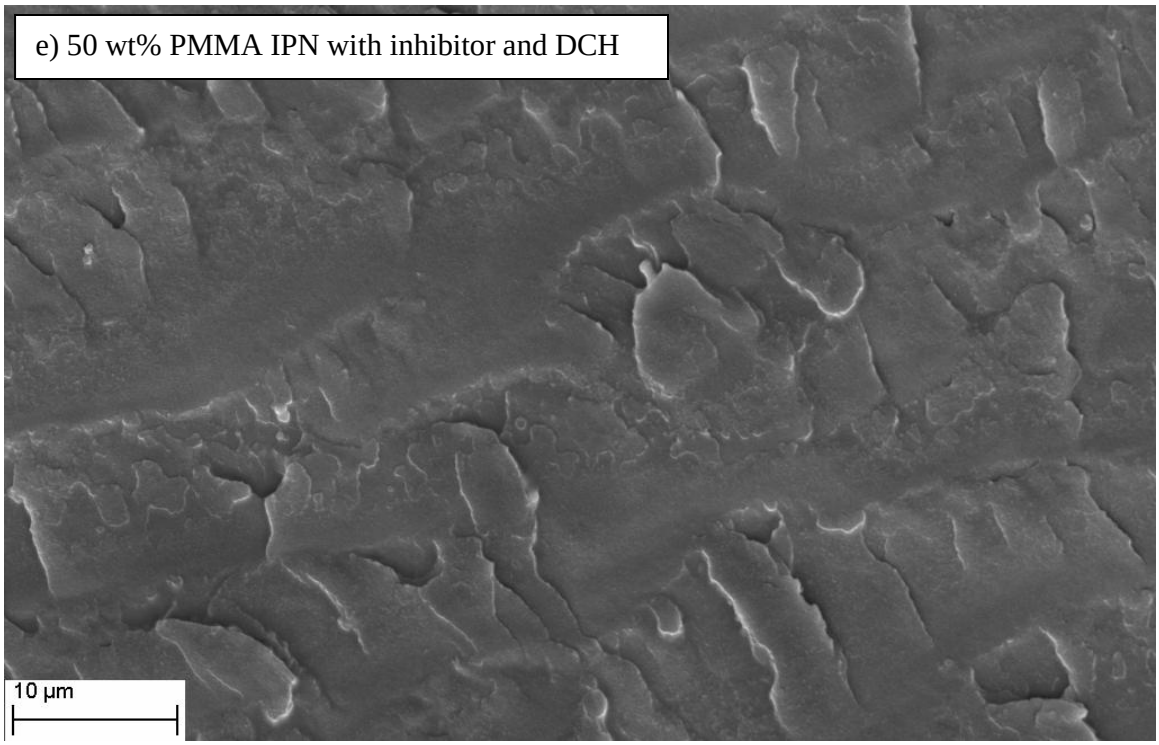
e) 50 wt% PMMA IPN with inhibitor and DCH
10 µm

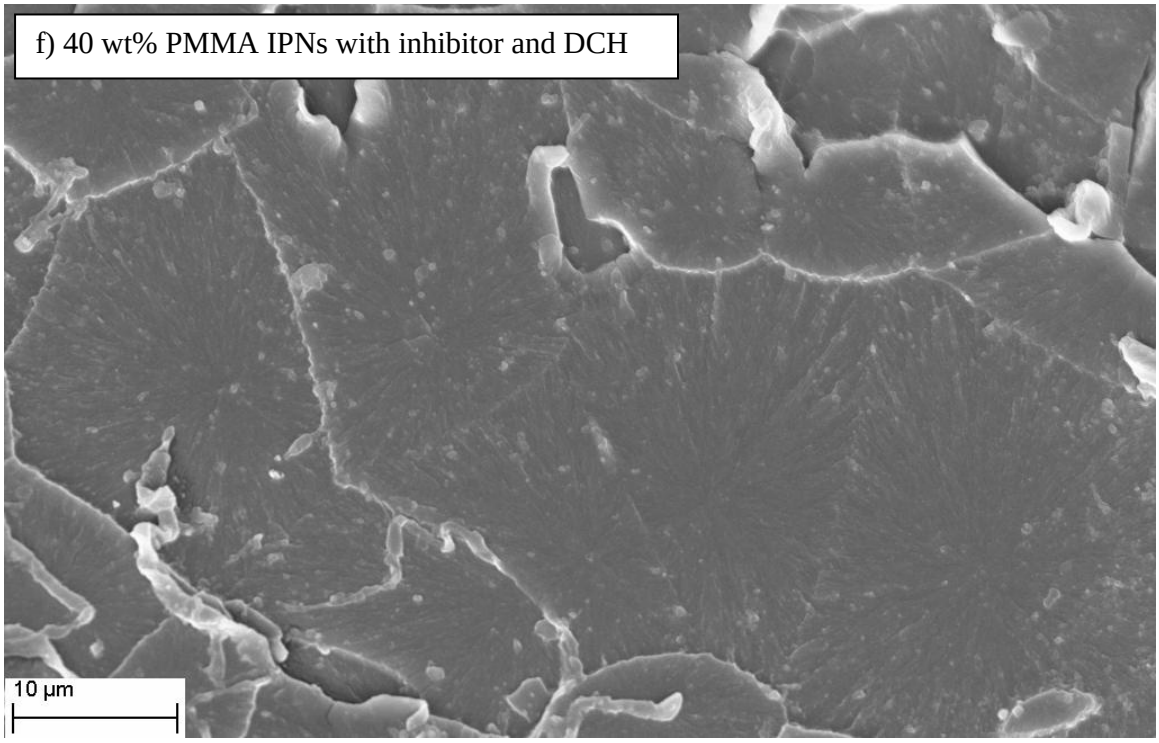
f) 40 wt% PMMA IPNs with inhibitor and DCH
10 µm

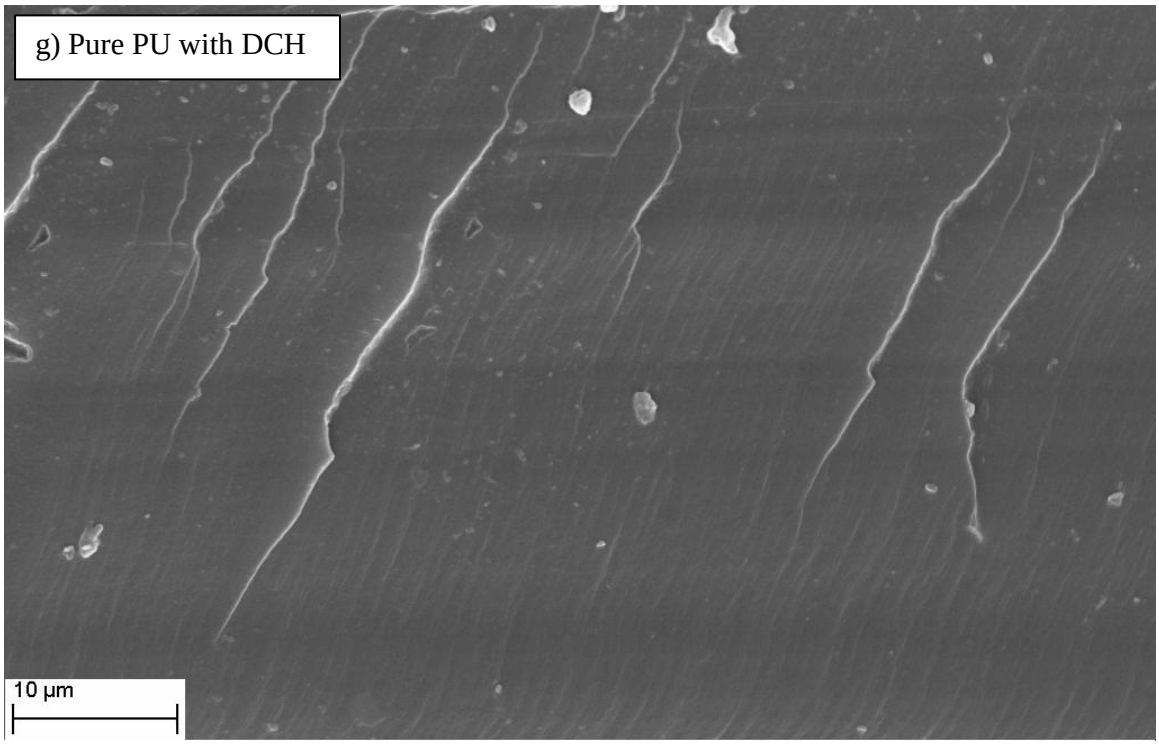

Figure II-8. SEM photos of a) commercial PMMA; IPNs with an inhibitor and DCH: b) 80 wt% PMMA c) 70 wt% PMMA d) 60 wt% PMMA e) 50 wt% PMMA, f) 40 wt% PMMA, and g) pure PU with DCH

In these SEM images, it appears that the presence of more PMMA included in an IPN created more surface area, suggesting that more energy was dissipated during the fracture process. These indications are similar to what was observed in the K_{Ic} values from fracture testing; a higher PMMA content in the IPN led to a higher K_{Ic} value and a higher degree of surface area after failure. This behavior is essential for the improvement in impact resistance for the IPNs. A higher degree of deformation energy a sample can withstand, then the less likely it will mechanically fail during its final application.

Another feature to note is the change in the surface area when more than 30 wt% PU is present in the IPN. The surface transitions from an extremely coarse surface to a smooth surface. This phenomenon may suggest that the IPNs underwent a phase inversion process, an inversion route

where the continuous phase between the phases converts from one polymer to the other, or instead of having one dominant phase, the two phases became co-continuous. This has been seen by other researchers as well [72, 75]. Figures 6-d, 6-e, and 6-f show some evidence where phase inversion during polymerization may have taken place.

Conclusions

In this part of the research, several different full-IPNs, consisting of PMMA and PU, were created based on various PMMA:PU weight ratios, the use of different isocyanates (aromatic versus aliphatic), and the synthesis of sequential and simultaneous IPNs through the presence of an inhibitor in the MMA monomer. Multiple characteristics were investigated, such as the morphology of the IPNs before and after brittle failure, the transparency, the thermo-mechanical properties, and the fracture behavior.

After careful analysis, it was concluded that samples which consisted of an MMA monomer without an inhibitor (simultaneous polymerization), PMMA content higher than approximately 80 wt%, an aromatic isocyanate (TDI), or a combination of these parameters exhibited dramatic phase separation, which negatively affected the mechanical and optical properties.

On the other hand, when IPN samples consisted of approximately 80 wt% PMMA or lower with the aliphatic isocyanate (DCH) and an inhibitor present in the MMA monomer (sequential polymerization), the best specimens were synthesized for transparent, impact-resistant material applications. Because these materials displayed minimal phase separation, the IPNs exhibited

high E’ and T_g values, relatively high transparencies, and small domain sizes. Additionally, these samples showed evidence for being tough, energy-absorbing materials capable of being potentially applied in real world scenarios. The findings in this part of the research set the foundation for subsequent experiments reported in this study.

CHAPTER III

INTERPENETRATING POLYMER NETWORKS WITH POLYURETHANE CONSISTING OF DIOLS OF VARYING MOLECULAR WEIGHT

Introduction

Expanding on the previous study, this part of the research focused on the morphological, optical, and thermo-mechanical effects caused by changing the network morphology of the PU phase. The purpose of changing the rubbery, soft phase was to observe if the properties studied in the previous chapter, such as fracture toughness, could be improved upon. In order to achieve this, diols of different molecular weight and chain lengths were used, including 650g/mol, 1400g/mol, 2000g/mol, and 2900g/mol. The consequences of increasing the molecular weight of the diol should be similar to what can be seen in Figure III-1, where the blue network represents the PU phase, and the red network represents the PMMA network.

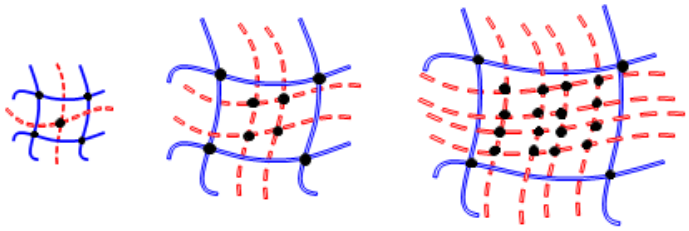

Figure III-1. Changes in network morphology as higher molecular weight diols are included in IPNs

The idea is that as the PU network has increasingly longer chains between cross-link points, then this system will have considerable changes in the final material properties. As an example, increasing the molecular weight of the diol should increase the flexibility of the PU phase, producing progress in impact-resistance and thus creating better materials for bullet-resistant type applications.

Some research groups and many others often discuss in their own studies the changes in their hard and soft segment content in pure, segmented PU. Generally, the soft segments are formed from macrodiols [90]. The hard segments can be synthesized by reactions involving diisocyanates with low-molecular weight diols, referred to as chain extenders [90], such as neopentyl glycol, hexamethylene diol, hydroxypivalic acid neopentyl glycol ester, butane diol, among others [91]. Even polyols, such as trimethylol propane and 1,2,4-butane triol can be used in the synthesis of hard segments [91].

It should be noted that the PU in this study is not considered or treated as a segmented PU with hard and soft segments, since no chain extenders are used and phase separation is undesirable. However, the similar work of others who did study these kinds of systems can still be compared to the currently reported materials.

Several other researchers have also studied the effects of changing the reactants for their pure PU systems, not in IPN form like this reported research. However, similar to this study, some individuals have looked into the effects of changing the molecular weight of the polyol for segmented PUs. For instance, O'Sickey et al. have studied the influence of the molecular weight

of soft segments of poly(urethane urea)s [92]. Li et al. [93] and Panwiriyarat et al. [94] have explored the effect of changing their polyurethane structures by using different molecular weight PCL diols .

Many other individuals have even looked at changing diols in IPNs, like Dadbin and Frounchi, who have investigated the effects of the molecular weight of the soft segment in their simultaneous IPNs consisting of PU and poly(allyl diglycol carbonate) [95]. Xiao et al. have also investigated the effects of changing the molecular weight of polyols for their IPNs with PU and methacrylate monomers, similar to the current study [96]. However, their research had several key differences from the current research, such as creating simultaneous IPNs with different reactants and where PU was the dominant system, versus this research which focused on sequential IPNs with PMMA as the dominant system.

One particularly popular topic among individuals who work with polymeric materials is the study of PU-based shape memory polymers (SMP)s. In this field, researchers have also explored the changes in the shape memory effects of having different soft segment lengths, such as Kim et al. [97] and J. R. Lin et al. [98]

In this section of the research, several material characteristics were studied, such as the optical and morphological properties, the thermo-mechanical properties, and the fracture properties of IPNs with diols of various molecular weights and chain lengths in the PU phase of the IPN. As mentioned before, the PU studied in this work is not considered a segmented PU, although there are elements of hard and soft segments present. As an example, the TRIOL and the DCH could

be regarded as a hard segment, but unlike PUs that are meant to be segmented, there is no chain extender present. Also, the diol in this research could be regarded as the soft segment. However, segmented PU is often used to promote phase separation, such as in the synthesis of SMPs. As shown in Chapter II, phase separation is undesirable, especially in an IPN, thus the PU synthesized for this research is not considered a segmented PU. The purpose of this research was to enhance the material properties that were seen in Chapter II while maintaining phase compatibility between PU and PMMA.

Materials and Methods

Materials

Reactants used in this part of the research involved many of the same chemicals in the previous chapter. For the PU phase, two polyols were used, 1,1,1-tris(hydroxymethyl) propane (TRIOL) from Acros Organics (U.S.) and poly(tetramethylene ether) glycol (PTMG) from Sigma Aldrich (U.S.). Since the main objective of this study was to determine the effects of varying the chain length of the PU phase, several PTMGs of different molecular weight were utilized, such as 650g/mol, 1400g/mol, 2000g/mol, and 2900g/mol. As before, each diol was combined with the triol beforehand, where they were both melted in an oven under a strong vacuum and mixed together. The isocyanate used was only the 1,6-diisocyanatohexane 99+% (DCH) from Acros Organics (U.S.), and the catalyst used was still dibutyltin dilaurate, 98% (DD) distributed by Pfaltz & Bauer (U.S.), with ethyl acetate as an analogue for DD.

In the PMMA phase, methyl methacrylate, 99% stabilized (MMA) from Acros Organics (U.S.) with the inhibitor still included and trimethylolpropane trimethacrylate (TRIM) from Sigma Aldrich (U.S.) were still employed. The initiator was 2,2'-azobis(2-methylpropionitrile), 98% (AIBN) from Sigma Aldrich (U.S,), with ethyl acetate as an analogue.

Methods

Similar to what was studied before, the reaction took place as a one-step, bulk polymerization with all reactants mixed together at ambient temperature. After the PMMA and PU precursors were first mixed separately, both precursors were mixed together. After thorough stirring, DD was added to catalyze the PU system, and then the IPN mixtures were placed in the oven at 60°C for 24 hours, followed by additional curing at 80°C for another 24 hours.

Although the ratios of the PU phase changed for different systems since each diol was of a different molecular weight, the same ratios between the reactants for the PMMA phase were used: PMMA to TRIM (95:5 by mass), and 1.3mL of AIBN solution for every 123.5g of MMA.

Since diols of varying molecular weight were added in the PU phase, different ratios of the reactants were mixed together. In order to determine the amount of diol, triol, and isocyanate needed so that all –OH groups would react with all –NCO groups, Equations III-1 and III-2 were used [99].

$$\text{Equivalent weight} = \frac{\text{MW}}{\text{\# functional groups}} \qquad \text{Equation III-1}$$

$$\text{Equivalent (eq)} = \text{Equivalent weight}^{-1} \text{ x mass of reactant} \qquad \text{Equation III-2}$$

$$= \frac{\text{\# functional groups}}{\text{MW}} \text{ x mass of reactant}$$

The equivalent ratio that was used in Chapter II between the polyols and the isocyanate was found to be the following: 0.19eq TRIOL: 0.12eq PTMG: 0.31eq DCH. Using these values, the amount of each diol, with a different molecular weight, that was needed for each experiment was calculated.

Instead of doing a wide range of sample ratios as before, from 80:20 to 50:50 (PMMA:PU), only samples with the ratios 80:20 and 70:30 were analyzed. Regardless of what molecular weight PTMG was being prepared, all IPNs were synthesized in the same manner with the exception of which PTMG/TRIOL mixture was included. Table III-1 shows the different IPN samples that were synthesized during this study.

Table III-1. IPNs samples synthesized in this study

Molecular Weight (g/mol)	650		1400		2000		2900	
PMMA:PU (wt%)	80:20	70:30	80:20	70:30	80:20	70:30	80:20	70:30

Techniques

The TEM used to study the morphology of the IPN samples was a Zeiss EM 10C 10CR Transmission Electron Microscope. Samples prepared for observation under the TEM underwent the same staining treatment as before where specimens were immersed in osmium

tetroxide (OsO_4) for at least a week to ensure a sufficient amount would penetrate the materials. Samples were then microtomed and studied. Although different molecular weight of the PTMG were used, the pure PU phase still absorbed the dye in every case, and the pure PMMA phase still remained unstained. This allowed the different phases in the IPNs to be distinguished.

Thermo-mechanical properties were studied through dynamic, strain-controlled 3-point bending tests with a TA Instruments RSAIII Dynamic Mechanical Analyzer (DMA). Testing parameters used included: frequency of 1.0Hz, initial temperature between 25°-30°C (or lower temperature for liquid nitrogen), final temperature of 200°C, ramp rate of 5°C/min, and a strain of 0.1%. Some tests were also conducted using liquid nitrogen; all testing parameters remained the same except for the starting temperature.

Thermal properties of pure PUs and IPNs were also observed using a TA Instruments Q2000 Modulated Differential Scanning Calorimeter (DSC). The procedure used to analyze the samples was the following: equilibrate at -80°C, modulate ± 1.00°C every 60 seconds, isothermal for 5 minutes, ramp 10.00°C/min to 250°C, ramp 10.00°C/min to -80°C, equilibrate at -80°C, isothermal for 5 minutes, ramp 10.00°C/min to 250°C, ramp 10.00°C/min to -80°C.

A UV-visible 2450 Spectrophotometer from Shimadzu Scientific Instruments was used to study the transparency of the IPNs; the surrounding air was used as the standard.

Another aspect that was studied in this section was the cross-link density of the IPNs and the pure PUs. In order to do this, a pycnometer and distilled water was used at room temperature to

find the samples' physical density. Obtaining swelling information involved placing specimens into glass vials and submerging them in tetrahydrofuran (THF). At different time intervals the samples were taken out of the vials, blotted to remove any extra THF, and had their masses recorded. Before performing the density and swelling tests, all samples were dried in an oven at approximately 80°C for a couple of hours to remove any residual moisture that may have been present in the samples. The following equations were used to find the molecular weight between cross-links and cross-link density [100]:

$$s = \frac{1}{\Phi_p} = 1 + \frac{W_s}{W_p}\frac{\rho_p}{\rho_s} \qquad \text{Equation III-3}$$

$$\bar{M}_c = -V_1 \rho_p \frac{{\Phi_p}^{1/3} - {\Phi_p}^{1/2}}{\ln(1-\Phi_p) + \Phi_p + X{\Phi_p}^2} \qquad \text{Equation III-4}$$

$$\nu_e = \frac{\rho_p N}{\bar{M}_c} \qquad \text{Equation III-5}$$

The corresponding variables represent:

Φ_p = polymer volume fraction in a swollen gel

W_p = weight of dried polymer

W_s = weight of absorbed polymer

ρ_p = density of dried polymer

ρ_s = density of solvent

V_1 = molar volume of solvent

X = Flory-Huggins interaction parameter between solvent and polymer = 0.477

N = Avogadro's number

The Flory-Huggins interaction parameter is based on the Flory-Rehner equation, which basically describes the relationship between a lightly cross-linked polymer in a solvent in terms of its maximum swelling equilibrium, thus giving an idea of its cross-link density [56]. The value that was used in these experiments was an estimate, since only values for the interaction between PMMA and THF could be found. Since the initial reactants and the method of synthesis can generate many different structures of polyurethane, as discussed in Chapter I, there is no one X value for PU. However, it is known that THF is a common solvent for PU [101]. Having a PU and PMMA together in an IPN creates even further complications for determining X. Extensive studies to resolve on a more accurate value could involve very many experiments, so for this research, 0.477 was used for comparative purposes [102].

As before, quasi-static fracture analysis was performed with the ASTM D5045 testing standard for determining the critical-stress intensity factor, K_{Ic}, also known as the crack initiation toughness, for the IPNs. Testing materials were prepared by machining the cured IPN sheets into rectangular coupons with dimensions of 80mm x 20mm x 8mm, followed by an edge notch of 6mm in length being cut into each sample, where the notch tip was sharpened with a razor blade. These single edge notched bend (SENB) samples were then loaded onto a 3-point bending apparatus in a displacement control mode and with a testing speed of 0.25mm/min. Load vs. deflection data was recorded until crack initiation and, if any occurred, during stable crack growth. Using this information, K_{Ic} values were calculated using the equations shown in the previous chapter.

Results and Discussion

Similar to Chapter II, synthesis of the IPNs consisted of a sequential polymerization, with the PU phase synthesizing first while the PMMA precursor swelled its network; following this, the PMMA then synthesized afterwards. The key difference in this part of the research was the starting reactants in the PU phase. Increasing the molecular weight and chain length of the diol should affect many material properties on not only the PU phase and the PMMA phase, but also the IPN network.

Thus, in order to understand the effect of including diols of different molecular weight in the PU phase, the first material property that was important to study was the morphology of the IPNs. As seen in the previous chapter, the final network morphology of an IPN is ultimately the characteristic that will affect subsequent behaviors in other types of properties. Thus, the morphology is discussed first, followed by its correlation with the thermo-mechanical, fracture, and optical properties.

Morphology

When observed under the TEM, it was apparent that the phase morphology of the IPNs changed as the molecular weight of the diol used in the PU phase varied. These photos can be seen in Figure III-2. The domain size of the PMMA seemed to increase as the molecular weight and the chain length of the diol increased for the PU phase. This could be associated to fewer cross-links, and longer chain lengths, being present in the PU phase, therefore allowing more PMMA to conglomerate in one area and form larger domains. It should be remembered that since the PU

phase polymerizes first, its final network morphology will govern how the PMMA phase's network will form.

For each molecular weight, major differences in morphology could be observed between samples with 80 wt% PMMA and 70 wt% PMMA. As more PU was included in the IPN sample, the PMMA domains became smaller but more numerous. This can be explained by the PU network; having more PU present should theoretically create a denser network where less PMMA can be accommodated and swell the PU phase.

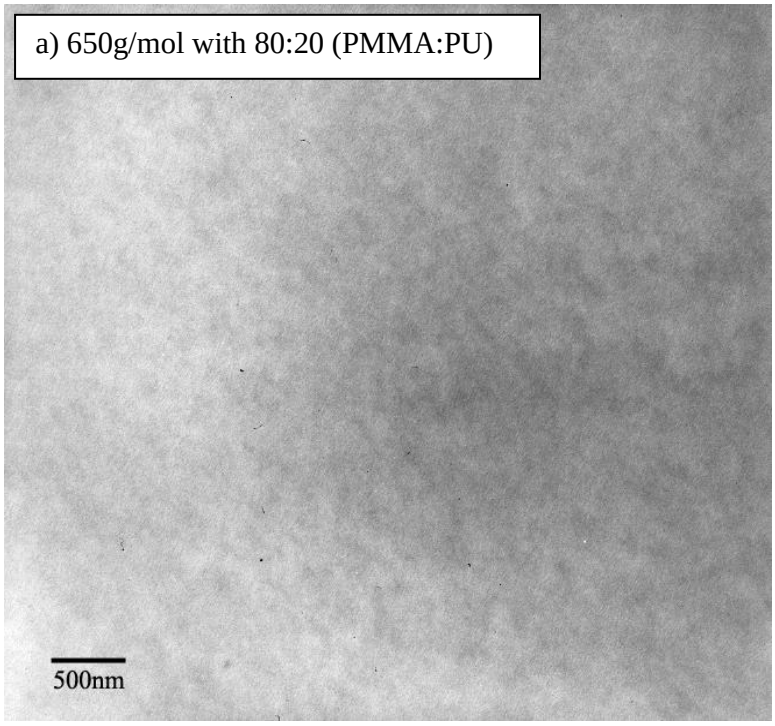

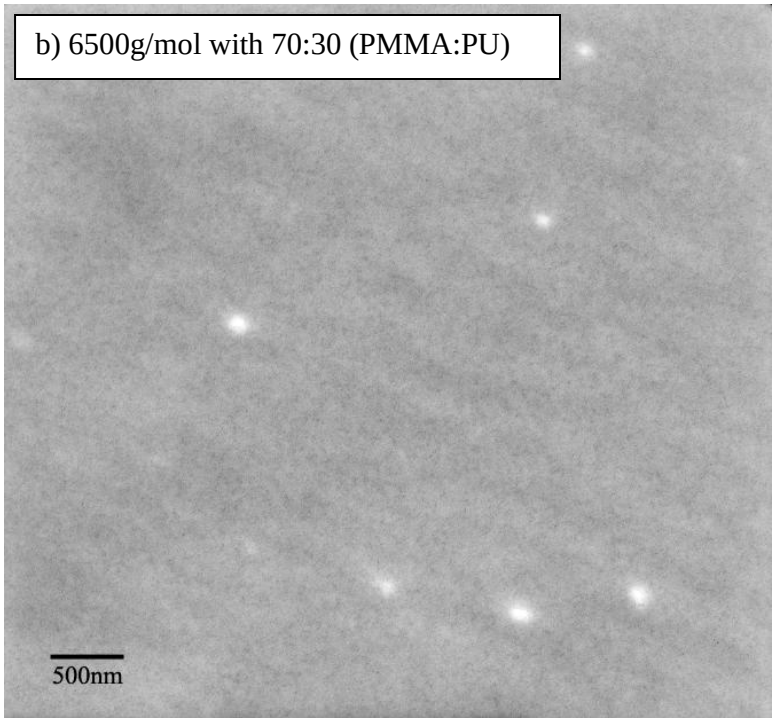
b) 6500g/mol with 70:30 (PMMA:PU)
500nm

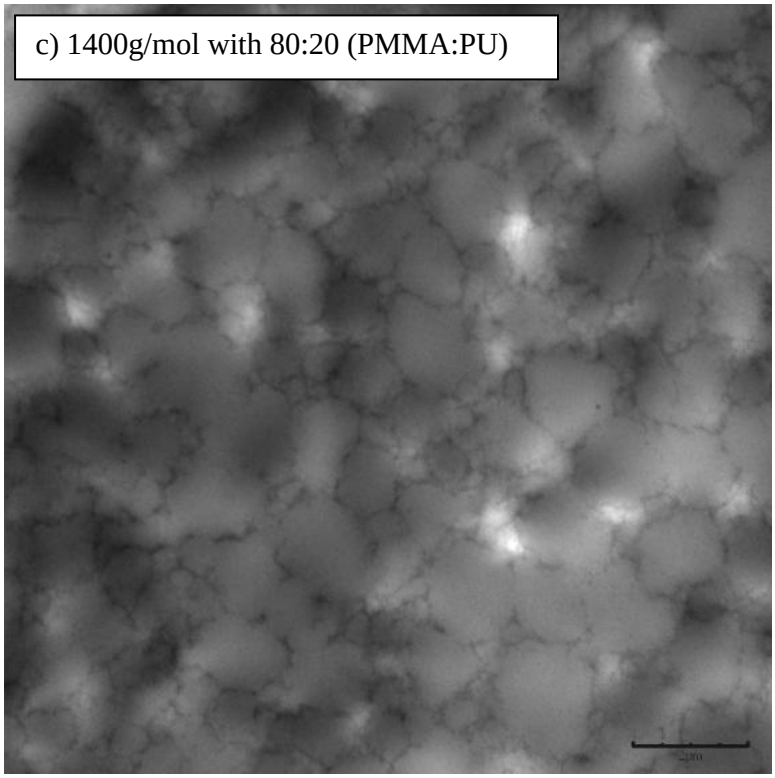
c) 1400g/mol with 80:20 (PMMA:PU)

d) 1400g/mol with 70:30 (PMMA:PU)

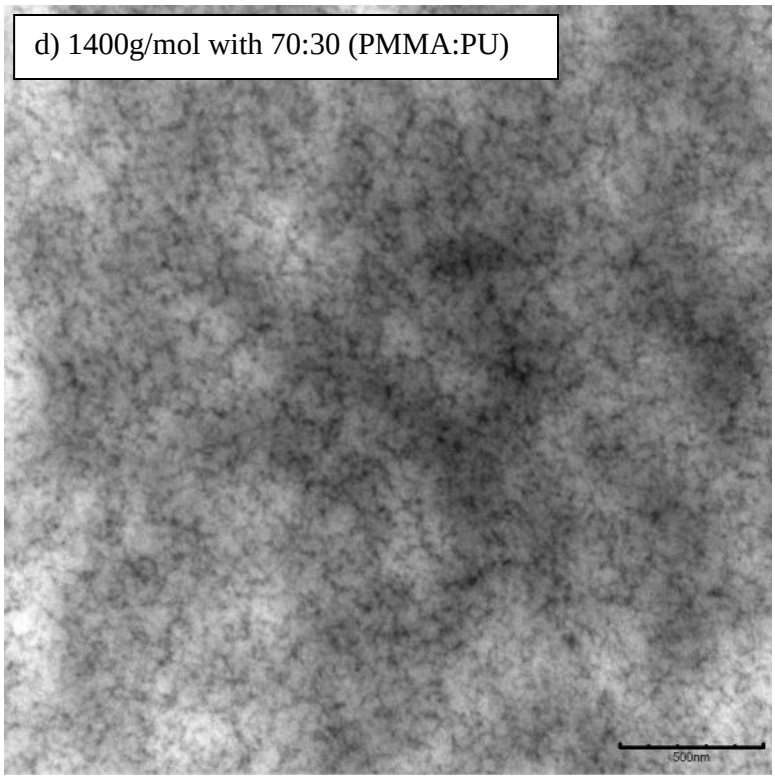

e) 2000g/mol with 80:20 (PMMA:PU)

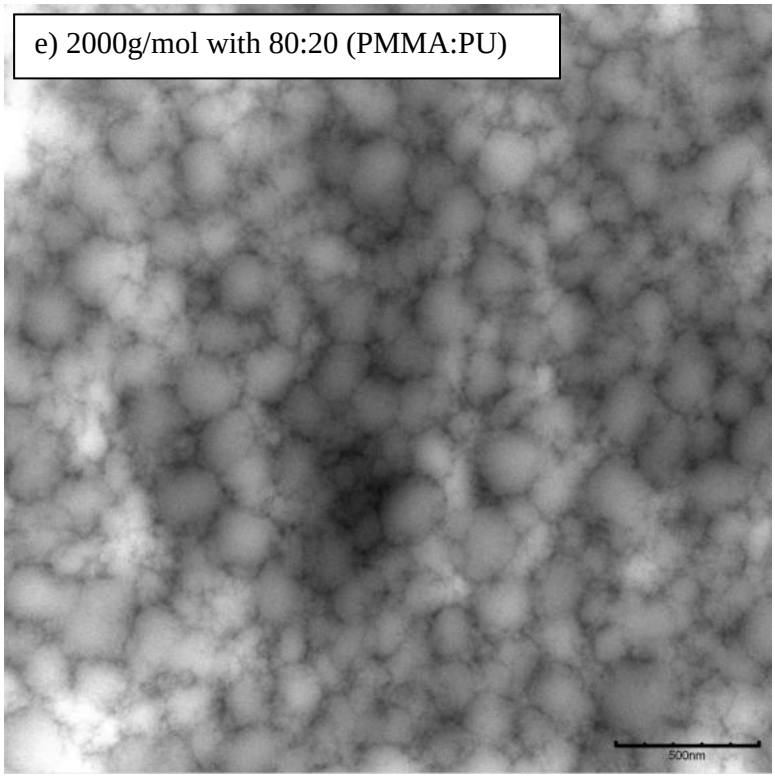

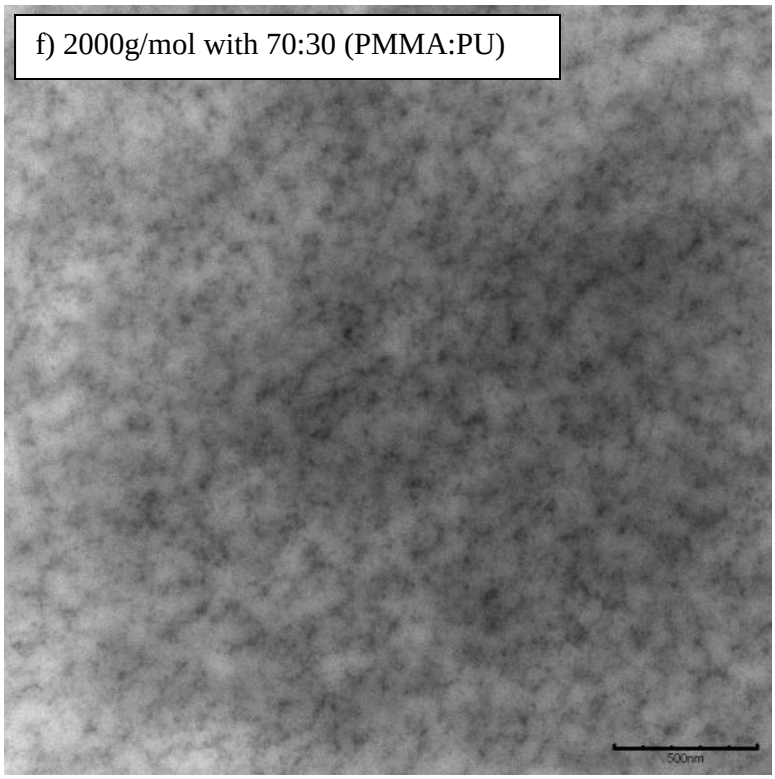
f) 2000g/mol with 70:30 (PMMA:PU)
500nm

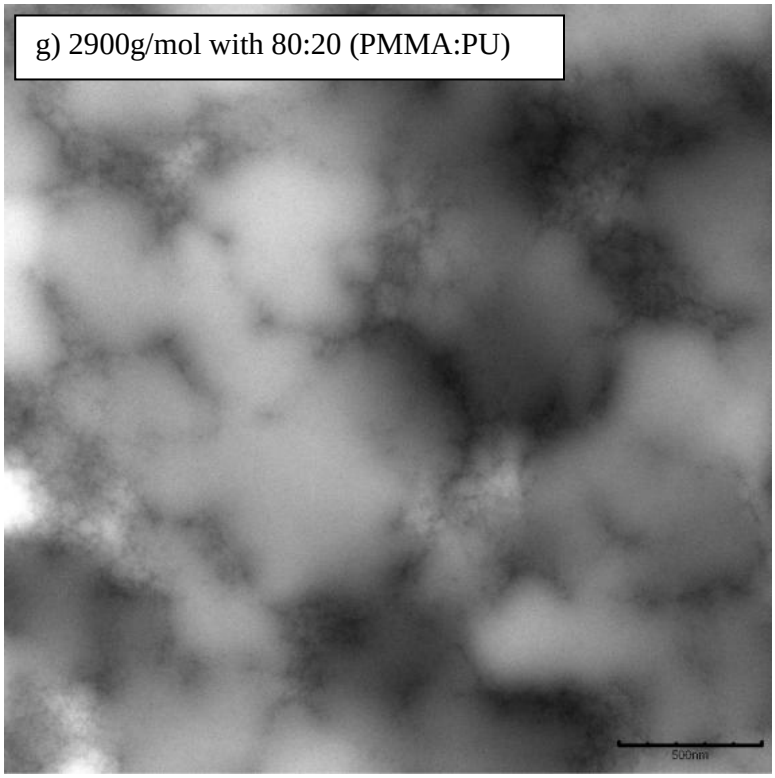
g) 2900g/mol with 80:20 (PMMA:PU)
500nm

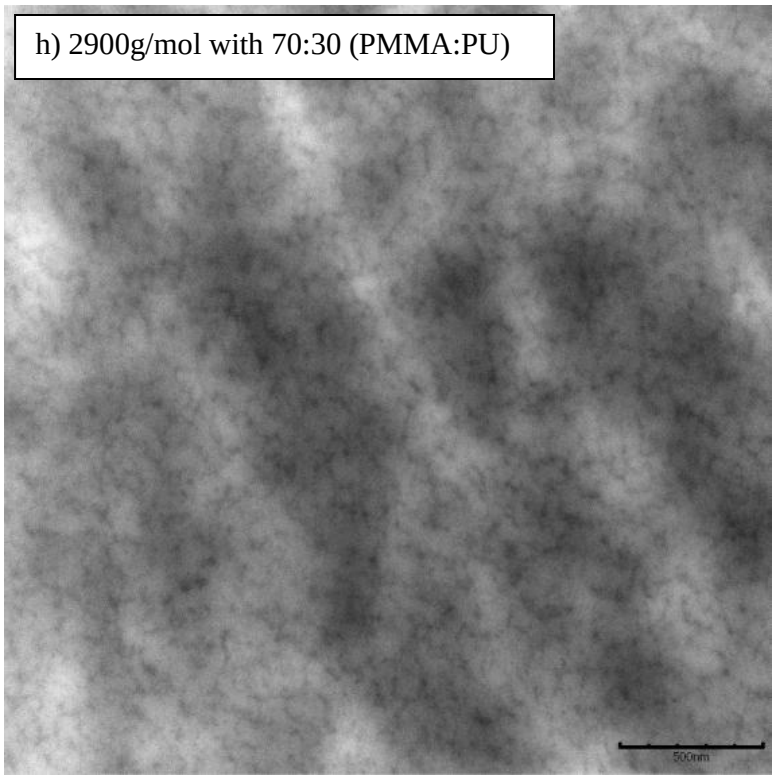

Figure III-2. TEM photos of IPNs (PMMA:PU) with diols of molecular weights a) 650g/mol (80:20), b) 650g/mol (70:30), c) 1400g/mol (80:20), d) 1400g/mol (70:30), e) 2000g/mol (80:20), f) 2000g/mol (70:30), g) 2900g/mol (80:20), and h) 2900g/mol (70:30)

Xiao et al. noted a similar phenomenon with their simultaneous IPNs with a PMMA system consisting of MMA and ethylene glycol dimethacrylate (EGDMA) as a cross-linker and a PU system consisting of PTMG and 4,4' diphenylmethane diisocyanate (MDI). IPNs that consisted of lower molecular weight polyols showed some smaller PMMA phase domains, but when the molecular weight increased, phase separation became more prominent, and the PMMA regions gradually became larger with clearer boundaries [93].

Many other research groups are finding similar results for their experiments. For instance, in O'Sickey and his coworkers' studies, they discovered that for their particular systems consisting of poly(urethane urea)s and poly(propylene glycol) (PPG) soft segments, when these soft

segments increased in molecular weight, higher degrees of phase separation occurred [92]. In agreement with this, Xiao et al. found that phase compatibility improved and phase separation decreased when their IPNs with PU and PMMA consisted of a lower molecular weight polyol present in the PU network [103]. In their work, Dadbin and Frounchi concluded that when a lower molecular weight polyol was used in the soft segment for their IPNs, interlocking and interpenetration increased between the two phases, thereby promoting great miscibility and finer microstructures. The most notable areas where these phenomena occurred were at the phase boundaries. Samples with lower molecular weight soft segments also showed a co-continuous morphology, while on the other hand, when samples included a higher molecular weight, a two-phase morphology formed, meaning that microphase separation took place. It is possible that this may be attributed to the less dense PU network that formed which resulted in less interlocking between the polymer phases [95]. These conclusions found by other researchers could explain why the currently studied system shows phase separation with higher molecular weight diols, as illustrated through the TEM pictures.

In order to further elucidate how the final morphology of the IPNs formed, swelling tests were performed which were later used to calculate the cross-link density and the molecular weight between cross-links. Since both the PMMA and the PU phases were both synthesized as networks instead of linear polymers, swelling experiments were possible. Results of swelling pure, cross-linked PU specimens can be seen in Table III-2, and Table III-3 shows swelling for IPNs consisting of various PMMA:PU ratios with a diol of molecular weight 1400g/mol. The calculated molecular weight between cross-links and the cross-link density for pure, cross-linked PU samples as well as IPNs with different PMMA:PU ratios and diols can be seen in Table III-4.

Table III-2. Swelling experiments of pure, cross-linked PU samples with different molecular weight diols

Pure PU	Day 1	Day 2	Day 3	Day 4
650g/mol	127.53 ± 1.71	127.22 ± 3.20	127.64 ± 0.72	127.48 ± 1.54
1400g/mol	136.83 ± 7.01	150.45 ± 3.34	150.86 ± 4.68	151.82 ± 4.68
2000g/mol	149.82 ± 5.32	165.01 ± 1.48	164.31 ± 0.92	164.46 ± 0.51
2900g/mol	215.67 ± 3.66	221.16 ± 1.30	218.52 ± 2.42	216.44 ± 2.82

Table III-3. Swelling experiments of IPN samples consisting of a 1400g/mol diol with varying amounts of PMMA:PU

(PMMA:PU)	Day 1	Day 2	Day 3	Day 4
0:100	136.83 ± 7.01	150.45 ± 3.34	150.86 ± 4.68	151.82 ± 4.68
70:30	125.73 ± 15.28	160.45 ± 14.10	161.13 ± 9.67	161.66 ± 9.72
80:20	100.19 ± 12.31	121.94 ± 23.97	117.61 ± 24.80	114.91 ± 26.77

Table III-4. Molecular weights between cross-links and cross-link densities for pure, cross-linked PU samples and IPNs with different molecular weight diols

(PMMA:PU)	Molecular Weight between Cross-links [g/mol]	Cross-link Density [mol/mL]
650g/mol Pure PU (0:100)	129.77	4.84×10^{21}
650g/mol 70:30	258.84	2.54×10^{21}
650g/mol 80:20	258.10	2.37×10^{21}
1400g/mol Pure PU (0:100)	231.33	2.70×10^{21}
1400g/mol 70:30	971.79	6.99×10^{20}
1400g/mol 80:20	347.27	2.00×10^{21}
2000g/mol Pure PU (0:100)	270.33	2.35×10^{21}
2000g/mol 70:30	488.07	1.41×10^{21}
2000g/mol 80:20	246.25	2.66×10^{21}
2900g/mol Pure PU (0:100)	861.32	7.00×10^{20}

2900g/mol 70:30	1118.12	$5.96x10^{20}$
2900g/mol 80:20	310.49	$2.28x10^{21}$

Table III-2 shows that pure PU samples with higher molecular weight diols swelled significantly higher than those with lower molecular weights diols. This phenomena correlates to observations made from studying the TEM photos; when a higher molecular weight diol was utilized, there was more room for the PMMA phase to occupy. Perhaps having a less dense PU phase translated into having the ability to swell more in a solvent, such as THF.

Using this information, it was also calculated, using the equation shown earlier, that pure, cross-linked PU samples with increasingly higher molecular weight diols exhibited increasingly higher molecular weights between cross-links and increasingly lower cross-link densities. These results can be seen in Table III-4. Using a diol with a longer chain length should have created networks with a higher molecular weight between cross-links, thus making a less dense network in a given area.

When looking at samples with a diol of the same molecular weight, the results were not as clear as when pure, cross-linked PU samples are compared. Table III-3 shows that the sample with 30 wt% PU swelled slightly higher than the pure, cross-linked PU network, followed by the 20 wt% PU. It was interesting to note that the pure, cross-linked PU did not swell the most, since this was the expected outcome. It was thought that having more of the flexible network, the PU phase, would lead to IPNs with higher amounts of PU to exhibit higher degrees of swelling. Similar trends were also found for samples with 2000g/mol and 2900g/mol. This can also be seen in Table III-4, where the samples that had lower molecular weights between cross-links and

cross-link densities were 30 wt% PU. Samples with 650g/mol PTMG showed the expected trend as the PU content increased. However, when diols of 1400g/mol and higher were used, these results did not follow this trend. Upon further investigation with DSC, it was discovered that these samples exhibited crystalline regions. This could possibly be the reason why swelling did not increase as PU content increased. Results from DSC tests can be seen in Table III-5.

Table III-5. DSC results for pure, cross-linked PU samples and IPNs with different molecular weight PTMGs

Sample	Crystallinity [°C]	ΔH_c [J/g]	Melting [°C]	ΔH_m [J/g]
Pure PU 650	-	-	-	-
650 80:20	-	-	-	-
650 70:30	-	-	-	-
Pure PU 1400	-	-	-	-
1400 80:20	-	-	-	-
1400 70:30	-	-	-	-
Pure PU 2000	-32.38	26.68	8.53	30.74
2000 80:20	-35.34	4.72	13.03	7.83
2000 70:30	-38.56	2.59	11.51	4.51
Pure PU 2900	-14.24	38.28	12.51	36.27
2900 80:20	-19.36	7.92	18.23	7.97
2900 70:30	-19.37	11.01	17.24	7.70

Apparently, crystallinity was present for IPNs and pure, cross-linked PU samples with diols of 2000g/mol and 2900g/mol. Although no crystallization was detected by DSC for samples with the diol of molecular weight 1400g/mol, this could be the approximate molecular weight where crystallinity began to come into prominence since crystallinity did appear for all pure, linear PU samples, including 1400g/mol, as shown in Table III-6.

Table III-6. DSC results for pure, linear PU samples with different molecular weight PTMGs

Sample	Crystallinity [°C]	ΔH_c [J/g]	Melting [°C]	ΔH_m [J/g]
650g/mol	13.75	25.92	40.97	15.75
1400g/mol	-23.29	34.34	18.26	39.52
2000g/mol	-21.32	43.10	20.8	70.65
2900g/mol	-7.54	53.04	22.14	54.86

Although not in IPN form, Li et al. also noted that with their segmented polyurethanes, samples consisting of low molecular weight soft segments did not show crystallinity. On the other hand, when samples had soft segments of higher molecular weight, crystallinity did become evident. They also mentioned that the ability of their PCL diols to crystallize was significantly depressed due to the connection with the hard segments [93]. Although, in this research, hard and soft segments were not considered, it may be comparable to shorter chains and lower molecular weights in the IPNs having a lower chance of forming crystalline regions because there were more cross-link points that hindered any organizational structure.

It may be possible that polyurethane in the presence of another network, or even by itself in network form, prohibited it from being able to form crystalline arrangements. For instance, a linear chain will have no interference except for itself in forming crystalline regions. With a polymer in a three-dimensional network, the presence of cross-links could hinder chains to form lamellae structures. Furthermore, having a completely different network present in the same area as a cross-linked PU, such as in the case of the IPNs with PMMA, would increase the chances of the PU chains interacting with other components that would further restrict any kind of crystalline organization. Not only would physical entanglements hinder crystalline regions from forming, but intermolecular bonding with other polymeric species could also play a role.

Optical Characteristics

When synthesizing segmented PUs or SMPs, phase separation is a desirable trait for the switching of the shape memory effect. However, for the purposes of obtaining a transparent material in this research, this was not the case. As shown in the previous chapter, one indication of phase separation was through optical studies. If a sample was completely opaque after curing, major phase separation occurred. On the other hand, if there was minimal phase separation, good homogeneity and intermolecular mixing between the PU and PMMA phases would result, and the IPNs appeared as clear, transparent specimens.

Figure III-3 shows results of UV-vis analysis of commercial PMMA along with IPNs with 80 wt% and 70 wt% PMMA with diols of varying molecular weight. The commercial PMMA almost reached 100% transparency, while the synthesized IPNs exhibited lower, but still relatively high, transparency values. Comparing Figures III-3a and III-3b, it seemed that in most cases, the samples with 70 wt % PMMA showed higher transparency tendencies than their 80 wt % counterparts, especially for samples with diols of molecular weight 2000g/mol and 2900g/mol.

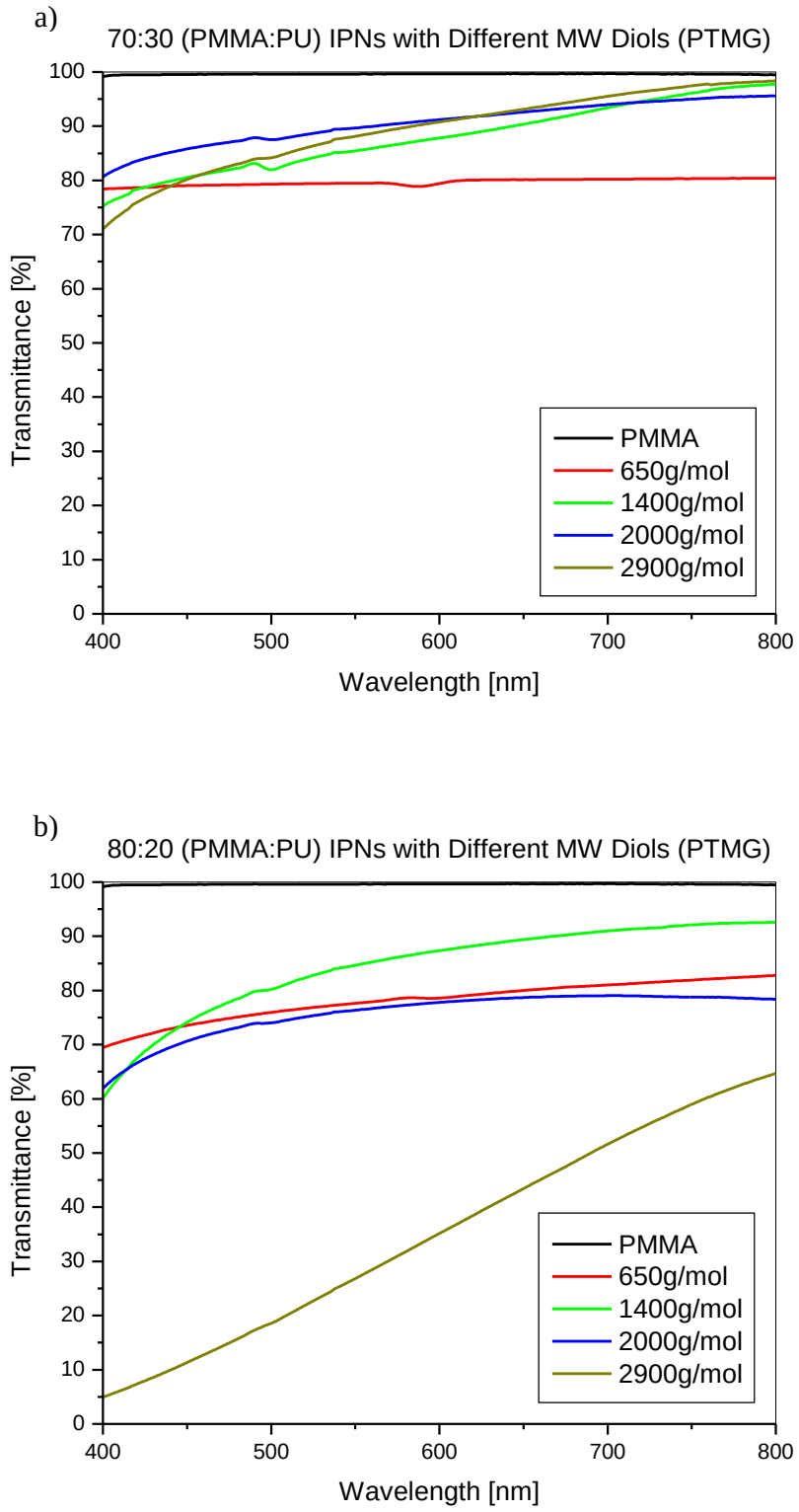

Figure III-3. UV-vis analysis of a) 70:30 and b) 80:20 (PMMA:PU) IPN samples consisting of different molecular weight diols

In the previous chapter, when the 650g/mol diol was used in the IPNs, phase separation became apparent starting at around 90 wt% PMMA and 10 wt% PU. It was concluded that too much of the PMMA phase was present, thereby inhibiting the PU phase from forming a substantial network system capable of accommodating PMMA domains while remaining intact. In other words, instead of the PMMA swelling the PU phase, the PU reacted separately and independently of the PMMA phase, followed by the synthesis of the PMMA phase outside of the PU network. This phase separation between the two networks contributed to low values of transparency. The same kind of phenomena was also observed for the IPN samples consisting of diols with molecular weights of 1400g/mol, 2000g/mol, and 2900g/mol.

With the currently studied IPNs with higher molecular weight PTMGs, phase separation seemed to occur when even lower amounts of PMMA were included in the IPN. For instance, phase separation for IPNs with 1400g/mol, 2000g/mol, and 2900g/mol PTMGs appeared to phase separate when the PMMA:PU ratios were 80:20. This could correlate to decreased values of transparency. Additionally, the presence of crystallinity in the IPNs with a higher molecular weight may have also contributed to lower values.

In their work, Dadbin and Frounchi mentioned that with their simultaneous IPNs consisting of PU and poly(allyl diglycol carbonate), when a lower molecular weight polyol was used in the PU phase, excellent optical transparency was achieved, which indicated a very similar refractive index between the two systems [95]. This may also be the case for the studied IPN materials in this research, where transparency correlated to a high degree of phase compatibility.

This same trend was seen in the TEM photos, which were shown previously. The photos of samples with 80 wt% PMMA showed irregular shapes for the PMMA domains, especially for IPNs with a 2900g/mol PTMG. When this occurred, domain areas of PMMA almost blended together while distinctive patches of PU formed in other regions. On the other hand, samples which contained 70 wt % PMMA displayed homogeneity with regularly shaped domains of the PMMA phase. This fine structure at the molecular level may be the reason why high transparencies were observed through optical studies with the naked eye as well as with UV-vis analysis, particularly with the 70:30 (PMMA:PU) IPNs.

Thermo-mechanical Characteristics

Another parameter of interest in this study was the effect of the morphology on the thermo-mechanical behavior, more specifically the E' and T_g values. As discussed earlier, and proven in Chapter II, the morphology plays a vital role in the final thermo-mechanical properties. Figure III-4 shows E' values slightly above room temperature (30°C) for samples with various diols. IPNs with 80 wt% PMMA had values of E' in the range of $6x10^8 – 1x10^9$ Pa, and IPNs with 70 wt% PMMA had values in the range of $3x10^8 – 9x10^8$ Pa.

It appeared that increasing the molecular weight of the diol in the PU phase did not have a profound effect on the E' values. It was initially expected that increasing the weight would translate into having a more flexible PU network, and in turn, a more flexible IPN. However, since crystallization was present for some of these IPNs, these structured regions acted as physical reinforcement. It is for this reason that increasing the molecular weight of the diol appeared to not affect the storage modulus.

Furthermore, a trend was observed when the E' of the 80:20 (PMMA:PU) samples were compared with the 70:30 (PMMA:PU) IPNs. For each diol, no matter what the molecular weight, samples with 80 wt% PMMA had a higher modulus than samples with 70 wt% PMMA. Despite the presence of crystalline structures for the higher molecular weights, the rigidity of the PMMA must have overpowered the rigidity of the crystalline regions. Hence the reason why samples with higher PMMA content had a higher E' than samples that would exhibit more crystallinity.

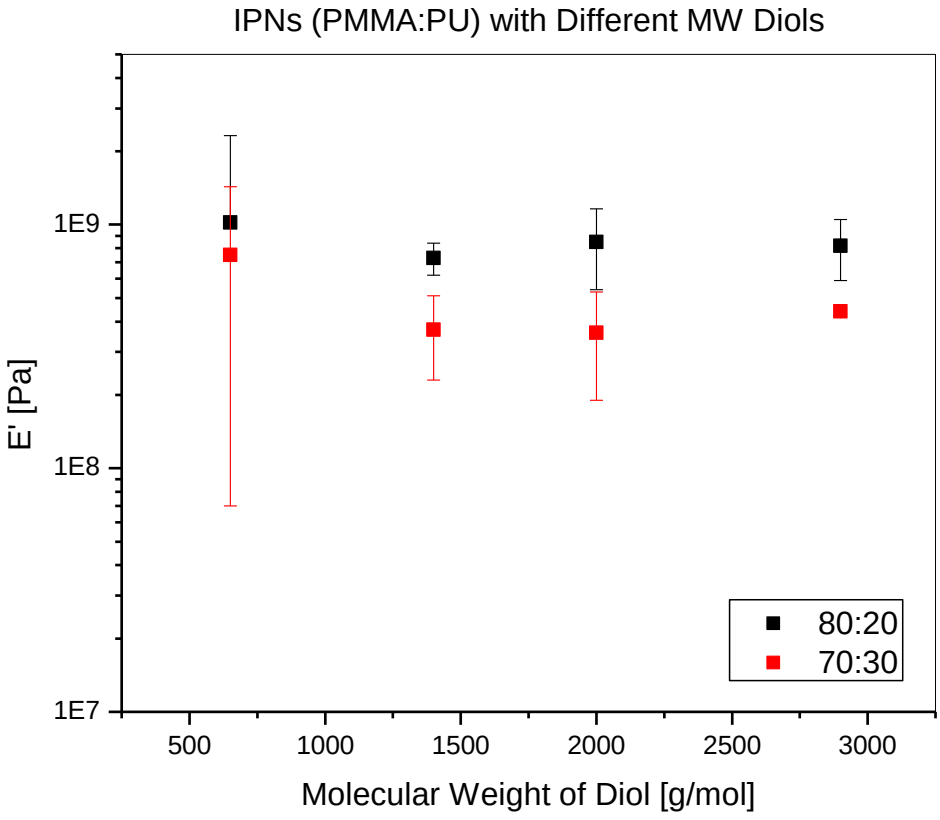

Figure III-4. E' of IPNs with different molecular weight diols

A clearer trend could be observed when looking at the glass transitions with increasing molecular weight PTMGs in Figure III-5. The T_g value increased as the molecular weight of the diol increased for both 80:20 and 70:30 (PMMA:PU) IPNs. This was expected because usually samples with longer polymer chains will have higher T_g's. Shorter and lower molecular weight diols have more chain ends than longer diols, and these chains ends are more active in movement than the middle of the molecule. When longer diols are present, there are more units in the middle of the molecule that are not as active. The energy needed to make these units more active is the reason why the T_g is higher [104]. It is also possible that the T_g observed is really the T_g that corresponds with the PMMA phase, since more phase separation did take place with higher molecular weight diols.

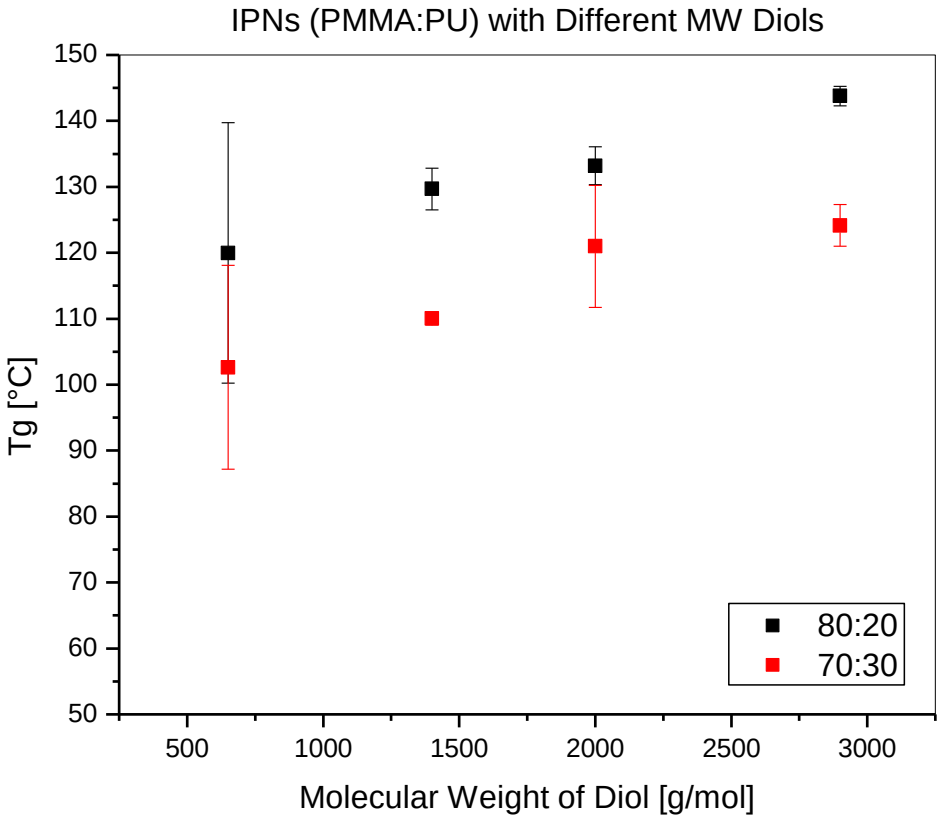

Figure III-5. T_g of IPNs with different molecular weight diols

Not only were IPNs studied, but pure, cross-linked PU samples were also investigated using DMA, and the E' and T_g values can be seen in Table III-7.

Table III-7. Summary of thermo-mechanical properties for pure, cross-linked PU samples with different PTMGs

Molecular Weight	E' [MPa] (10°C)	T_g [°C]
650g/mol	2.83 ± 1.64	-11.23 ± 0.25
1400g/mol	4.60 ± 0.25	-46.80 ± 0.72
2000g/mol	8.24 ± 2.99	-64.61 ± 1.28
2900g/mol	18.72 ± 4.43	-68.57 ± 0.42

The trends previously mentioned are the opposite with the pure, cross-linked PU samples. Here when a higher molecular weight diol was included, the E's were higher and T_g's were lower. This is what was initially expected; a lower molecular weight and a shorter chain length should create a denser and more rigid network, requiring more energy to transition from a glassy state to a rubbery state, thus raising the T_g. Perhaps here, the effect of having crystallinity present in the samples was the less dominant feature, compared to the IPNs.

Fracture Properties

Quasi-static fracture analysis, performed by Dr. Hareesh Tippur's research group in the Department of Mechanical Engineering at Auburn University, Alabama, was also used to study the effect of changing the molecular weight of the diol on the fracture toughness of the IPNs. Samples that were studied included 70:30 (PMMA:PU) IPNs with 650g/mol, 1400g/mol, 2000g/mol, and 2900g/mol molecular weight PTMGs. The results for the 650g/mol PTMG (from Chapter II) can be seen in Figure III-6-a, and 1400g/mol, 2000g/mol, and 2900g/mol PTMGs can be seen in Figure III-6-b.

a)

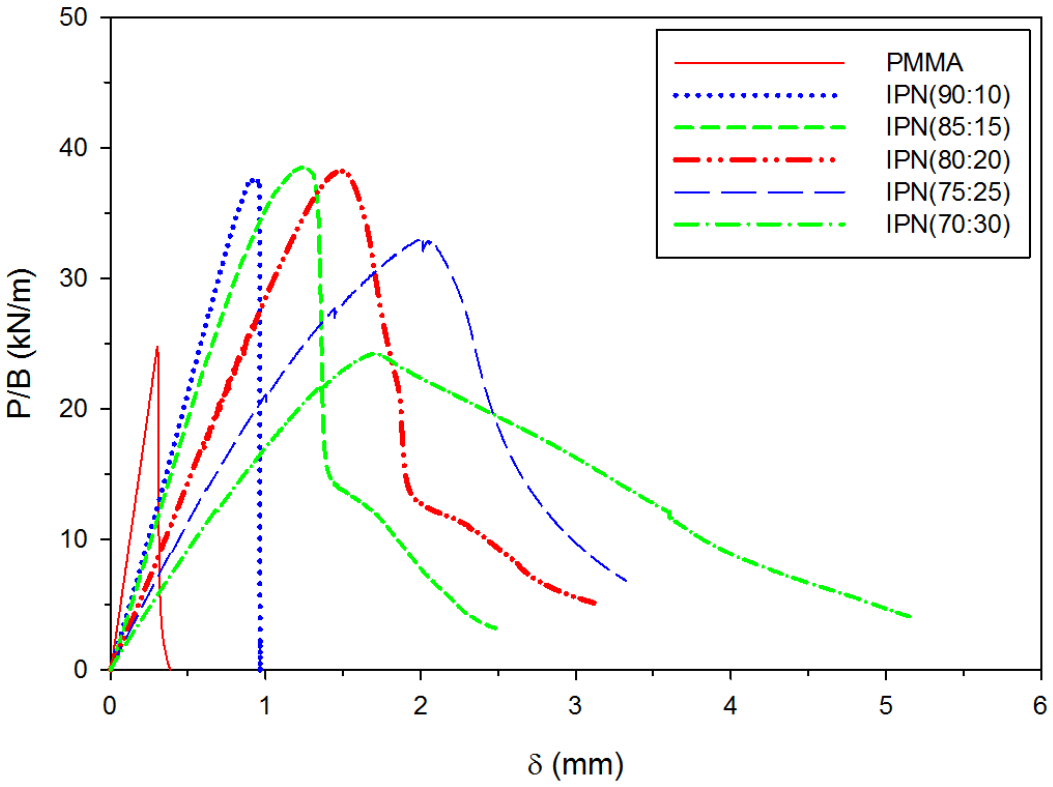

b)

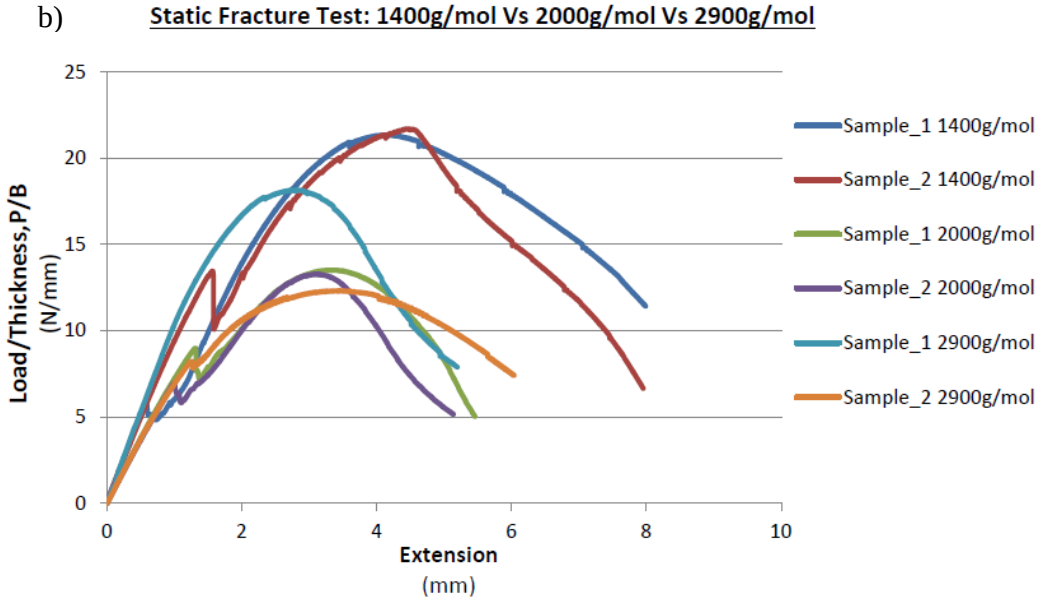

Figure III-6. Quasi-static fracture analysis of IPNs with a) 650g/mol PTMG, b) 70:30 (PMMA:PU) IPNs with 1400g/mol, 2000g/mol, and 2900g/mol PTMG

As seen in the figures, the IPNs with 650g/mol and high PMMA wt% displayed a higher stiffness, but IPNs with a lower PMMA wt% eventually exhibited plastic deformation at an extension close to 2mm. On the other hand, IPNs with 1400g/mol, 2000g/mol, and 2900g/mol could not sustain as high a loading like the IPNs with 650g/mol PTMG, but instead were able to maintain a longer extension and exhibit plastic deformation.

Increasing the molecular weight of the diol in the PU system from 650g/mol to higher values increased the amount of load the IPNs could withstand, especially when 1400g/mol was included. Perhaps this phenomenon was possible through the creation of a more flexible network in the PU system. The ability of the PU phase, and subsequently the IPN, to flex allowed the samples to absorb more energy and withstand more deformation before failure.

Another parameter that was investigated was the fracture toughness. A summary of IPNs with 70:30 (PMMA:PU) and diols of different molecular weight can be seen in Table III-8. It appeared that the IPN with the 2000g/mol diol exhibited the highest K_{Ic} value, or fracture toughness, with an average of 1.31 MPa $m^{1/2}$.

Table III-8. Fracture toughness of 70:30 (PMMA:PU) IPNs with different molecular weight diols

Molecular Weight 70:30 (PMMA:PU)	**Quasi-static fracture toughness (KIc) [MPa $m^{1/2}$]**
1400g/mol	0.92 ± 0.01
2000g/mol	1.31 ± 0.04
2900g/mol	0.74 ± 0.01

Conclusions

In the previous chapter, different parameters for the synthesis of IPNs consisting of PU and PMMA were explored and tested. Building from these experiments, this part of the research investigated the changes that would occur when diols of different molecular weight and chain lengths were used in the PU phase, or in other words, when the network structure of the PU phase was altered. It was found that several key aspects were affected, such as the transparency, the phase morphology of the components' domains as well as the final IPN structure, the thermo-mechanical behavior, and finally the mechanical properties.

The morphology of the IPNs did change when different diols were incorporated, as evidenced by TEM photos and UV-vis analysis. Large, distinct domains of PU and PMMA phases and opacity in the final IPNs with higher molecular weight PTMGs exhibited increasingly more phase separation. On the other hand, when lower molecular weights were used, the transparency remained high, especially when a substantial amount of PU was present in the IPNs to accommodate the PMMA phase before synthesis, such as in the 70:30 (PMMA:PU) samples.

The presence of crystallinity not only played a role in the ability of the IPNs and pure PUs to swell in a solvent, but these structures acted as physical reinforcement, thereby increasing the E' values.

The glass transition temperatures of the IPNs increased when both the PMMA content and the molecular weight of the diol increased, suggesting that more physical entanglements were

present with possibly increased phase separation. On the other hand, decreasing values of T_g when diols of increasing molecular weight were used in pure, cross-linked PU was observed. It is possible that there was another phenomena taking place for pure, cross-linked PUs that differed from how the IPNs behaved. For instance, the PU network may have had increasingly "looser" and more flexible networks that required less heating to reach a rubbery state.

Improvement in the fracture toughness of the samples showed promising results. The 70:30 (PMMA:PU) IPN with 650g/mol exhibited the capability to withstand a high load, but plastic deformation at low extensions. Samples with higher molecular weight diols displayed increased plastic deformation while also showing relatively high values in K_{1c}.

CHAPTER IV

INTERPENETRATING POLYMER NETWORKS WITH POLYURETHANE CONSISTING OF DIFFERENT DIOL TO TRIOL RATIOS

Introduction

The previous chapters have shown that successful IPNs, consisting of PMMA and PU, were synthesized with variables such as sequential versus simultaneous synthesis, ratios of PU to PMMA, curing profiles, and the inclusion of aromatic and aliphatic isocyanates for the PU phase. The effect of changing the PU phase by using diols of varying molecular weight was also explored and reported. For this chapter, the objective was to find another way to possibly enhance the properties of the IPNs by changing the PU phase in a different manner.

This part of the research, the focus was on creating different flexibilities in the PU phase by adjusting the degree of cross-linking and size of the network through changing the diol:triol ratio. Consequently the effects on the morphology and the thermal, optical, and thermo-mechanical properties were studied.

In this system and in the previous systems, both a triol (three –OH groups) and a diol (two –OH groups) were used in the synthesis of PU. A triol was needed to create a three-dimensional cross-linked network capable of forming a full-IPN with another polymer. The diol was

included to allow for control of the network size of the PU. Changing the relative amounts of these reactants was how the flexibility and the "mesh holes" of the PU network were adjusted. Doing this not only affected how stiff the PU phase was, but it also changed how much PMMA would be accommodated and be able to swell within the PU phase. A diagram of how changing the diol:triol ratio affects the IPN network morphology can be seen in Figure IV-1.

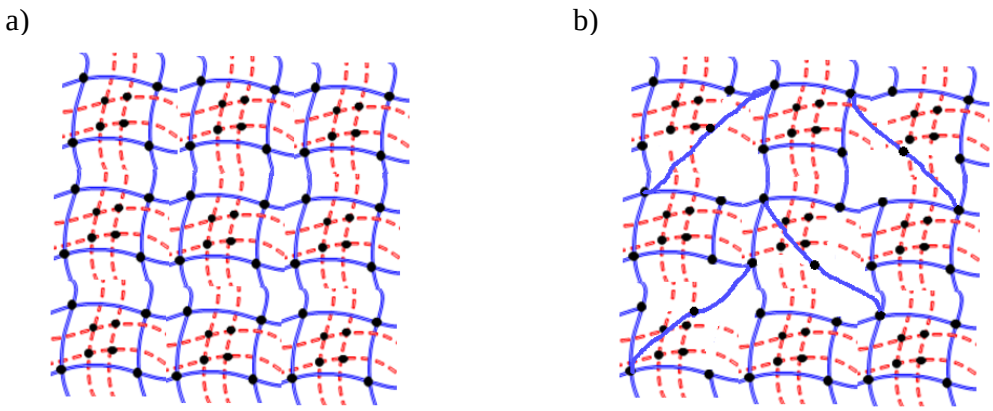

Figure IV-1. Diagram depicting a) original IPN in Topic 1 and b) IPN with more diol than triol and larger "mesh sizes" in PU phase

The molecular weight of the diol remained constant at 650g/mol in order to compare these samples to those synthesized in Chapter II's studies. The chemical structures of the diol, or PTMG, can be seen in Figure IV-2-a, and the triol can be seen in Figure IV-2-b.

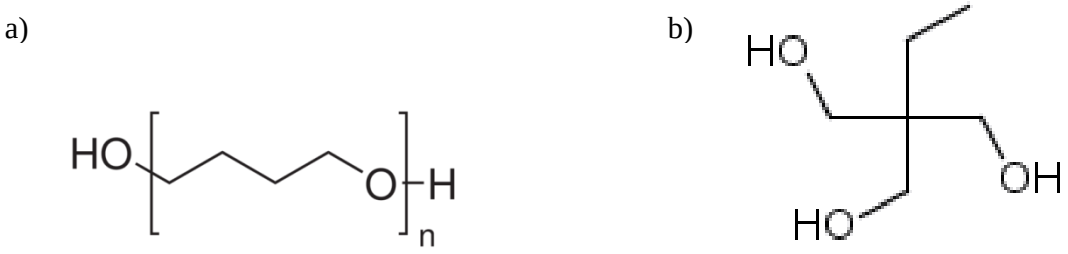

Figure IV-2. Chemical structures of the a) diol (PTMG) [105] and b) triol (TRIOL) [106] used in this research

Some researchers, like Dadbin and Frounchi, have looked into PU systems and have reported the effects of changing the hard segment to the soft segment by using different amounts of diol to triol [95]. As mentioned before, although the PU studied in this research does have some aspects of a segmented polyurethane, it is not considered to have hard and soft regions, especially since this is an undesirable trait that promotes phase separation. However, the work of others can still be compared to the reported results to help elucidate the mechanisms behind the effects of changing the diol:triol ratios.

Materials and Methods

Materials

The PU phase consisted of two different polyols: the triol was 1,1,1-tris(hydroxymethyl) propane (TRIOL) from Acros Organics (U.S), and the diol was poly(tetramethylene ether) glycol (PTMG) of molecular weight 650g/mol from Sigma Aldrich (U.S.). The diol and the triol were combined beforehand, and the mixture was melted in an oven under a strong vacuum to remove residual moisture. The isocyanate used was 1,6-diisocyanatohexane 99+% (DCH) from Acros Organics (U.S.), and the catalyst used was dibutyltin dilaurate, 98% (DD) distributed by Pfaltz & Bauer (U.S.). Ethyl acetate was utilized as an analogue for DD.

The PMMA phase consisted of methyl methacrylate, 99% stabilized (MMA) from Acros Organics (U.S.) and trimethylolpropane trimethacrylate (TRIM) from Sigma Aldrich (U.S). The TRIM was simply used as a cross-linker to create a three-dimensional network for the PMMA

phase. 2,2'-azobis(2-methylpropionitrile), 98% (AIBN) from Sigma Aldrich (U.S.) was used as an initiator.

Methods

Synthesis of the IPNs took place in a one-step, bulk polymerization with all of the reactants mixed together at room temperature, but with the PMMA and PU phases initially prepared separately. Once the PMMA system was prepared by mixing MMA, TRIM, and AIBN, and the PU phase was prepared with the PTMG/TRIOL mixture and DCH, these precursor solutions were thoroughly stirred together. DD was then added to catalyze the PU system. The IPN precursors were cured at 60°C for 24 hours and 80°C for an additional 24 hours.

Several IPNs of varying PMMA:PU content were synthesized, namely 80:20 and 70:30, using this method. Samples with varying PU chain flexibility were synthesized in the same manner with the only difference being the PTMG/TRIOL mixture.

The following ratios were used for the PMMA phase: PMMA to TRIM (95:5 by mass), and 1.3mL of AIBN (with ethyl acetate as an analogue) for every 123.5g of MMA. For the PU phase, the constituents were added in proportions different to what was previously studied in Chapter I in order to change the diol:triol ratio.

For the previous studies in Chapters II and III, the diol:triol ratio remained constant. In order to determine the percentage of diol, or flexible chains, present in each IPN, Equations IV-1, IV-2, and IV-3 were used [99], similar to the last chapter. Equation IV-1 shows how the equivalent

weight of a chemical is calculated. Using the inverse of this value and multiplying it by the mass of that chemical used in the synthesis of the polyurethane, the equivalence is determined. Dividing the equivalence value of PTMG by the summation of equivalence values of PTMG, TRIOL, and DCH and then multiplying by 100, the percentage of flexible chains can be calculated. Another method of calculating the percentage of flexible chains would be to simply calculate the percentage based on the mass of the PTMG compared to the mass of all of the constituents together. The reason why equivalence values were used was so that the change in the percentage of flexible chains would be adjusted in a more systematic manner.

$$\text{Equivalent weight} = \text{x } \frac{\text{MW}}{\text{\# functional groups}} \qquad \text{Equation IV-1}$$

$$\text{Equivalent (eq)} = \text{Equivalent weight}^{-1} \text{ x mass of reactant} \qquad \text{Equation IV-2}$$

$$= \frac{\text{\# functional groups}}{\text{MW}} \text{ x mass of reactant}$$

$$\text{\% Flexible chains} = \left[\frac{\text{PTMGeq}}{(\text{PTMGeq}+\text{TRIOLeq}+\text{DCHeq})}\right] \text{ x } 100 \qquad \text{Equation IV-3}$$

Mentioned in Chapter III, the equivalent ratio that was used in previous studies was found to be the following: 0.19eqTRIOL:0.12eqPTMG:0.31eqDCH. Using the equations, these systems had a percentage of flexible chains of 19.35%. In order to increase the flexibility, different equivalence values were used, such as switching the values for the PTMG and TRIOL, and then increasing the equivalency value of PTMG even more. By varying the equivalences of the PU system, different percentages of chain flexibilities were produced. Ultimately, the difference

stemmed from changes in the ratio of PTMG to TRIOL. Table IV-1 shows the different percentage of chain flexibilities of this study that were calculated.

Table IV-1. Equivalence values and their respective percentages of chain flexibility

TRIOL	PTMG	DCH	Chain Flexibility
0.19eq	0.12eq	0.31eq	19.35%
0.12eq	0.19eq	0.31eq	30.65%
0.06eq	0.25eq	0.31eq	40.32%
0.00eq	0.31eq	0.31eq	100% (linear)

It should be noted that these "flexibilities" do not reflect any mechanical testing that would show sample flexibility. This is merely a nomenclature developed to describe the type of system that was being investigated.

Techniques

Thermo-mechanical analysis was conducted using a TA Instruments RSAIII Dynamic Mechanical Analyzer (DMA). The following testing parameters were used for 3-point bending tests: frequency of 1.0Hz, initial temperature between 25°-30°C (or lower temperature for liquid nitrogen), final temperature of 200°C, ramp rate of 5°C/min, and a strain of 0.1%.

A TA Instruments Q2000 Modulated Differential Scanning Calorimeter (DSC) was used for investigating the thermal behavior of the pure PUs The testing procedure used in these studies included the following: equilibrate at -80°C, modulate ± 1.00°C every 60 seconds, isothermal for

5 minutes, ramp 10.00°C/min to 250°C, ramp 10.00°C/min to -80°C, equilibrate at -80°C, isothermal for 5 minutes, ramp 10.11°C/min to 250°C, ramp 10.00°C/min to -80°C.

A UV-visible 2450 Spectrophotometer from Shimadzu Scientific Instruments was used for determining the transparency of the IPN samples, where air was used as the standard.

The density of the IPNs and pure PUs was determined using a pycnometer at room temperature with distilled water. Following the procedure described in Chapter III, studies on the swelling behavior of the samples involved placing specimens into glass vials filled with tetrahydrofuran (THF), and comparing their swollen masses with their original masses at different time intervals. Samples were dried beforehand in an oven at approximately 80°C for a couple hours to remove any residual moisture for both density and swelling experiments. The equations shown in Chapter III were also used to analyze the cross-link density and molecular weight between cross-links of samples with varying ratios of diol:triol. Once again, the Flory-Huggins interaction parameter was used as an estimate with the value being 0.477, since this is the value when PMMA interacts with THF [102].

In order to study the morphology of the IPNs, a Zeiss EM 10C 10CR Transmission Electron Microscope (TEM) was used, and the same sample preparation procedure was used for the TEM as from the previous studies. After cut samples sat in the dye for at least a week to ensure a sufficient amount would penetrate the materials, the samples were microtomed. It was determined during the previous study that when using this technique, the PMMA remained unstained while the PU phase appeared to turn a dark, black color. It was this distinction

between the two phases that enabled the study of the domain formation and phase separation processes for the IPN systems. Other research groups have also studied the morphologies of their IPN systems using this technique [75, 76, 84, 107].

Results and Discussion

The aspects that were studied in this part of the research were the morphological, thermo-mechanical, and thermal changes that resulted from using different amounts of diol to triol in both IPNs and in pure PU samples. As before, changing the morphology to create improved toughness was the purpose of this work, so the network morphology was analyzed first.

Morphology

As expected, the phase morphology drastically changed depending on the polyol mixture included in the PU. Figure IV-3 shows TEM images of IPNs with 19.35%, 30.65%, and 40.32% chain flexibility, or in other words, varying ratios of diol to triol. Noted earlier, the PU phase was able to absorb the osmium tetroxide dye, while the PMMA phase remained unchanged. In the photos, the PU phase appeared to be a bridged network, while the PMMA phases appeared as circular domains within the PU phase.

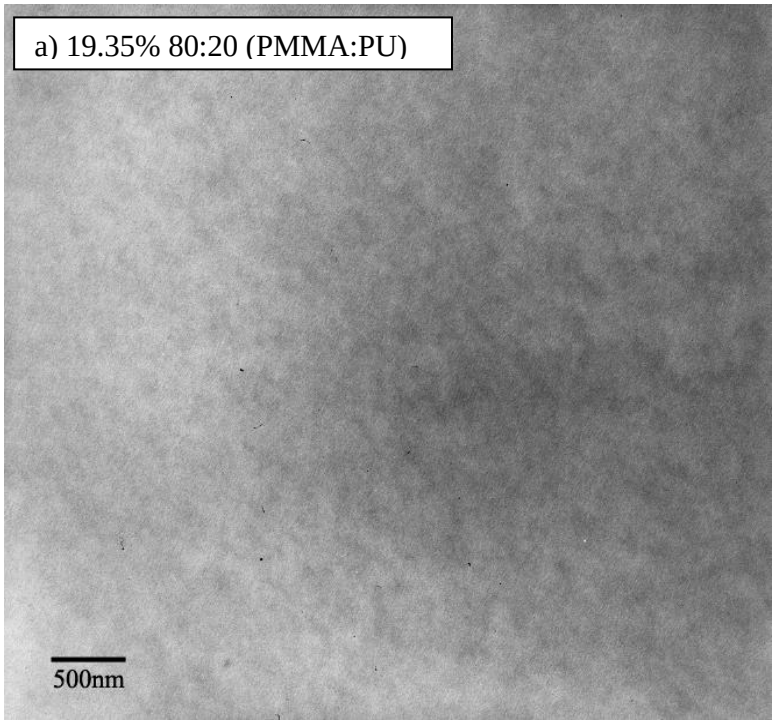
a) 19.35% 80:20 (PMMA:PU)
500nm

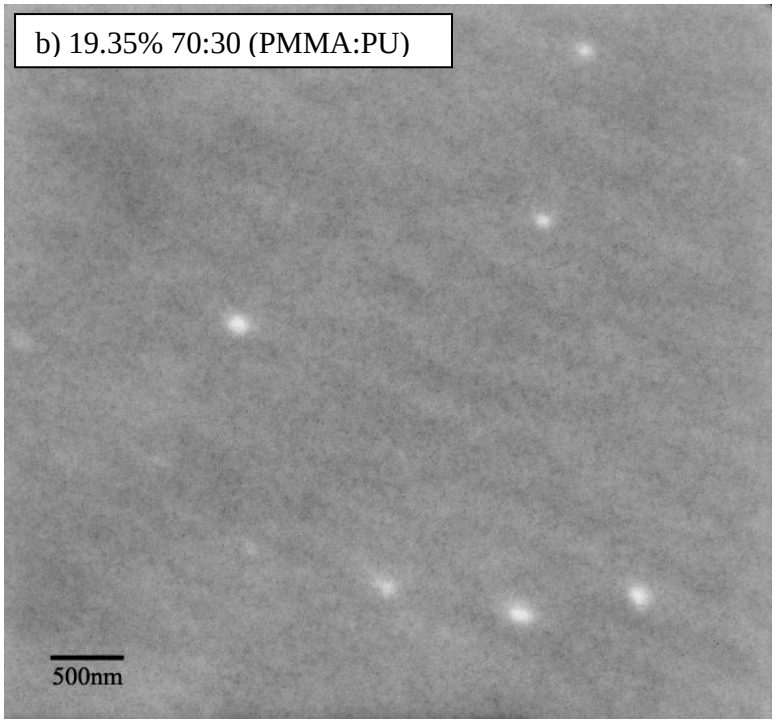
b) 19.35% 70:30 (PMMA:PU)
500nm

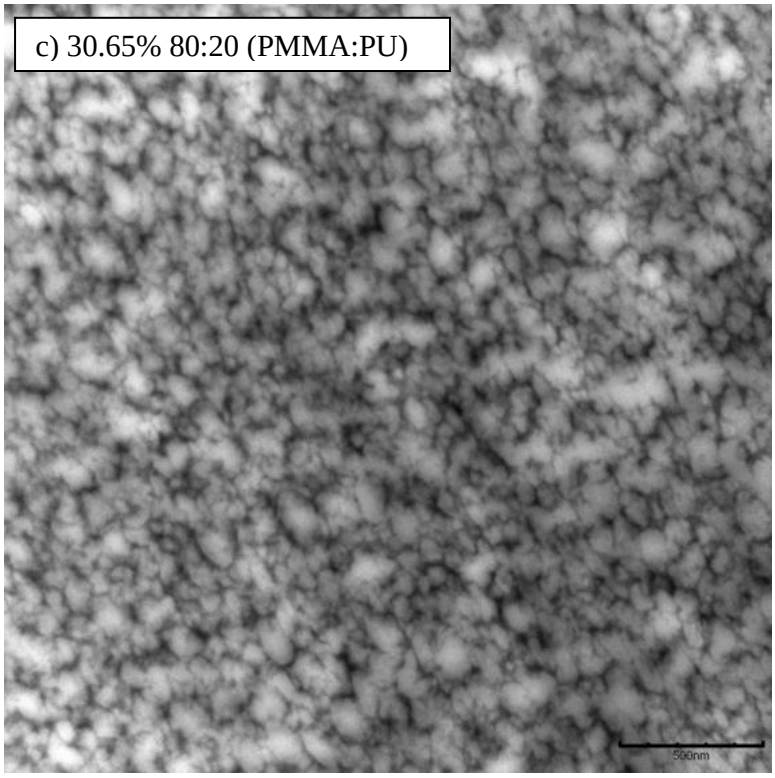
c) 30.65% 80:20 (PMMA:PU)
500nm

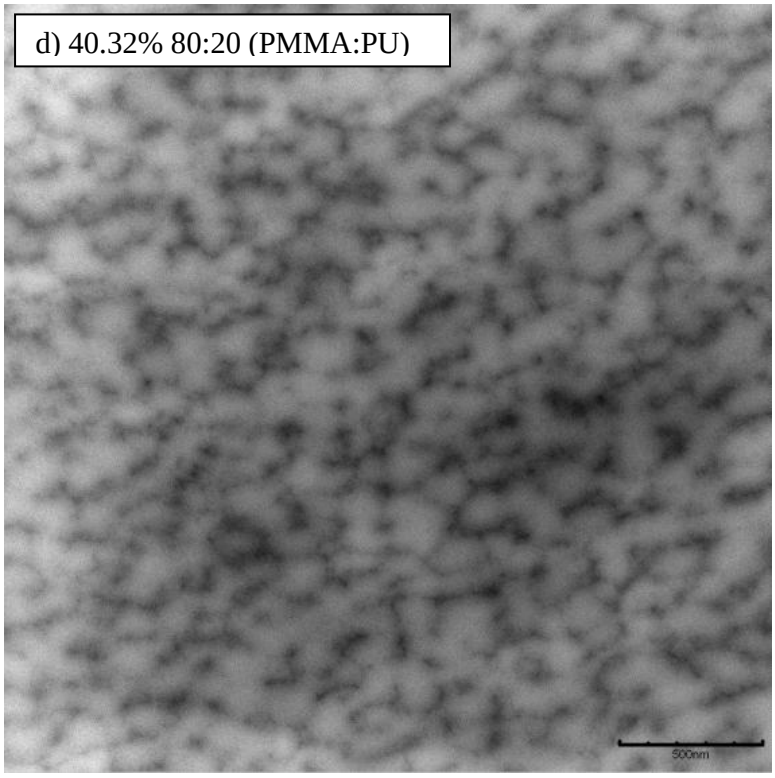
d) 40.32% 80:20 (PMMA:PU)
500nm

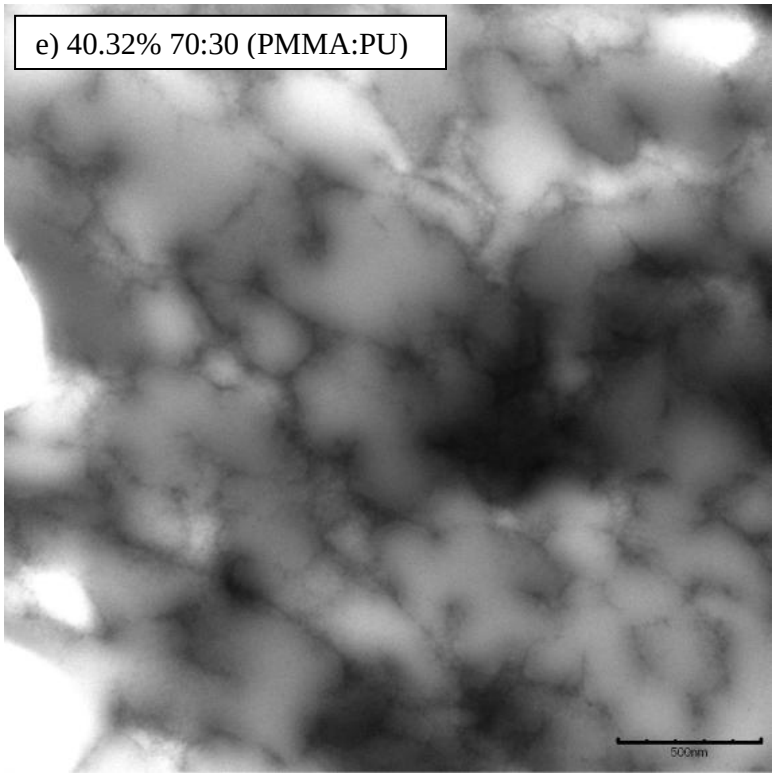

Figure IV-3. TEM photos of IPNs (PMMA:PU) containing 650g/mol PTMG with flexibilities of a) 19.35% (80:20), b) 19.35% (70:30), c) 30.65% (80:20), d) 40.32% (80:20), and e) 40.32% (70:30)

By comparing the 80:20 (PMMA:PU) samples in Figures IV-3-a, c, and d, when more diol and less triol were included and the percentage of chain flexibility increased, the domain size of the PMMA became larger, corresponding to a less dense PU network. This is logical since having less of the cross-linking agent, triol, would theoretically allow more space for the PMMA to occupy. Concurrently, with more diol included in the IPN, the larger the "mesh holes" became, allowing the accommodation of more PMMA within the PU network. Having such distinct phases in large domains suggests phase separation was present in the 80:20 (PMMA:PU) IPNs. Dadbin and Frounchi noted with their simultaneous IPNs that heterogeneity in their TEM photos correlated to phase separation, which is what was also observed with the TEM photos shown in Figure IV-3 [95].

Furthermore, when the degree of chain flexibility increased, the PMMA domains seemed to interconnect more than when the PU chain flexibility was lower. It is possible that the increase in flexibility allowed the PMMA domains to swell the PU phase in a manner so that the domains were able to be less separate.

Another interesting feature to mention is the drastic change in the network morphology between the Figures IV-3d and IV-3e, which show 40.32% 80:20 and 70:30 (PMMA:PU), respectively. The network for the sample with more PU present is much more open compared to the IPN with less PU.

The differences in the network morphology in these photos indicate that just by changing the diol and triol amounts in the PU system, it is possible to manipulate the final network morphology of the IPNs. In order to further explain the phenomenon taking place, swelling experiments were conducted.

Swelling experiments were possible in this research since both polymeric phases were cross-linked, similar to the previous studies. It is generally known that linear and branched polymers can be completely dissolved to form homogeneous solutions; on the other hand, cross-linked networks will only swell in compatible liquids [100]. So for this experiment, both the PU and PMMA networks could, for the most part, swell in a solvent without degrading or dissolving. Even pure PU was able to swell since it was synthesized specifically to be a three-dimensional, cross-linked network. When immersed in THF, in a few hours, pure cross-linked PU and IPN

samples expanded to about twice their original sizes. In fact, many samples tripled in size over a period of a few days. Experimental results can be seen in Figures IV-4 and IV-5, where Figure IV-4 shows the swelling of pure PU samples of different diol:triol ratios, or chain flexibilities, and Figure IV-5 shows IPNs that had a 30.65% chain flexibility in the PU network with varying amounts of PMMA:PU.

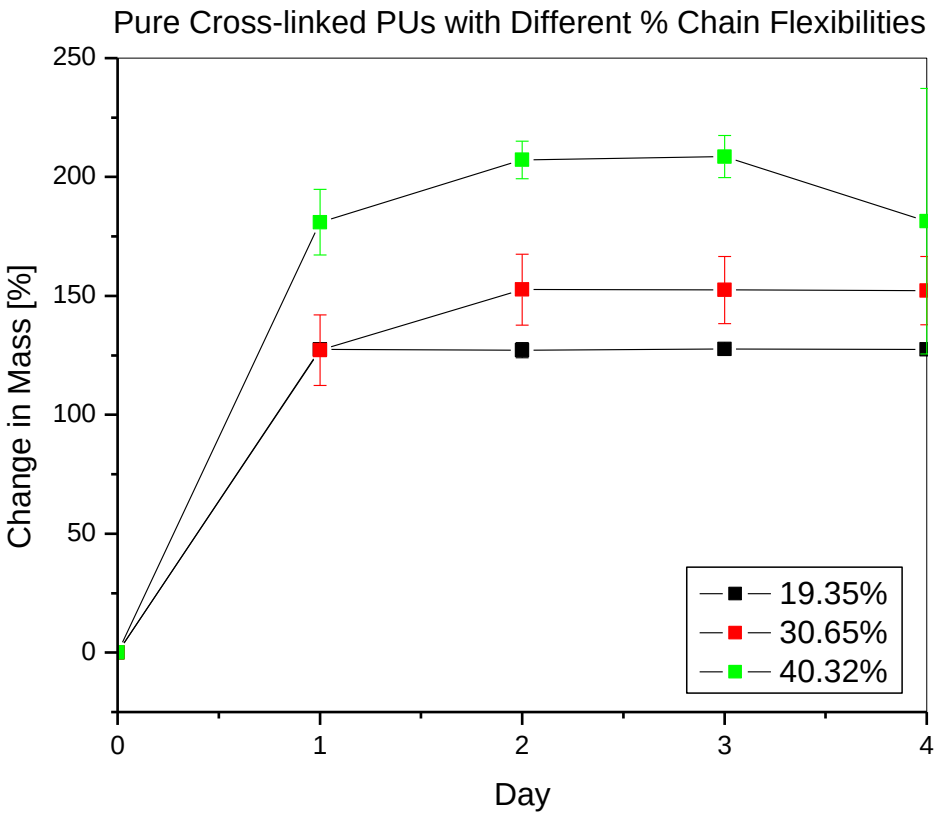

Figure IV-4. Swelling experiments of pure cross-linked PU samples with different percentages of flexibility

Looking at the figure above, it can be seen that the PU network with more diol present, or with a higher percent chain flexibility, was able to swell much more than the network with more triol

present. This was expected since having more of a flexible network present should allow more of the solvent to penetrate within the IPN.

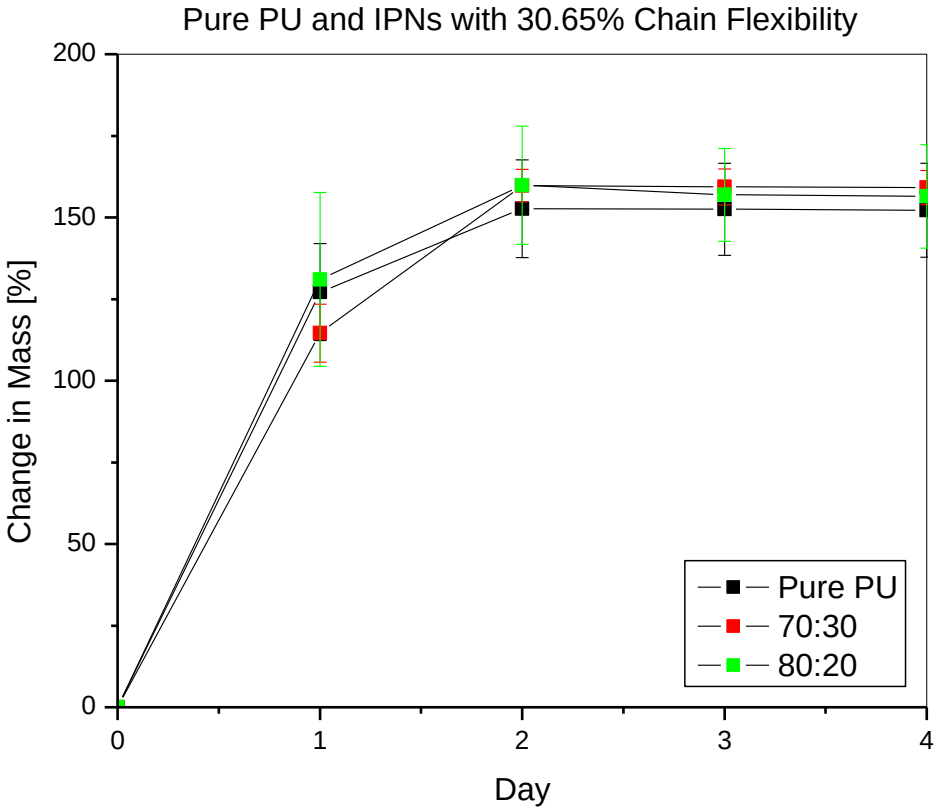

Figure IV-5. Swelling experiments of IPNs samples consisting of 30.65% chain flexibility with varying amounts of PMMA:PU

Figure IV-4 shows for IPNs with 30.65% flexibility that after the second day of being submerged in THF, swelling equilibrium was reached. IPNs containing more PU in the system could swell, to some extent, more than samples with less PU. This may be caused by the inherent characteristics of PMMA and PU materials; PU is a more flexible material and PMMA is rigid. Having more of the flexible phase in the IPN would mean the IPN would be able to swell more when immersed in a solvent. A summary for all pure cross-linked PU and IPN samples and their

respective highest percent change in mass, molecular weight between cross-links, and their cross-link density can be seen in Table IV-2.

Table IV-2. Highest percent change in mass, molecular weight between cross-links, and cross-link density for pure cross-linked PU and IPN samples

Sample (PMMA:PU)	Highest % Change in Mass	Molecular Weight between Cross-links [g/mol]	Cross-link Density [g/mol]
19.35% (0:100) – Pure PU	129.26 ± 0.18	129.77	4.84×10^{21}
19.35% (70:30)	156.00 ± 20.80	258.84	2.54×10^{21}
19.35% (80:20)	148.00 ± 25.55	258.10	2.37×10^{21}
30.65% (0:100) – Pure PU	153.05 ± 14.60	163.27	3.78×10^{21}
30.65% (70:30)	160.13 ± 5.08	473.80	1.51×10^{21}
30.65% (80:20)	159.95 ± 18.02	371.11	1.83×10^{21}
40.32% (0:100) – Pure PU	208.88 ± 8.97	443.16	1.34×10^{21}
40.32% (70:30)	210.94 ± 1.64	514.70	1.33×10^{21}
40.32% (80:20)	45.81 ± 0.67	15.33	4.15×10^{22}

As seen in Figure IV-5, the highest swelling for samples of different chain flexibility in Table IV-1 was exhibited by samples with 30 wt% PU, even more than pure cross-linked PU. This may be attributed to the PMMA disrupting the network of the PU phase, therefore allowing more spacing within the IPN network. This translates into the THF solvent being able to penetrate into the IPN network more than the pure cross-linked PU network. Additionally, for most cases, these IPN samples had the highest molecular weight between cross-links and the lowest cross-link density.

The swelling results can be related to the TEM pictures shown earlier; the system with 40.32% flexibility had larger PMMA domains where the THF could also penetrate. With the smaller, denser network of 30.65% flexibility, less THF would be able to penetrate into the domains within the PU network.

Figure IV-6 shows TEM images of 80:20 (PU:PMMA) IPNs of either 19.35% or 30.35% chain flexibility before and after they were swelled with THF.

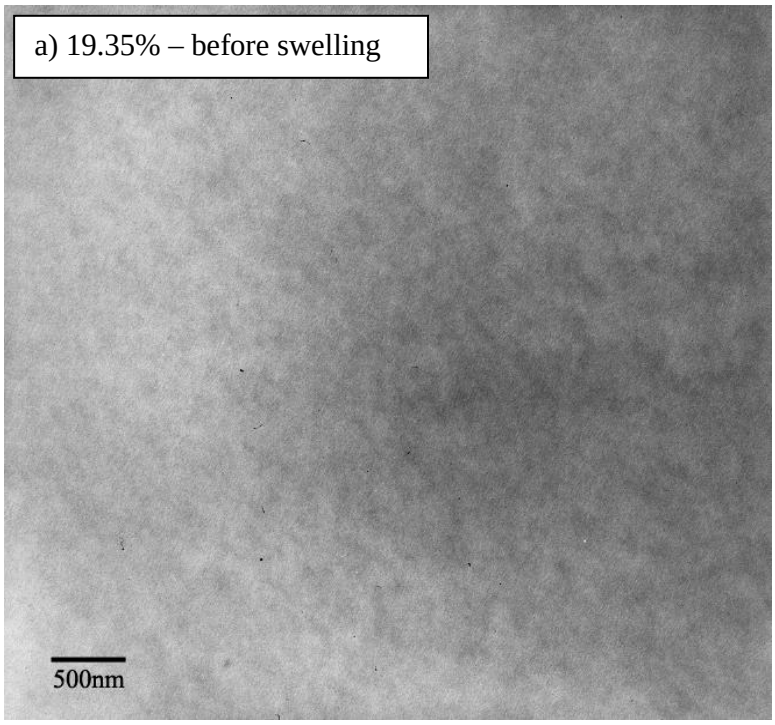

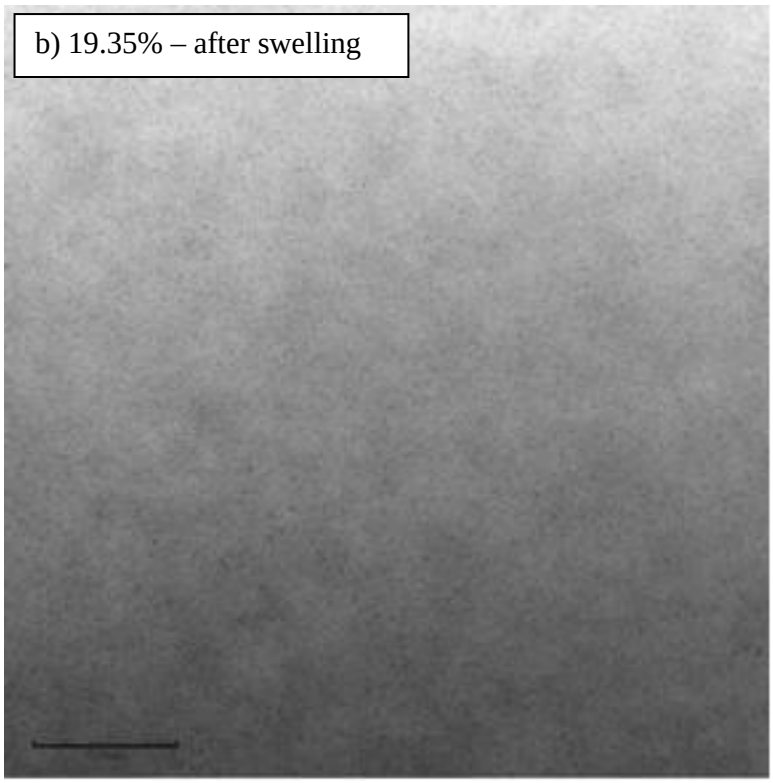
b) 19.35% – after swelling

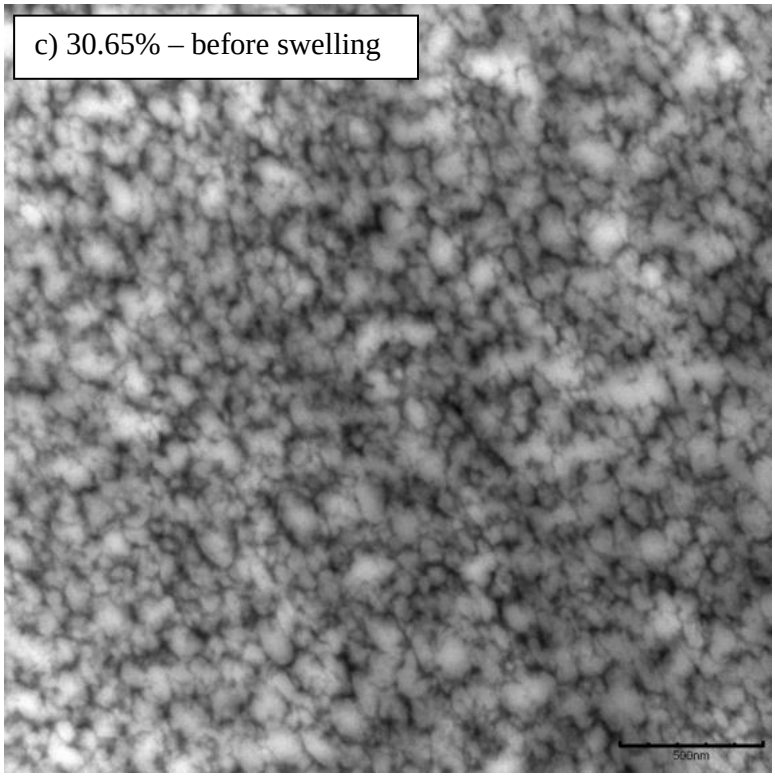
c) 30.65% – before swelling
500nm

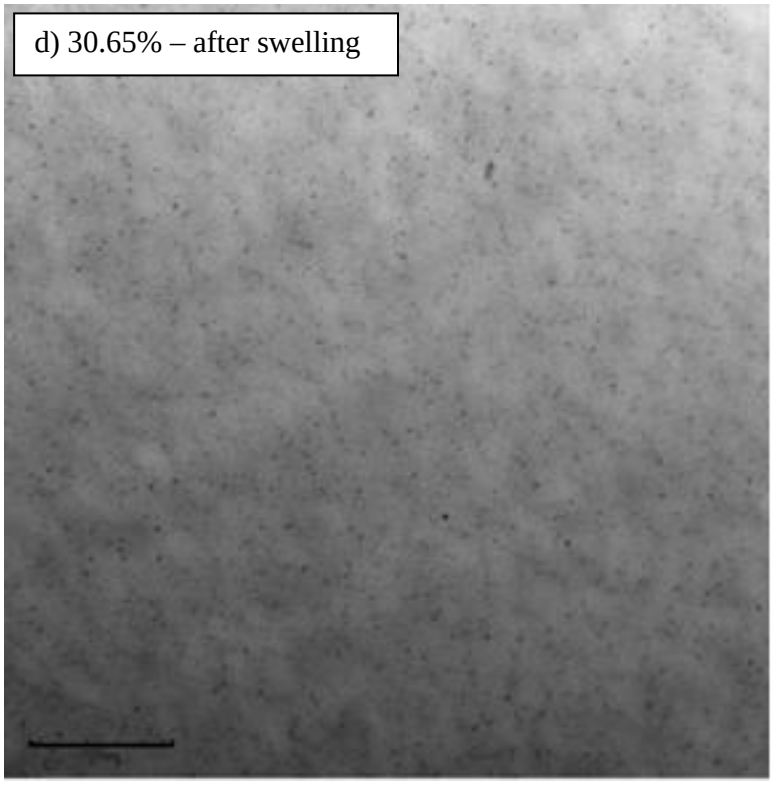

Figure IV-6. TEM photos of 80:20 (PMMA:PU) IPNs containing 650g/mol PTMG with flexibilities of a) 19.35% before swelling, b) 19.35% after swelling, c) 30.65% before swelling, and d) 30.65% after swelling

Figures IV-6-a and IV-6-c, which are 80:20 (PMMA:PU) IPNs with 19.35% and 30.35% chain flexibility, respectively, were shown earlier in this chapter. When comparing the two pictures with 19.35% chain flexibility, Figures IV-6-a and IV-6-b, no prominent change was observed.

On the other hand, when the photos of the 30.35% chain flexibility, Figures IV-6-b and IV-6-d, were compared, there was a drastic change in the morphology of the sample. The IPN appeared to have transitioned from a continuous network of PU with PMMA domains to a network consisting of PMMA with very small PU domains. It is possible that the PU network was not completely interlocked with the PMMA phase, which explains why it was able to swell so much compared to samples with 19.35% chain flexibility. This lack of interlocking would have

allowed some of the PU phase to be extracted during swelling with THF so that small globular structures would have formed within the PMMA network. If this mechanism occurred, then phase separation would have taken place and perhaps been the reason why the samples with 30.35% and 40.32% chain flexibility were able to swell to a higher degree than samples with 19.35% chain flexibility.

Thermo-mechanical Characteristics

Another property that was studied was the thermo-mechanical behavior of pure cross-linked PU samples as well as IPNs. Figure IV-7 shows the glass transition temperature, T_g, of pure PU specimens with varying amounts of diol:triol ratios. As expected, as the flexibility of the network increased, the T_g of the PUs decreased. Since a PU with a higher amount of diol will have a higher degree of flexibility, when studying the T_g, it should be expected that less heat would be needed to reach the rubbery phase than PU samples with less diol and more triol.

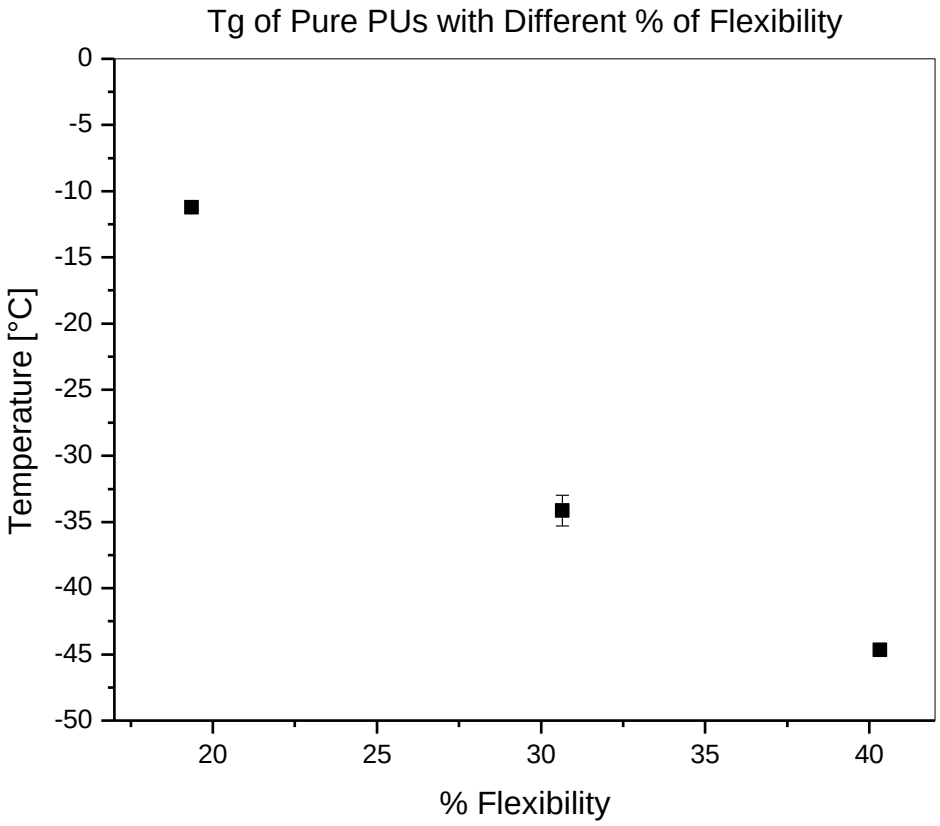

Figure IV-7. T_g values of pure cross-linked PU samples consisting of different percentages of flexibility based on diol:triol ratios

On the other hand, when PUs of different flexibilities were used in the making of IPNs, samples with PU consisting of more diol had a higher T_g than those with less diol. This trend can be seen in Figure IV-8. Perhaps this is due to the final network morphology of the IPN. When fewer but larger domains of PMMA form, this could raise the T_g of the IPN, compared to when more, smaller domains form. This T_g may also correspond more with the PMMA since increasing the chain flexibility showed increased phase separation. This phase separation may lead to higher T_g values that correlate to the PMMA phase.

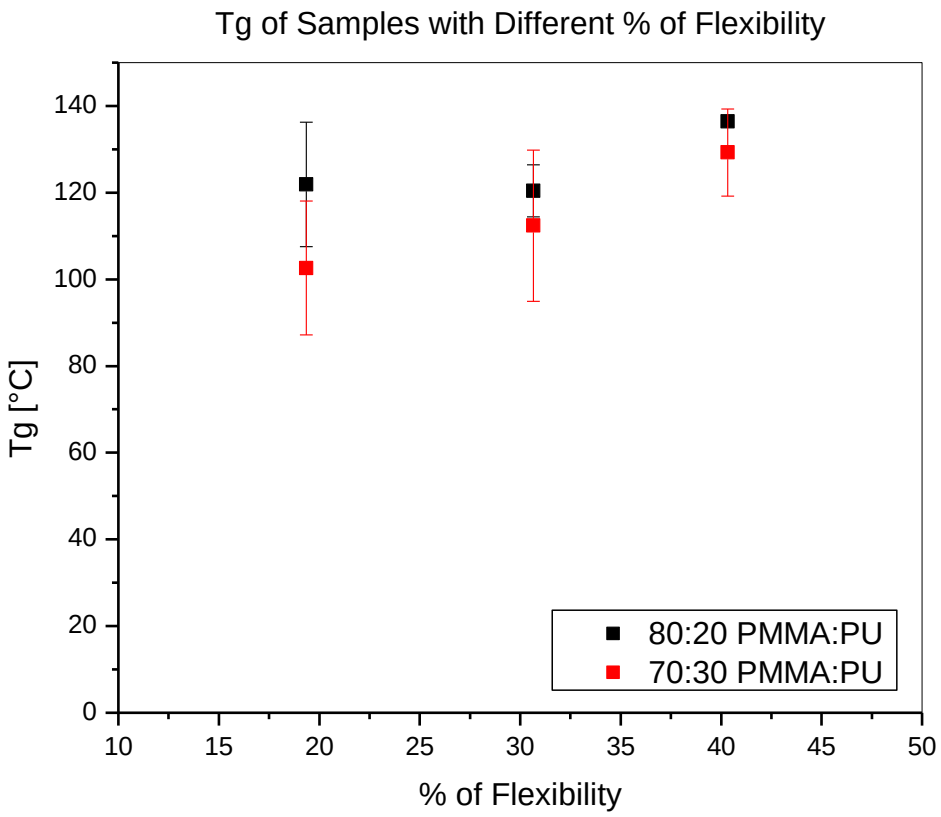

Figure IV-8. T_g values of 80:20 and 70:30 (PMMA:PU) IPN samples consisting of different percentages of flexibility based on diol:triol ratios .

The E' values of IPNs at approximately room temperature with different flexibilities can be seen in Figure IV-9. Samples consisting of 80:20 (PMMA:PU) were in the range of $6x10^8 – 8x10^8$ Pa, and samples consisting of 70:30 (PMMA:PU) were in the range of $2x10^8 – 8x10^8$ Pa. Those samples with less PMMA and more PU present were generally lower in stiffness than samples with more PMMA. However, when looking at the same ratio of PMMA:PU, the stiffness did not show significant difference when different flexibilities, or amounts of diol, were included.

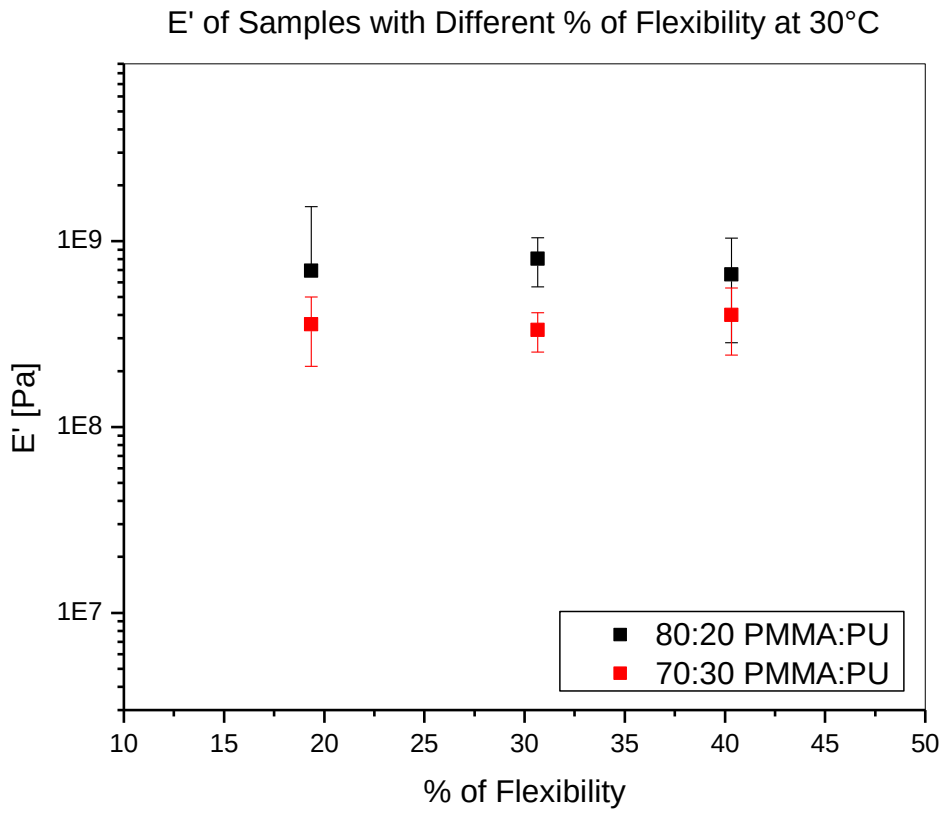

Figure IV-9. E' values at 30°C of 80:20 and 70:30 (PMMA:PU) IPN samples consisting of different percentages of flexibility based on diol:triol ratios

DSC analysis was used to give enlightenment behind the trends of the T_g and E' of the IPN samples. Generally, increasing the flexibility of a network phase should therefore increase the flexibility of the whole IPN. However, by using a modulated DSC program for observing the samples, it was found that cold crystallization was present, which may have affected the thermo-mechanical properties.

A modulated DSC (MDSC) analysis involves the same linear heating mechanism as in conventional DSC analysis, but a sinusoidal heating mechanism is also used. Using the

sinusoidal heating mechanism in MDSC analysis allows the heat flow to be determined by heat capacity and kinetic components. When only using conventional DSC, only the sum of these components can be observed [108]. The heat capacity and kinetic components are sometimes referred to as the reversible and nonreversible thermal events. Reversible thermal events include T_g and melting. On the other hand, nonreversible thermal events can include oxidation, curing, relaxation and cold crystallization (T_{cc}) [109].

Polymeric samples, such as poly(ethylene terephthalate) (PET), are cooled quickly where they remain amorphous materials. When these materials are reheated above the glass transition temperature, and cooled slowly, crystallization will occur. This crystallization, referred to as a cold crystallization, is different from melt crystallization, and it can be monitored using MDSC [110, 111]. Table IV-3 shows the cold crystallization temperatures and correlating heat flows for pure cross-linked PUs and IPNs of varying chain flexibilities obtained from MDSC analysis.

Table IV-3. Cold crystallization temperatures and correlating enthalpies for pure, cross-linked PU and IPNs with different chain flexibilities

Sample	Chain Flexibility	Ratio	T_{cc} [°C]	ΔH [J/g]
Pure cross-linked PU	19.35%	0:100	-	-
	30.65%	0:100	-	-
	40.32%	0:100	-3.93	8.75
IPN	19.35%	70:30	-	-
		80:20	-	-
	30.65%	70:30	Not tested	Not tested
		80:20	26.94	4.71
	40.32%	70:30	22.02	42.26
		80:20	24.12	32.59

This cold crystallization could be the factor that raised the storage modulus for the IPNs when the chain flexibility increased. Having cold crystallization present could make the materials more rigid. Looking at Table IV-3, only those samples with a high chain flexibility experienced cold crystallization. This may be due to the presence of an increased amount of cross-links in the samples with lower chain flexibilities since these could act as restrictions for crystalline regions to form. A schematic of how these crystalline regions may appear can be seen in Figure IV-10.

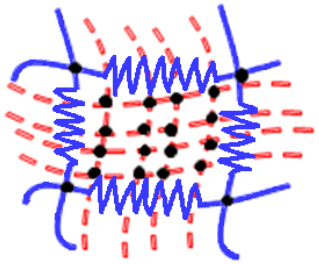

Figure IV-10. Schematic showing the formation of crystalline regions in a cross-linked network

Despite little change in E' values, impact resistance of the material may still be affected by flexibility. The material may be rigid during normal conditions, but during times when the material is struck, such as in high-impact scenarios, it may be possible that the morphology of the network will contribute to impact absorption.

Optical Characteristics

Another important aspect focused on in this research was the transparency of the IPNs. Studies using a UV-vis can be seen in Figure IV-11. Commercial PMMA was close to 100% transparency, and IPN samples of different diol:triol ratios were relatively high, although not quite as high as PMMA.

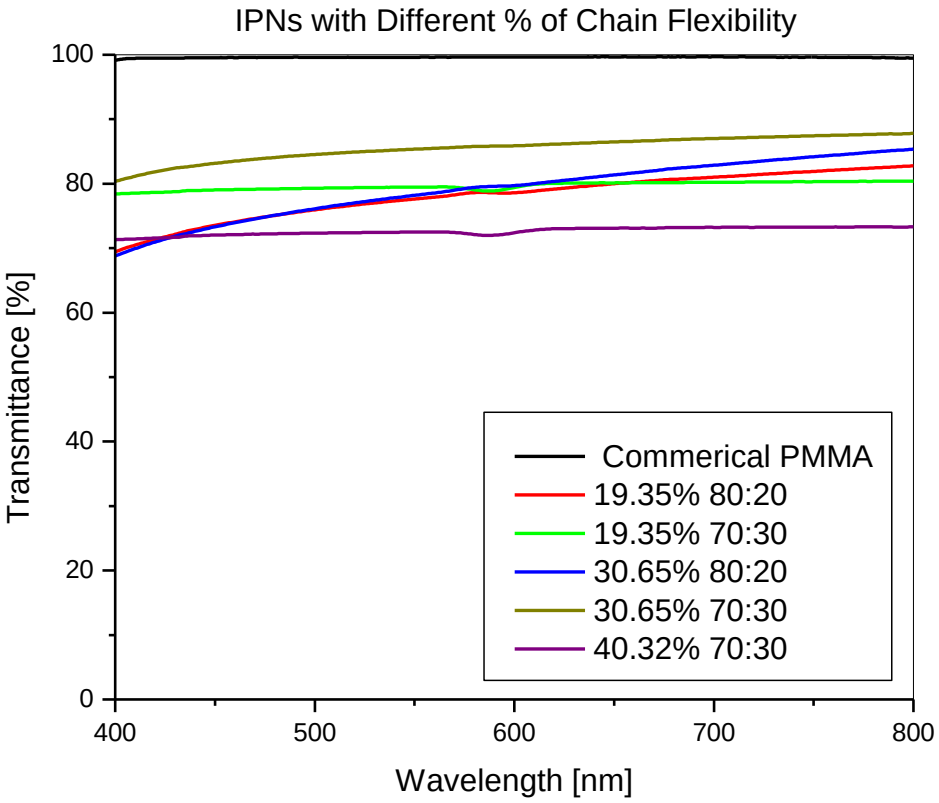

Figure IV-11. UV-vis analysis of IPNs consisting of different chain flexibilities

Looking at Figure 1V-11, it appears that samples with the 19.35% and 30.35% chain flexibility had the highest transparency values, and the 40.32% IPN with 70 wt% PMMA exhibited the lowest transparency. This can be attributed to the increase in phase separation with a higher chain flexibility, which was observed from the TEM photos.

Conclusions

In this study, several IPNs were synthesized with varying amounts of diol and triol in the PU phase. By doing this, the morphological structure was modified, and so were the subsequent

physical and thermo-mechanical properties. When more of the diol, the linear portion of the chain, was present, the network became more flexible and the domain sizes became larger, as evidenced by the TEM photos. Swelling experiments also showed a change in the structure when different amounts of diol and triol were included.

Despite the small change in E', the storage modulus showed a relatively high stiffness and offers room for improving impact resistance without drastically comprising the rigidity of the IPN. Additionally, the transparency of these samples was also high, a necessary characteristic for window-like applications.

CHAPTER V

GRAFT-INTERPENETRATING POLYMER NETWORKS WITH POLYURETHANE AND A METHACRYLATE-BASED COPOLYMER

Introduction

In this final part of the research, a different approach was taken for increasing miscibility between the polymer phases during the synthesis of transparent IPNs that would be suitable for impact-resistant applications. Instead of synthesizing a full-IPN, graft-interpenetrating polymer networks (graft-IPNs) and their effects on the morphological, thermo-mechanical, impact, and optical properties were created and studied.

Graft-Interpenetrating Polymer Networks

Graft-IPNs can be considered as full- or semi-IPNs, but what make these materials particularly unique are the additional cross-links between the two different polymer network phases. In other words, at certain points throughout the IPN network, cross-link points chemically connect the two polymers together. Full- and semi-IPNs do not have these extra chemical cross-links between the polymer phases; rather, there exist only physical entanglements with each phase intertwined with the other. An illustration of a graft-IPN can be seen in Figure V-1.

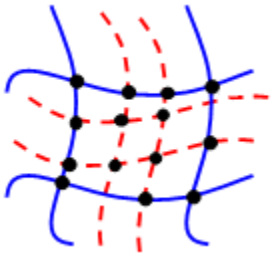

Figure V-1. A graft-IPN with cross-links connecting both-phases

The main aspiration of this study was to decrease the phase separation that had been previously observed with some of the IPNs with PU and PMMA in earlier experiments, especially those with a higher amount of PMMA present or a higher molecular weight diol in the PU phase. As discussed before, due to thermodynamic and kinetic differences between polymer networks, incompatibility between the constituent networks will result in decreased miscibility, increased phase separation, and lower properties [112]. It has been found that grafts induced into IPNs, may act as compatibilizers between two polymeric phases of differing characteristics. When a grafting reaction is included in an IPN synthesis, phase separation may decrease or even become non-existent. The decrease in phase separation could improve several factors, such as interfacial bonding, miscibility, and the interpenetration of the networks, thus improving physical and mechanical properties [113].

Other researchers have also looked into using graft-IPNs to enhance currently existing materials. Huang and Zhang, along with the rest of their research group, have looked into creating graft-IPNs using chitosan and polyurethane. These materials exhibited good mechanical properties, and they were biodegradable. They have also looked into graft-IPNs consisting of nitrolignin

and polyurethane with different NCO/OH molar ratios, and they discovered that they could improve the strength and toughness of the materials [114].

Graft-IPNs involving epoxies is of major interest, since pure epoxy can be brittle, therefore lacking good mechanical properties, such as impact strength, resistance to crack propagation, and elongation at break [115]. Sung and Lin have attempted linking epoxy (diglycidyl ether of bisphenol A or DGEBA) matrices with polydimethylsiloxane (PDMS) to form graft-IPNs [116]. Although they did not find initial success improving mechanical properties, compared to the pure epoxy, due to major incompatibility before network formation, they later found that adding a third component, polypropylene glycol (PPG), can increase the phase homogeneity throughout the IPN. In fact, having three networks present at once not only showed better homogeneity than graft-IPNs consisting of just epoxy/PPG or epoxy/PDMS, but it also increased damping properties [117].

Other research groups have studied graft-IPNs with epoxy, and DGEBA appears to be an extremely popular epoxy to include. For instance, Kostrzewa et al. have looked into graft-IPNs consisting of DGEBA and PU. They too were able to synthesize materials that lacked phase separation and enhance the mechanical properties based on pure DGEBA [115].

Hsieh et al. have also used DGEBA to create graft-IPNs with urethane-modified bismaleimide (UBMI), and they found materials with poly(butylene adipate)-based PUs exhibited improved Izod impact strength than pure DGEBA. On the other hand, graft-IPNs consisting of poly(oxypropylene)-based PUs exhibited an increase in fracture energy [118].

Even some researchers are going beyond synthesizing graft-IPNs by including additional reinforcement. Examples include Wang et al. who have studied graft-IPN composites consisting of PU and DGEBA with short carbon fiber and micro hollow glass beads. They found that damping properties and tensile strength could be improved upon with these fillers [119]. Furthermore, Lin et al. have studied the reinforcement of DGEBA/PU graft-IPNs with ultra high molecular weight polyethylene (UHMWPE) fibers [120].

In order to create a grafting synthesis during polymerization, like these research groups and many others, hetero-functional monomers or other chemical compounds are included as reactants in the IPN precursor. These chemicals should be able to react with multiple reactants so that different polymer networks will bind together [112]. For this research, cross-linking points were created between a hard phase consisting of a methacrylate-based copolymer and a soft phase, polyurethane, with one of the monomers in the copolymer phase having the ability to react with both polymer networks.

Bisphenol A Glycidyl Methacrylate and Triethyleneglycol Dimethacrylate Copolymer

Instead of using the previously synthesized PMMA from earlier chapters that would be unable to form cross-links with the PU phase, other methacrylate monomers were explored that had the capability of forming grafts. A copolymer resin commonly used in dentistry was found to be appropriate for this study: bisphenol A glycidyl methacrylate (BisGMA) and triethyleneglycol dimethacrylate (TRI-EDMA), sometimes also referred to as TEGDMA.

BisGMA is a long and rigid difunctional monomer that was invented in 1962 by Ray Bowen [121]. Since its discovery, it has been used as a dental resin due to its high molecular weight and mechanical properties [122]. One initial motivation why BisGMA was chosen for this research, that follows the reason why it is used in dentistry, was due to its structural features similar to that of polycarbonate (PC). PC has very high stiffness due to the two aromatic rings in its monomeric backbone chain [123]. BisGMA also has aromatic rings in its backbone and should therefore display similar stiffness properties. Figure V-2 shows the structures of BisGMA and a Lexan-version of polycarbonate synthesized with bisphenol A [124].

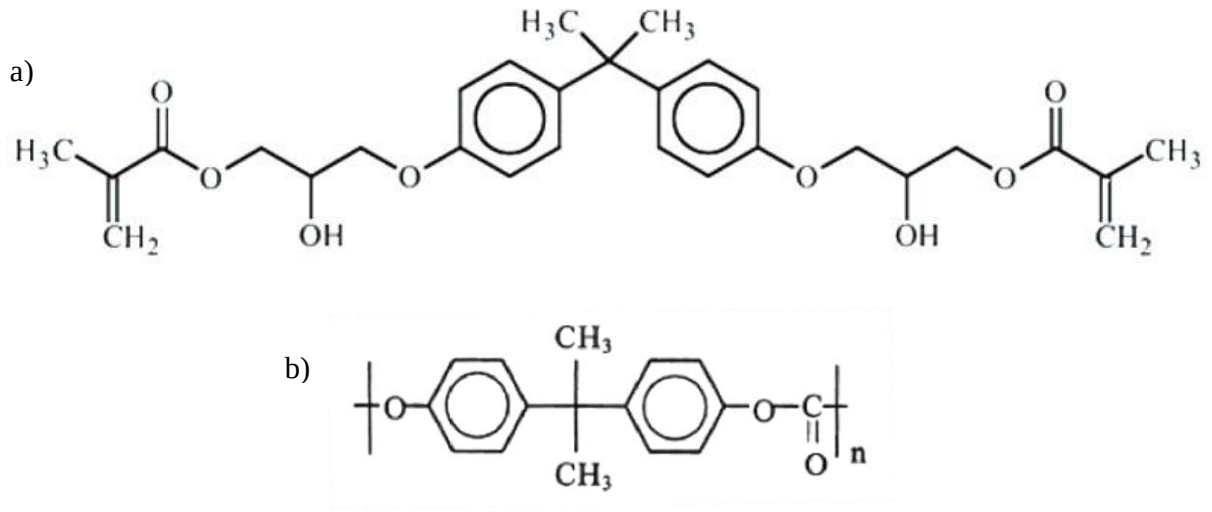

Figure V-2. Chemical structures of a) BisGMA [125] and b) polycarbonate [124]

Another major beneficial feature of BisGMA is its hydroxyl groups, which make it possible for this polymer to bond with the isocyanate groups in PU's backbone chain. The mechanism can be seen in Figure V-3.

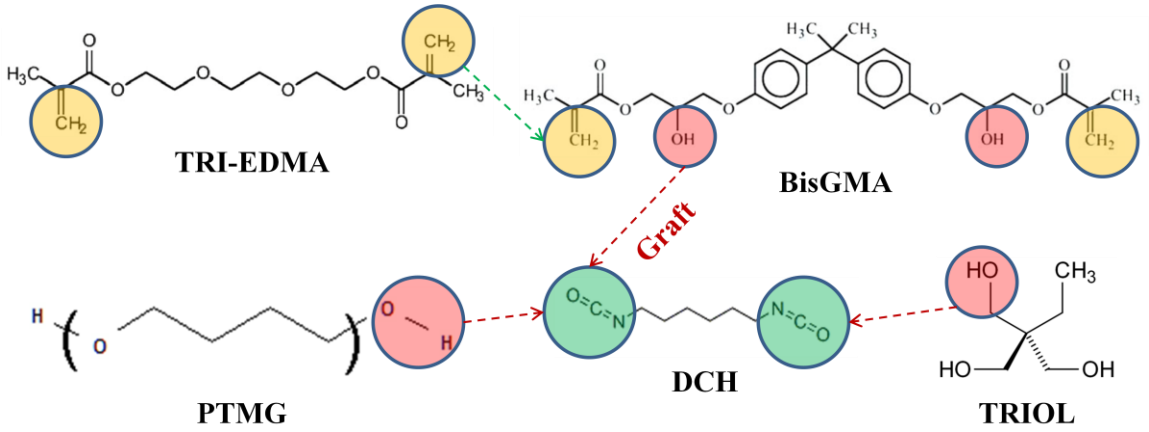

Figure V-3. Synthesis and mechanism of TRI-EDMA [126] and BisGMA [125] copolymer (hard phase) with PU (soft phase)

TRI-EDMA, which can also be seen in Figure V-3, is a lower molecular weight monomer that is commonly paired with BisGMA as a copolymer in dentistry to lower BisGMA's viscosity [121]. It was included in this research not only for this reason, but to also allow the ability to control how cross-linked the hard phase would be with the soft phase, or the PU. As seen in the figure above, not only will TRI-EDMA form a copolymer through its two reactive $=CH_2$ double bonds, but its two –OH groups can react with the –NCO groups in diisocyanatohexane (DCH), like the PTMG and TRIOL. Thus, TRI-EDMA will connect the methacrylate copolymer chain as well as the PU network.

Materials and Methods

Materials

The reactants used for the PU involved the same chemicals as the experiments reported in previous chapters. Two polyols were utilized, 1,1,1-tris(hydroxymethyl) propane (TRIOL) from Acros Organics (U.S.) and poly(tetramethylene ether) glycol (PTMG) from Sigma Aldrich

(U.S.). Three PTMGs were used: 650g/mol, 1400g/mol, and 2900g/mol. The equivalent weights used were 0.19eq TRIOL: 0.12eq PTMG: 0.31eq DCH for both diols, and calculations based on the equivalent weights were similar to those in Chapter III. Each diol was combined beforehand with TRIOL, and then the mixture was melted in an oven under a strong vacuum to remove residual moisture. The isocyanate and catalyst used were 1,6-diisocyanatohexane 99+% (DCH) from Acros Organics (U.S.), dibutyltin dilaurate, 98% (DD) distributed by Pfaltz & Bauer (U.S.), respectively. Ethyl acetate was still used as an analogue for the DD.

For the BisGMA and TRI-EDMA, both were used as delivered from ESSTECH, Inc (U.S.). Prior to experiments, a vacuum was pulled on BisGMA to remove residual moisture. The initiator used was 1 wt% benzoyl peroxide (BPO) from Fisher Scientific (U.S.).

In order to form cross-links between the copolymer phase (TRI-EDMA:BisGMA) and the PU phase, an excess amount of DCH was included in the graft-IPN precursor. The equivalent weights used were 1.0eq DCH:1.0eq BisGMA.

Methods

Copolymer samples simply involved mixing BisGMA and TRI-EDMA together, and then mixing in BPO once the viscosity of the copolymer precursor solution had substantially decreased. Curing involved placing the samples in an oven for 24 hours at 60°C and then another 24 hours at 80°C.

IPNs were synthesized by first mixing the PU and copolymer precursors separately. The BisGMA and TRI-EDMA monomers were mixed in one container, and once the viscosity had decreased, BPO was mixed into the solution. A diol and triol solution was mixed with DCH in a separate container. Following this the PU and copolymer precursors were combined; then DD was added to this solution. Curing took place at 60°C for 24 hours and 80°C for an additional 24 hours.

Several copolymer samples were synthesized with varying ratios of TRI-EDMA to BisGMA, namely 100:0, 75:25, 50:50, 25:75, and 0:100. For the graft-IPNs, three different sets of materials were synthesized: one set had a PTMG diol of molecular weight 650g/mol, and others had had a molecular weight of 1400g/mol or 2900g/mol. Table V-1 shows the ratios (by weight) used for synthesizing these materials.

Table V-1. Ratios (by weight) used for synthesizing graft-IPNs

Molecular Weight of PTMG	650g/mol	1400g/mol	2900g/mol
TRI-EDMA:BisGMA Ratio (Copolymer)	50:50	90:10	50:50
Copolymer:PU Ratio	95.24:4.76	90:10	95.24:4.76
	86.96:13.04	80:20	86.96:13.04
	71.43:28.57	70:30	71.43:28.57
	-	60:40	-

The copolymer consisted of a ratio between the TRI-EDMA and the BisGMA. This copolymer mixture was then used in different amounts with PU. For the sake of easy nomenclature, the

samples with 650g/mol and 2900g/mol will labeled as having the ratios of 95:5, 87:13, and 71:29 (Copolymer:PU).

Techniques

In order to study the thermo-mechanical properties, a TA Instruments RSAIII Dynamic Mechanical Analyzer (DMA) was used. The testing parameters followed involved: frequency of 1.0Hz, initial temperature between 25°-30°C (or lower temperature for liquid nitrogen), final temperature of 200°C, ramp rate of 5°C/min, and a strain of 0.1%.

Similar to the last chapter, the thermal properties of the graft-IPNs were also observed using a TA Instruments Q2000 Modulated Differential Scanning Calorimeter (DSC). The following procedure was used for analyzing samples: equilibrate at -80°C, modulate ± 1.00°C every 60 seconds, isothermal for 5 minutes, ramp 10.00°C/min to 250°C, ramp 10.00°C/min to -80°C, equilibrate at -80°C, isothermal for 5 minutes, ramp 10.00°C/min to 250°C, ramp 10.00°C/min to -80°C.

A UV-visible 2450 Spectrophotometer from Shimadzu Scientific Instruments was used to measure the transparency of the IPNs, and ambient air was used as the standard.

The density of the IPNs and pure PUs was determined by using a pycnometer at room temperature with distilled water. Studying the swelling behavior of the IPNs involved placing cut pieces of each sample into glass vials and submerging them in tetrahydrofuran (THF). The

masses of the samples were compared to their original masses at different time intervals. For both density and swelling experiments, the cut samples were placed in an oven at approximately 80°C for a couple hours so that any residual moisture would be removed.

Further studies on the morphology of the IPNS involved using a Zeiss EM 10C 10CR Transmission Electron Microscope (TEM). The sample preparation procedure was used for the TEM as described in previous chapters. Samples broken under liquid nitrogen sat in the dye for at least a week to ensure a sufficient amount would penetrate the materials, after which the samples were microtomed. Similar to the PMMA remaining clear after staining, the copolymer phase remained clear. The distinction between the clear copolymer phase and the dark PU phase enabled the study of the domain formation and phase separation processes for the IPN systems.

Results and Discussion

Instead of using PMMA, a completely new rigid phase was explored in this chapter. Thus, the first step in analyzing these new types of IPNs involved studying the rigid phase by itself, or in other words, only studying the copolymer consisting of BisGMA and TRI-EDMA.

Copolymer - Optical Properties

Copolymer samples were not analyzed with a UV-vis since the transparency and yellow color could be easily seen by the naked eye. Pure TRI-EDMA and pure BisGMA, along with copolymers with different ratios of these two components can be seen in Figure V-4. As can be seen in these photos, pure TRI-EDMA was extremely clear with no discoloration; however, upon

adding increasing amounts of BisGMA, a yellow color became darker, with BisGMA appearing the darkest. Additionally, all pure samples and copolymer samples were extremely transparent. This can be inferred by the printed colored image being discernable under the samples, as shown in the photos.

Figure V-4. Samples of a) pure TRI-EDMA, TRI-EDMA:BisGMA ratios of b)75:25, c)50:50, d) 25:75, and e) pure BisGMA

Copolymer - Thermal and Thermo-mechanical Properties

In order to obtain an understanding of the thermal properties of the copolymer, DSC was used to observe T_g values. However, as can be seen in Figure V-5, no major transitions could be observed for the samples.

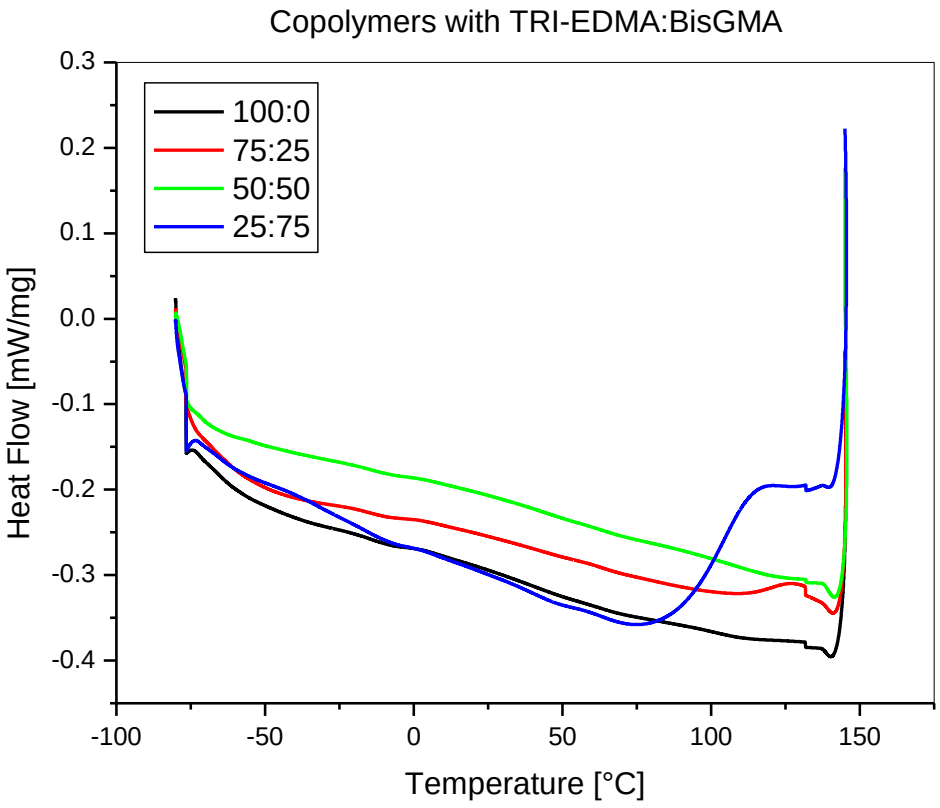

Figure V-5. DSC results of copolymers

Studying the graph above, there are no distinct peaks distinguishing the glass transition phase of the samples. From this, it was inferred that the T_g probably spanned a broad range due to two transition temperatures from both BisGMA and TRI-EDMA or different mechanisms of relaxation. Thus, the DMA was once again used to study the T_g. Test results from the DMA can be seen in Figure V-6.

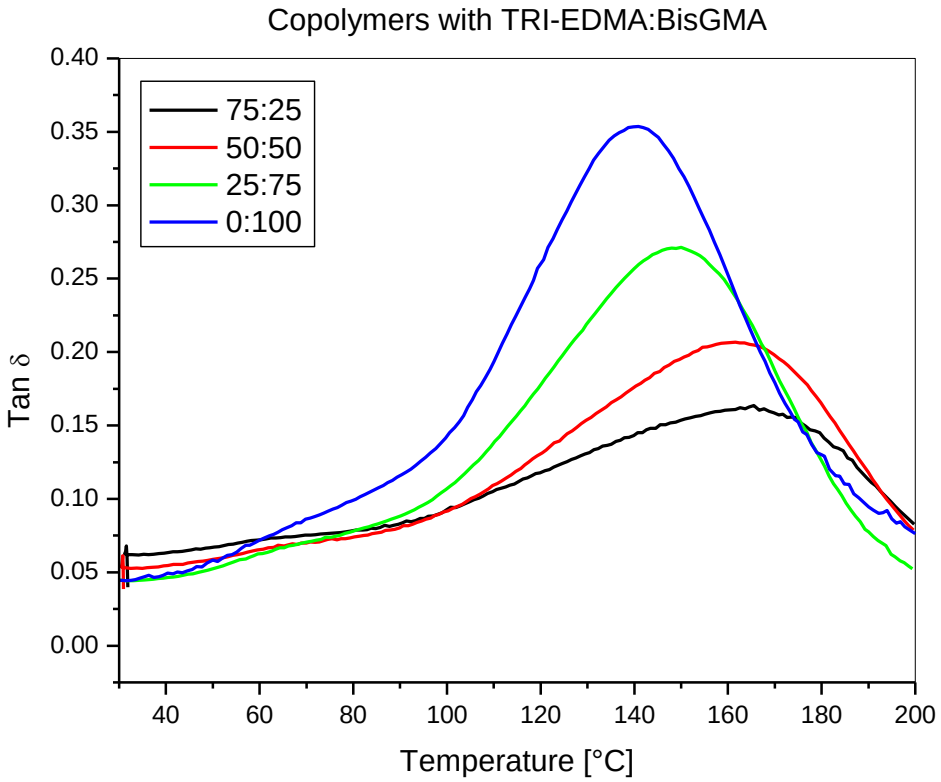

Figure V-6. Tan δ peaks of copolymers

As suspected, the T_g's of the different copolymers displayed wide-ranging peaks between 140-170°C. Although the peak of the pure BisGMA, labeled 0:100, also showed a relatively broad peak, it still had a more defined peak than the samples with increasing amounts of TRI-EDMA. The merging of the two T_g values of BisGMA and TRI-EDMA is the reason why no definitive peaks were observed with the DSC.

The pure TRI-EDMA could not be tested using 3-point bending due to its very brittle nature, but the T_g could still be estimated based on the shifts in the T_g for the copolymer systems. The T_g of TRI-EDMA was much higher than that of BisGMA, and this can be seen through the shifting of

the peaks to a higher temperature as more TRI-EDMA was included. Conversely, as more BisGMA was included in the copolymers, the T_g of the samples shifted to a lower temperature, closer to pure BisGMA.

Another aspect that should be mentioned is the fact that a copolymer must have formed since only one T_g peak can be observed. Had two peaks been present after performing DMA tests, this would have indicated that phase separation had occurred; however, only one peak for each copolymer is evident, and therefore, one heterogeneous polymer chain was synthesized.

The DMA was also used to investigate the storage modulus of the pure BisGMA and different copolymers. These results can be seen below in Figure V-7. Noted before, 3-point bending was not possible for the pure TRIEDMA due to its extreme brittleness.

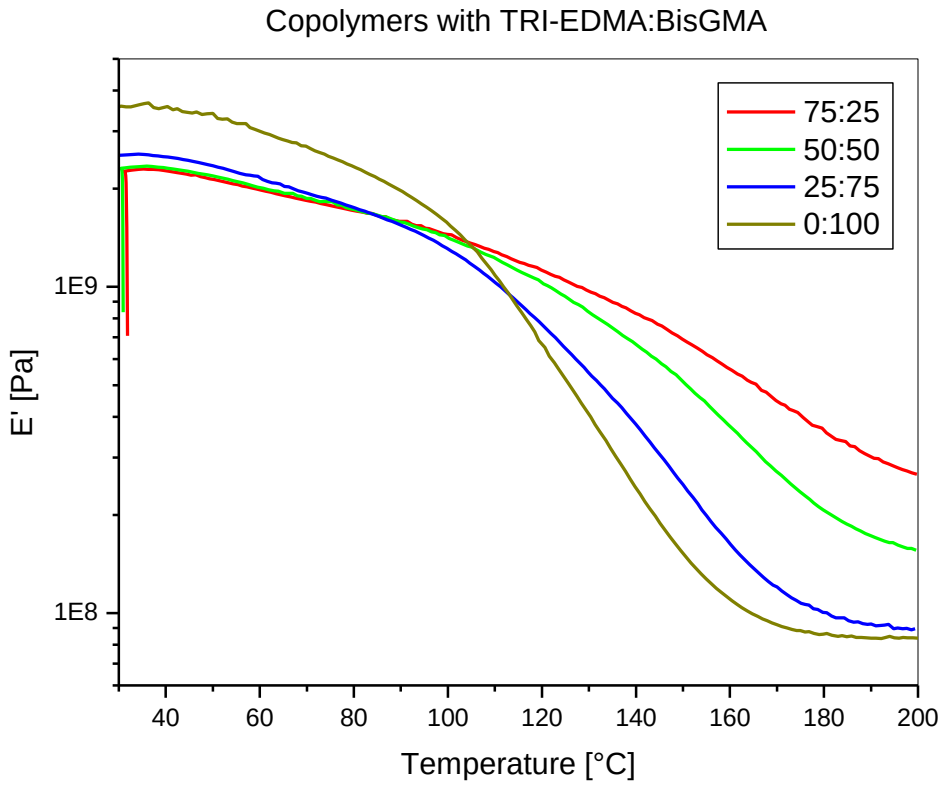

Figure V-7. E' values of copolymers and pure BisGMA

At lower temperatures, E' values were between 1.5-3.5 GPa. Furthermore, BisGMA exhibited a higher E' than the copolymer systems, but at higher temperatures, the E' was lower than the copolymers'. The same phenomenon can be seen when looking at only at the copolymers. When there was more BisGMA present, the initial value of E' at lower temperatures was higher, but at an increased temperature, the value of E' fell below those samples with less BisGMA and more TRI-EDMA. This is due to the glass transition temperature of each phase. At lower temperatures, BisGMA contributes more to the high stiffness than TRI-EDMA, and thus the E' of samples with more BisGMA present have a higher modulus. However, at higher

temperatures, after BisGMA's T_g and before TRI-EDMA's T_g, the high stiffness of the copolymers can be attributed more to the TRI-EDMA phase.

Copolymer - Morphology

For gaining a better understanding of the morphology and the cross-link density of the copolymer samples and pure BisGMA, the following equation was used to calculate the number of active chains [60]:

$$E' = 3nRT \qquad \text{Equation V-1}$$

'E'' is the modulus at temperature, 'T', 'R' is the gas constant, and n the number of active chains. For these calculations, the temperature used for 'T' was 200°C, or 473.15K.

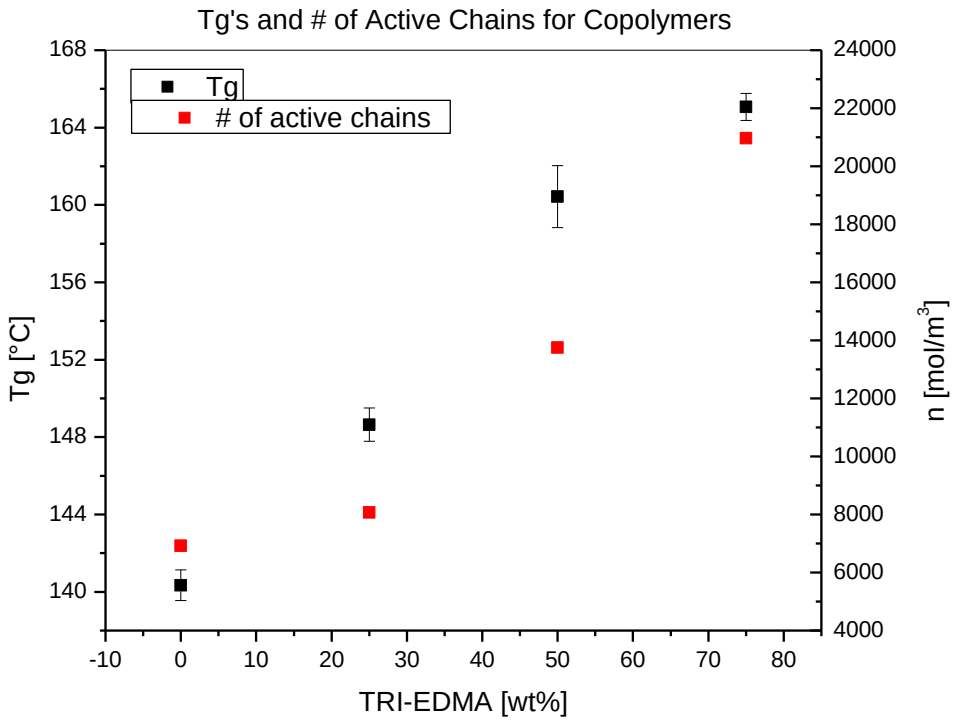

Figure V-8. T_g's and number of active chains for copolymers

It is understood that in a perfectly cross-linked network, every chain emanates from one cross-link point and joins another cross-link point [127]. In other words, there are no chains left unreacted and dangling, and no chains loop back around to have both ends emanating from the same cross-link. Equation V-1 is used to determine this kind of best-case-scenario where all chains have ideally reacted and are therefore, active chains.

Having a higher number of active chains corresponds to a higher degree of cross-links because more chains would have joined more cross-link points. Looking at Figure V-8, it appears that when there is more TRI-EDMA and less BisGMA present in a copolymer, there is a higher degree of cross-linking because the calculated number of active chains is higher. This follows

the trends observed from DMA experiments. Samples with more TRI-EDMA present had higher E' values at higher temperatures (seen in Figure V-7), and had higher T_g's. The high cross-link densities must have contributed to the stiffness of the materials and also raised the energy needed for the copolymers to transition from the glassy phase to the rubbery phase.

After studying the copolymer phase, the addition of polyurethane was investigated. Further studies with PU involved copolymers with the ratios of 50 wt% TRI-EDMA and 50% BisGMA. This copolymer ratio displayed high thermo-mechanical properties as well as transparency with slight yellowing. Since previous studies mainly involved using a PTMG of molecular weight 650g/mol, initial experiments also included this reactant. Later experiments included PTMGs with molecular weights of 1400g/mol and 2000g/mol.

Graft-IPNs with 650g/mol PTMG - Optical Properties

The addition of PU proved to affect the optical, morphological, thermo-mechanical, and mechanical properties of pure copolymer. For instance, when increasingly more amounts of PU was added to the TRI-EDMA:BisGMA copolymer in a graft-IPN, the transparency significantly decreased. This phenomenon can be seen in Figure V-9, where 100:0 is the pure copolymer consisting of 50:50 (TRI-EDMA:BisGMA).

When approximately 5 wt% PU was present in the graft-IPN, the transparency in the visible light region had a transmission value of about 90%, compared to commercial PMMA which had a transmission value of 100%. However, when approximately 29 wt% of PU was present in the graft-IPN, the transmission value dramatically decreased to half the value of commercial

PMMA. These results suggest that phase separation may have been present in the graft-IPNs when more PU was included. It has been observed in earlier chapters that if a sample has a low transmission value, this stems from poor intermolecular penetration of the networks.

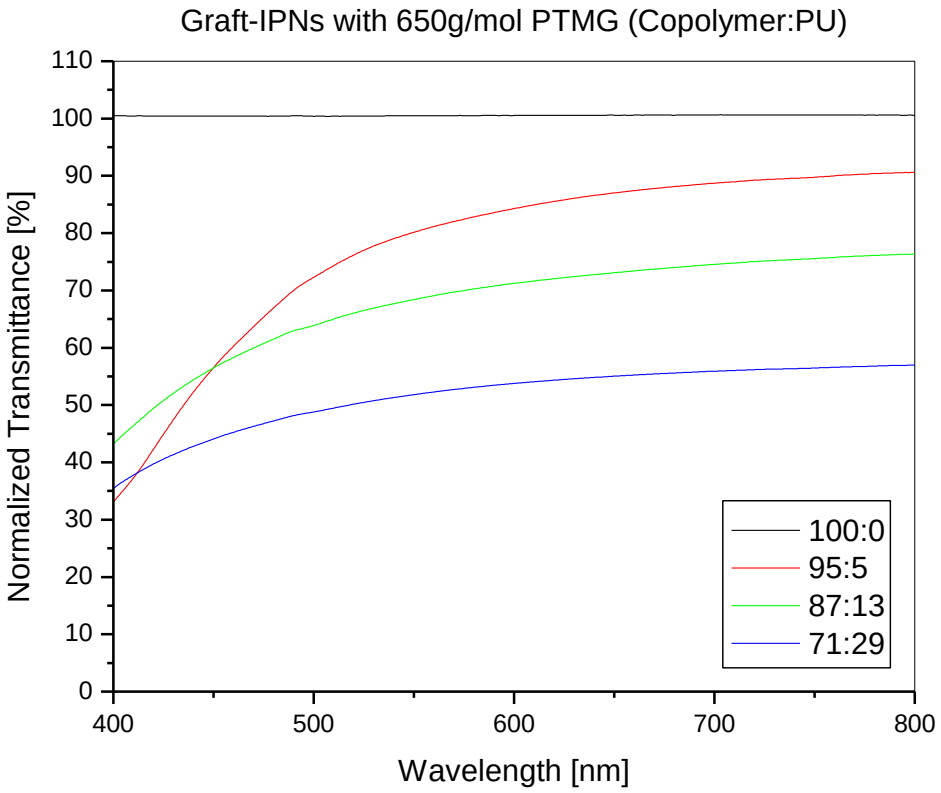

Figure V-9. UV-vis analysis of graft-IPNs with different copolymer:PU ratios and 650g/mol PTMG

In order to gain a better understanding of why the transparency was lower when more PU was added, the thermo-mechanical and mechanical properties were investigated.

Graft-IPNs with 650g/mol PTMG - Thermo-mechanical Properties

Figure V-10 shows pure copolymer (TRI-EDMA:BisGMA) and graft-IPNs with different amounts of PU. It appears that when more PU was included in the IPN, E' decreased. This was expected since having more of the rubbery phase and less of the rigid phase present should lower the overall stiffness of the samples.

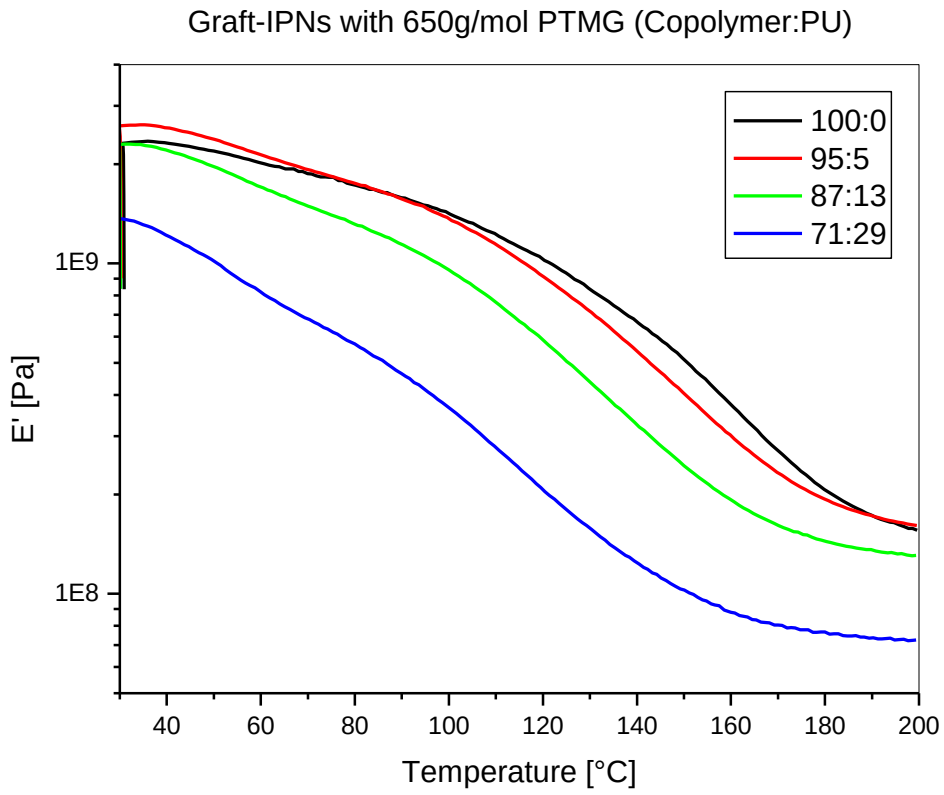

Figure V-10. E' of pure copolymer and graft-IPNs with 650g/mol PTMG

The tan δ curves from DMA testing can be seen in Figure V-11. With increasing amounts of PU, the T_g decreased from approximately 160°C to 120°C. This, too, was expected as this trend has been seen in Chapter II. Since PU is the soft, rubbery phase, the glass transition temperature would be much lower than that of a stiff, rigid phase such as a copolymer consisting of resins

TRI-EDMA and BisGMA. With more of the copolymer present, the higher the T_g will be, but more PU present the more the tan δ peak will shift to lower temperatures.

It is interesting to note that phase separation was not apparent for graft-IPNs since there were not two distinctive peaks corresponding to the different networks. Although there is a slight peak in all the graft-IPN materials, this probably corresponds to the BisGMA since a similar peak can be seen in the pure copolymer sample. Phase separation may not have played a role in decreasing the transparency; perhaps simply adding more of a less transparent material, such as an elastomeric PU may have simply decreased the transparency of a more transparent rigid phase.

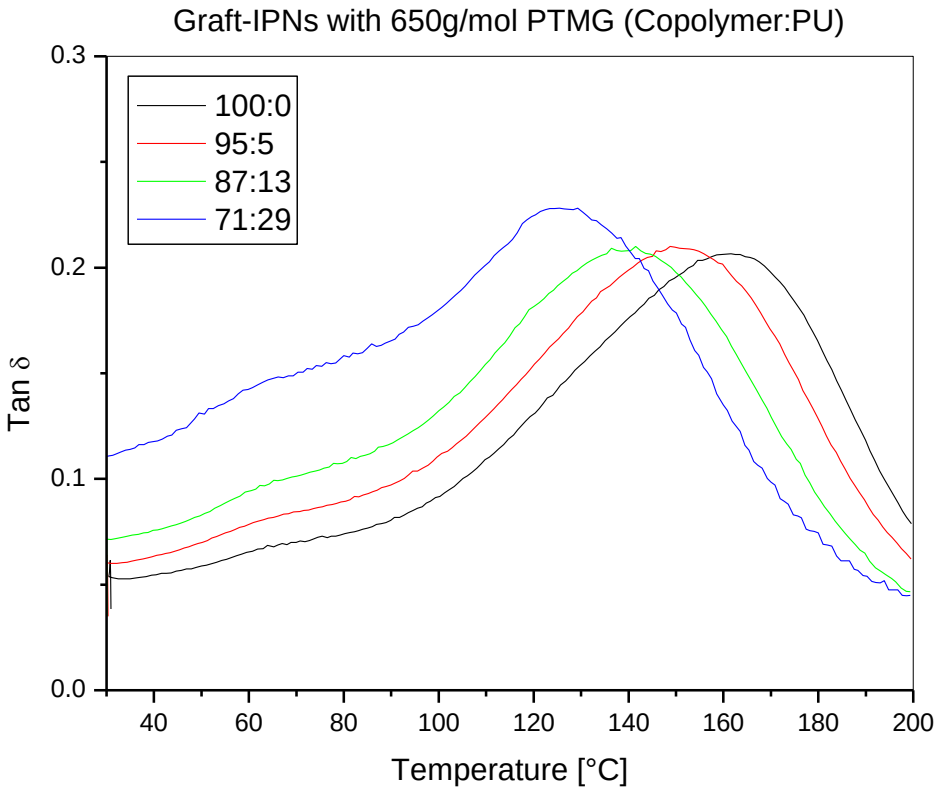

Figure V-11. Tan δ curves of pure copolymer and graft-IPNs with 650g/mol PTMG

Graft-IPNs with 650g/mol PTMG - Mechanical Properties

SEM micrographs can be seen in Figure V-12, which consist of pure copolymer with 50 wt% TRI-EDMA and 50 wt% BisGMA, and pictures of graft-IPNs with different amounts of copolymer to PU. Like those samples studied in Chapter II, these samples were immersed in liquid nitrogen for at least a minute, and then they were broken so that a brittle failure below the glass transition temperature could be observed.

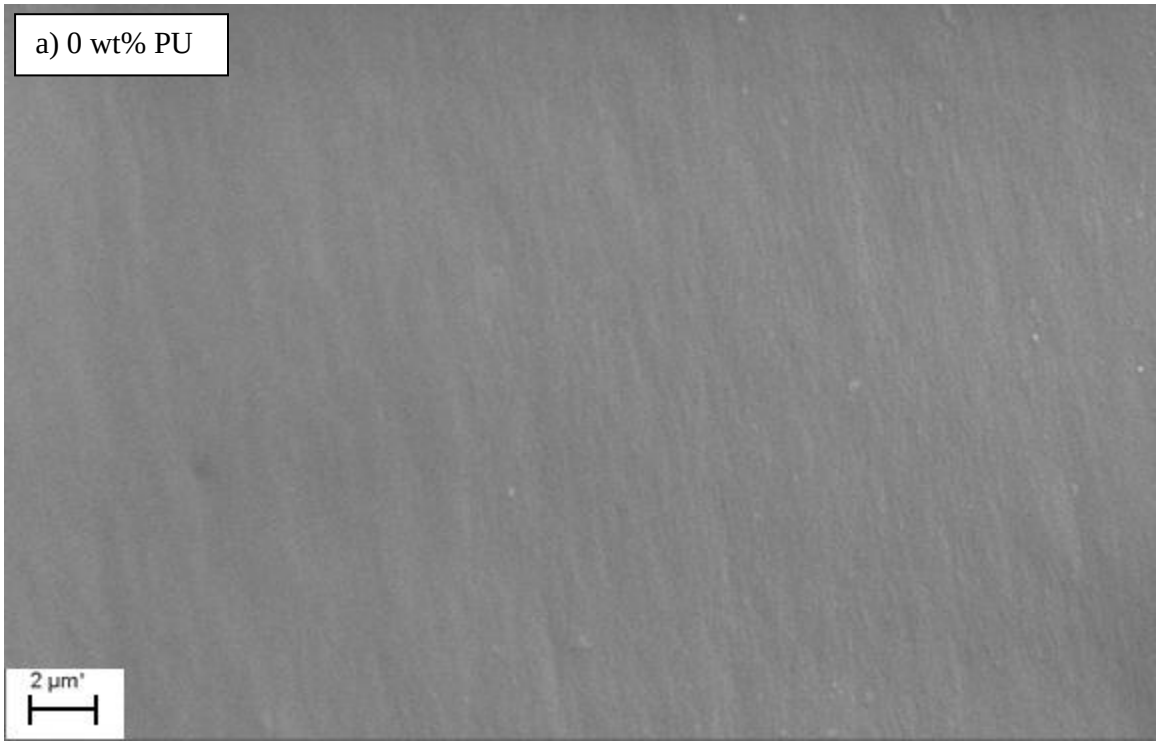

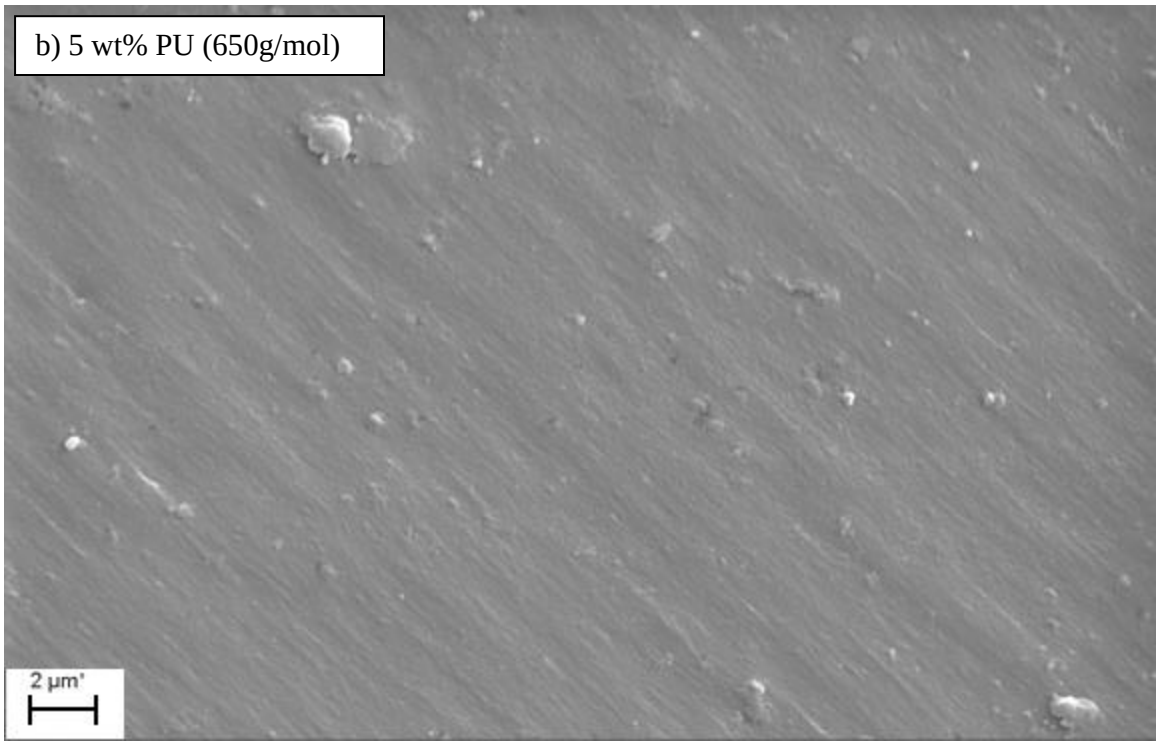
b) 5 wt% PU (650g/mol)
2 µm'

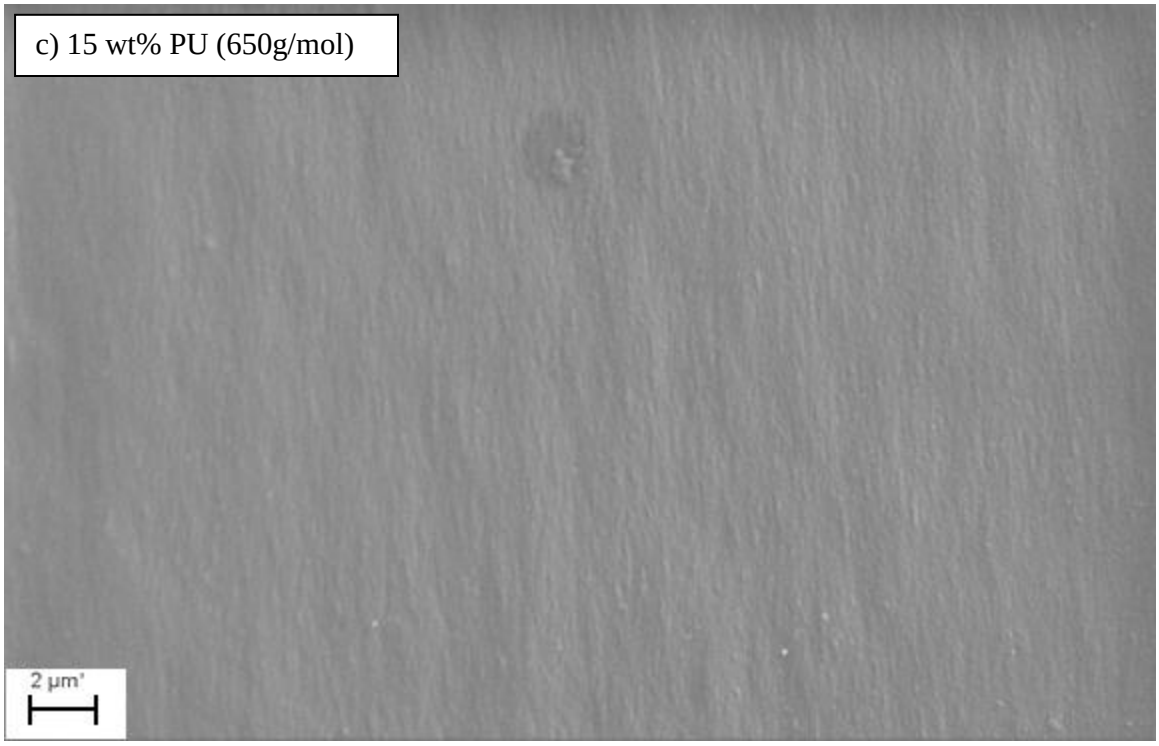
c) 15 wt% PU (650g/mol)
2 µm'

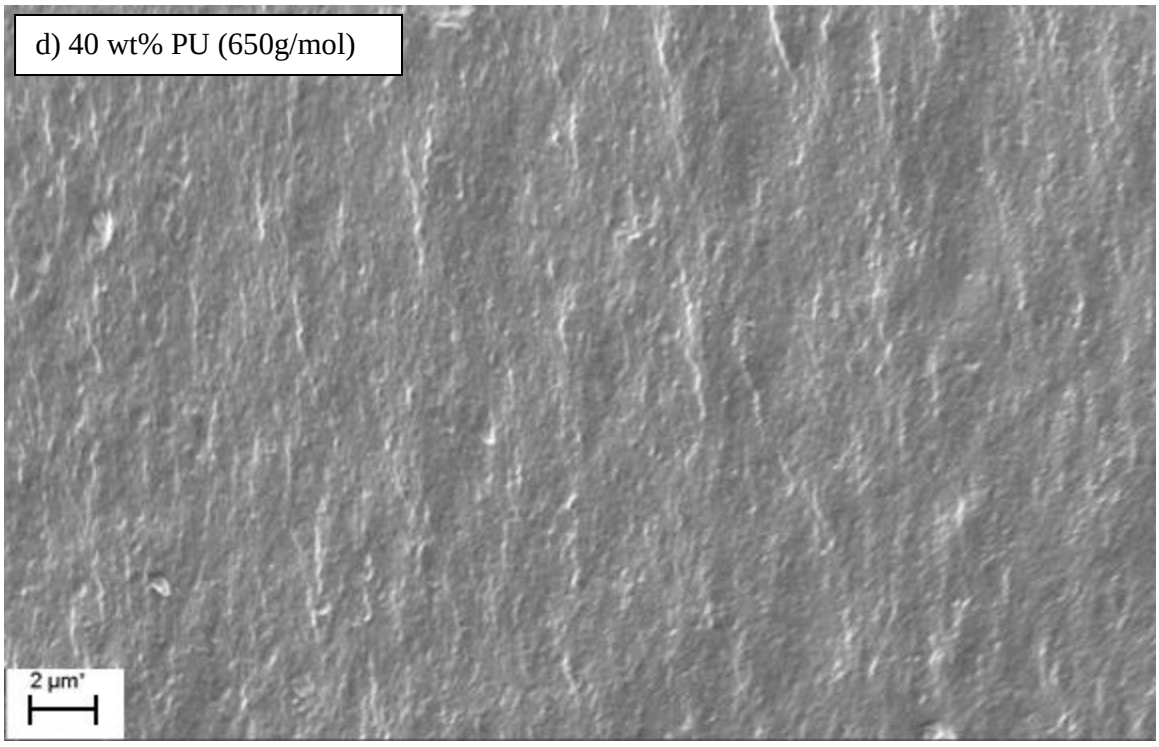

Figure V-12. SEM photos of 50:50 (TRI-EDMA:BisGMA) with 650g/mol PTMG and a) 0 wt%, b) 5 wt%, c) 15 wt%, and d) 40 wt% PU

Looking at Figure V-12-a, the surface of the pure copolymer is relatively smooth with slight indentations, most likely caused by very slight phase separation due to the two different resins present. However, when studying Figure V-12-b, a graft-IPN with a low amount of PU included, particle or glob-like structures appeared to have formed. This may be due to an insufficient amount of PU present to form a cross-linked network capable of being swelled by the copolymer phase. This same phenomenon occurred when there was not enough PU to form a network that could accommodate PMMA in its network, as discussed in Chapter II. Perhaps the large particles that can be seen in the photo are polyurethane particles.

The surface shown in Figure V-12-c appears smoother than the graft-IPN with 5 wt% PU, but slightly rougher than pure copolymer. This suggests that an adequate amount of PU was present

to form a cross-linked network that could provide accommodation of the copolymer phase within its network. Additionally, the rougher surface implies that more energy was dissipated due to the increase in surface area.

The SEM micrograph in Figure V-12-d shows a much rougher surface compared to all other samples. Increasing the PU content to almost one-third of the total graft-IPN created extremely tortuous ridges disrupted brittle failure. In other words, samples with a considerable amount of PU dissipated more energy than graft-IPNs with lower PU content.

By increasing the amount of PU, it was hoped that the fracture toughness of the materials could be improved upon. Table V-2 summarizes the glass transition temperature, the storage modulus (E'), as well as the critical-stress intensity factor (K_{Ic}). Interestingly, the K_{Ic} valued decreased from a copolymer to a graft-IPN with a low amount of PU present. As suggested by the SEM photo, this material may have exhibited slight phase separation; thus, the fracture toughness were negatively affected. Conversely, when higher amounts of PU were included, the K_{Ic} increased to a higher value. The SEM photo of the graft-IPN with the most PU content present showed a rough surface that possibly meant that more energy could be dissipated. Fracture tests confirm that slightly more energy could be absorbed by this material.

Table V-2. Thermo-mechanical and mechanical properties of graft-IPNs with 650g/mol

Sample (Copolymer:PU)	**T_g [°C]**	**E' (35°C) [GPa]**	**K_{Ic} [MPa $m^{1/2}$]**
100:0	160.44 ± 1.61	2.40 ± 0.09	0.587
95:5	150.50 ± 2.50	2.50 ± 0.18	0.549

87:13	139.24 ± 3.17	2.32 ± 0.07	0.688
71:29	126.81 ± 1.89	1.30 ± 0.01	0.682

Although improvement in the mechanical properties were observed by adding increasing amounts of PU, the K_{Ic} values were not high enough to be comparable to other materials currently on the market, such as Plexiglas®. Additional studies were needed to find a better method of reaching values closer to those commercially available.

Graft-IPNs with 2900g/mol PTMG – Optical Properties

Since adding PU with a diol of molecular weight of 650g/mol did not significantly improve the fracture toughness of the graft-IPNs, compared to pure copolymer, a diol with a higher molecular weight was utilized. PTMG was still part of the PU precursor, but the molecular weight chosen for this part of the experiment had a molecular weight of 2900g/mol. Figure V-13 shows how graft-IPNs with 50:50 (TRI-EDMA:BisGMA) with a diol of molecular weight 2900g/mol appeared.

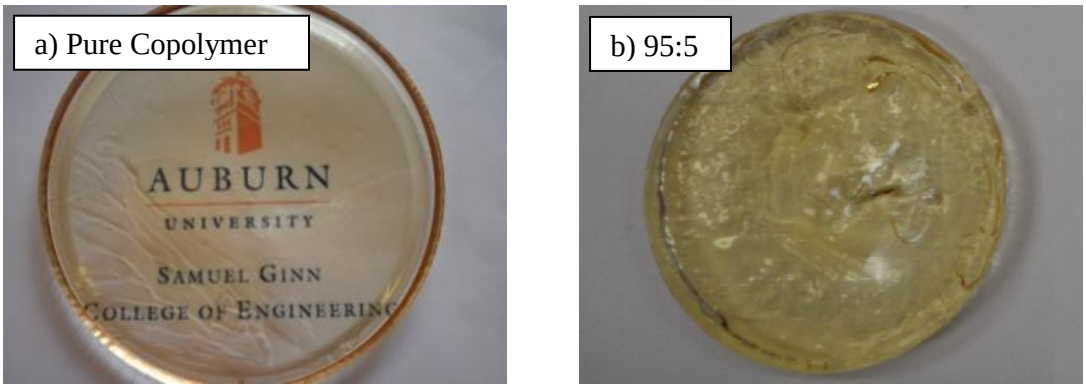

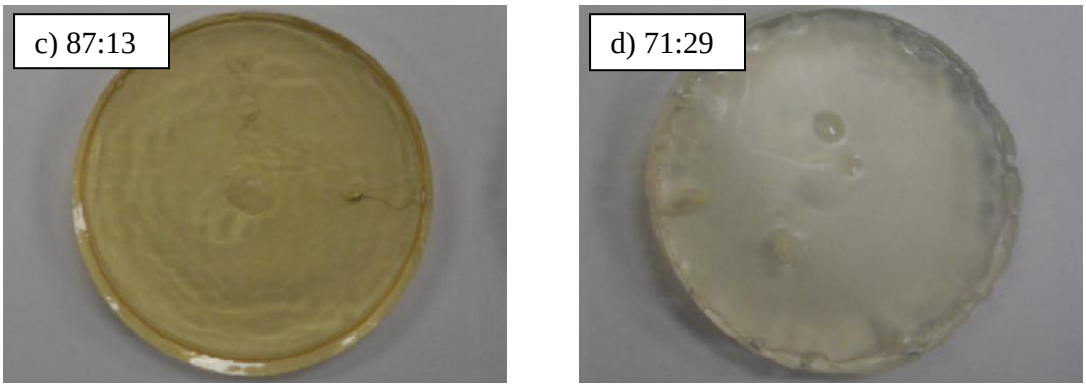

Figure V-13. Samples of a) pure copolymer and graft-IPNs with PU consisting of 650g/mol PTMG in ratios of b) 95:5, c) 87:13, and d) 71:29 (TRI-EDMA:BisGMA)

Since improving the mechanical properties of these graft-IPNs was the main issue, analysis with DMA was the first step in characterizing these materials, followed by observation of failed samples with SEM and fracture test experiments.

Graft-IPNs with 2900g/mol PTMG - Thermo-mechanical and Mechanical Properties

DMA results can be seen for graft-IPNs with 50:50 (TRI-EDMA:BisGMA) with 2900g/mol PTMG in Figure V-14, where Figure V-14-a shows the tan delta curves, and Figure V-14-b shows the E' values. It appears that the T_g's were in the range of 130°C-180°C. Additionally, for all the materials, whether PU was included or not, there was no phase separation present in the systems. A very slight peak may be visible at lower temperatures, but as before with the 650g/mol molecular weight diol, this is probably due to the BisGMA, especially since this peak is observed in the pure copolymer.

Also seen previously, as more PU was included in the graft-IPNs, the tan delta peak, or the T_g, shifted more toward lower temperatures. This was expected since gradually having more of the phase with a low T_g should continually move the T_g value to lower temperatures. Lin et al. also

noted with their graft-IPNs consisting of PU/epoxy that the T_g values shifted to lower temperatures, compared to the pure epoxy, when more PU was included [120].

The E' values also shifted to lower values when more PU was included. This trend has been consistently seen with the full-IPNs as well as the graft-IPNs studied in this research. When more of the soft, rubbery phase is involved, the thermo-mechanical properties will tend to decrease.

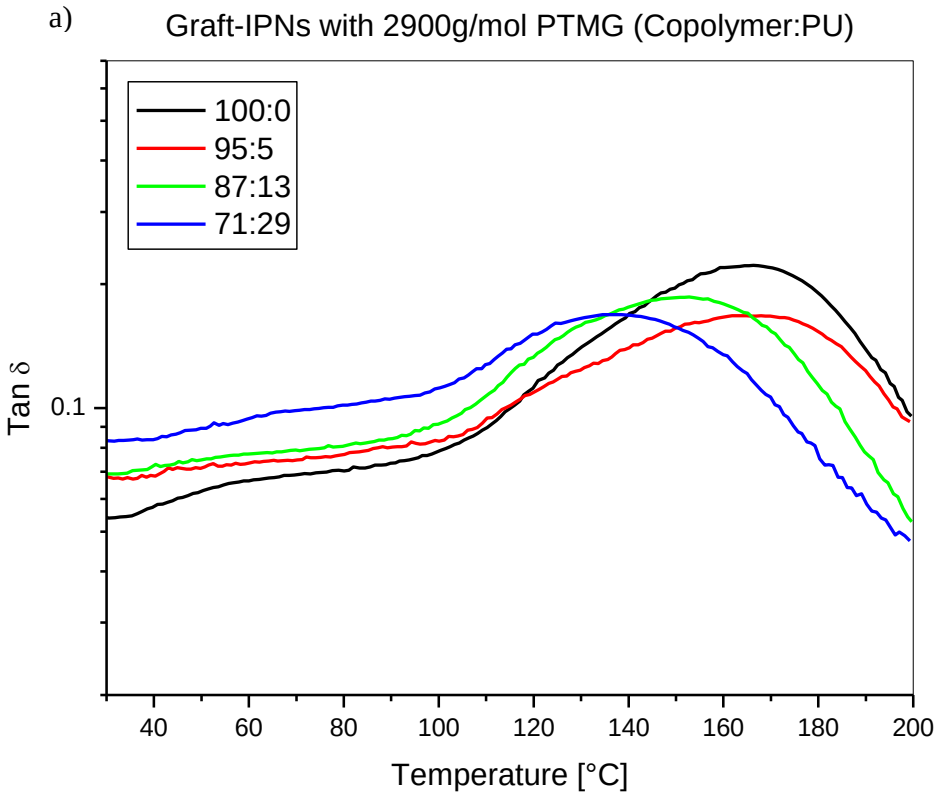

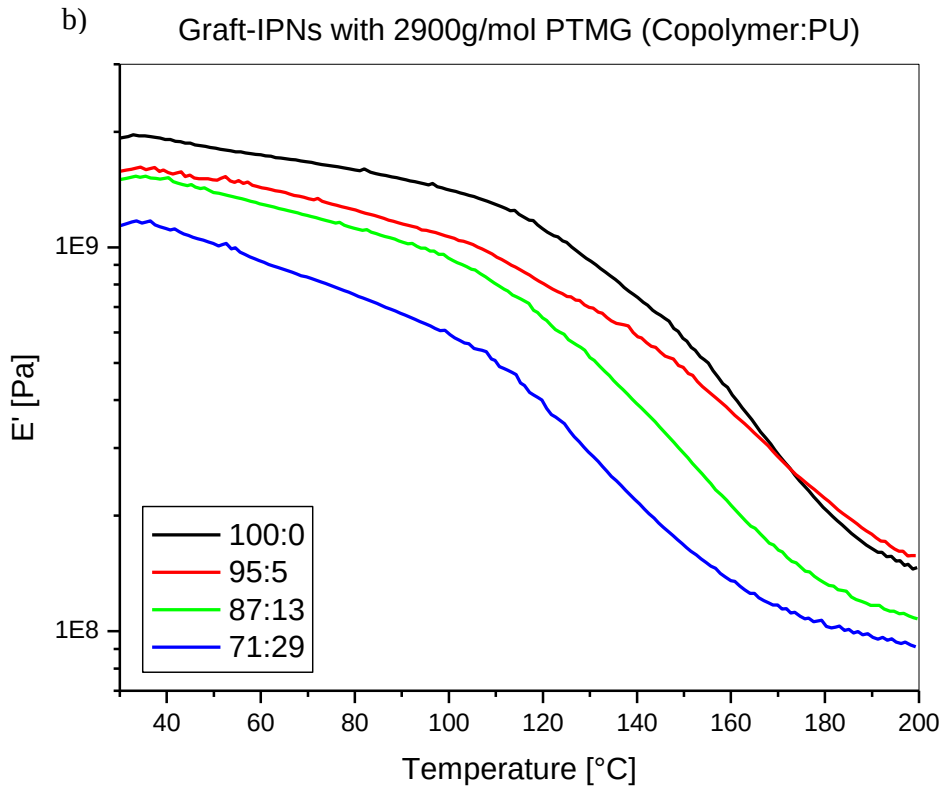

Figure V-14. DMA results of pure copolymer and graft-IPNs with 2900g/mol PTMG

Analysis of the mechanical properties was additionally investigated for graft-IPNs with the PU phase having a molecular weight diol of 2900g/mol. Figure V-15 shows SEM photos taken of graft-IPN samples with different PU amounts and with a diol of molecular weight 2900g/mol after brittle failure following submersion in liquid nitrogen. The SEM photos of 50:50 (TRI-EDMA:BisGMA) with 650g/mol PTMG in Figure V-12 can be used as a comparison for the SEM photos in Figure V-15; however, it should be noted that Figure V-15's magnification is twice that of Figure V-12's.

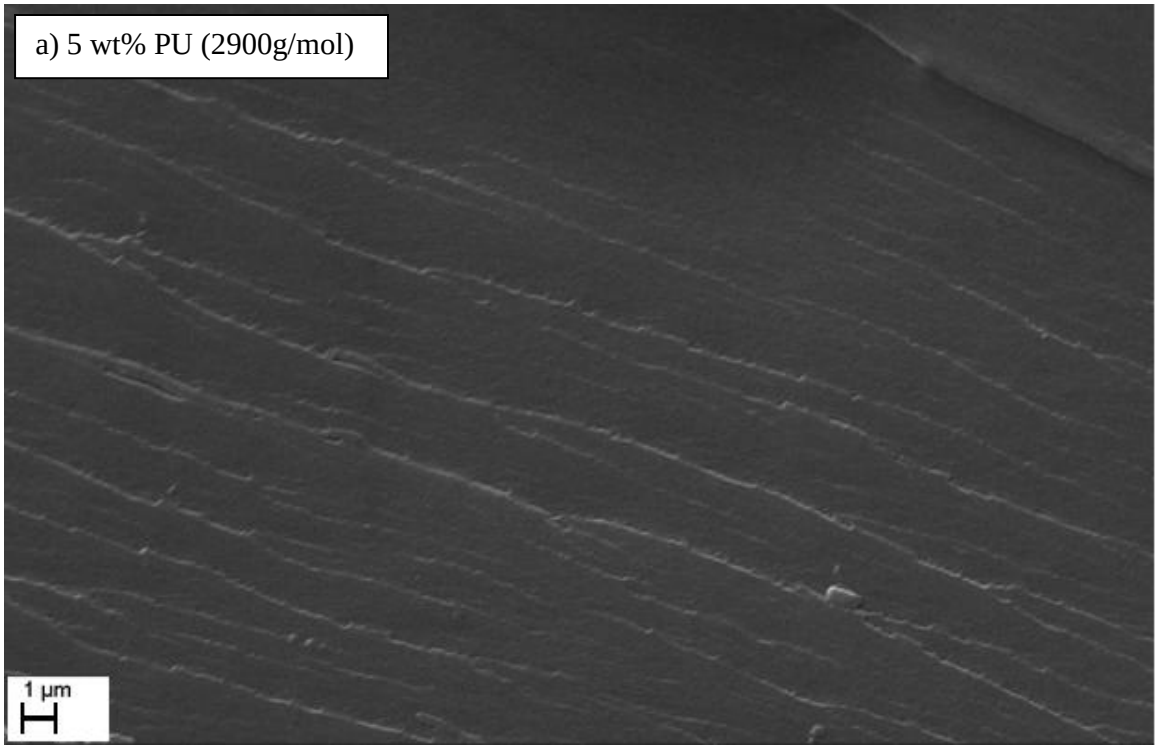
a) 5 wt% PU (2900g/mol)
1 µm

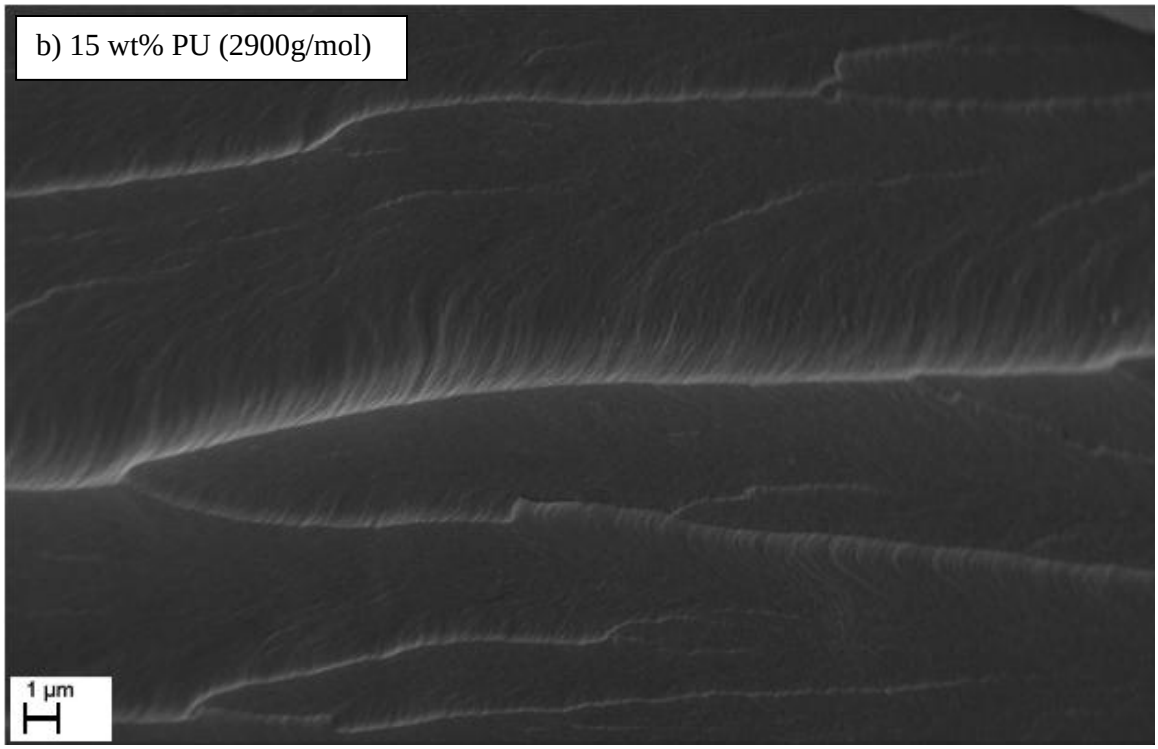
b) 15 wt% PU (2900g/mol)
1 µm

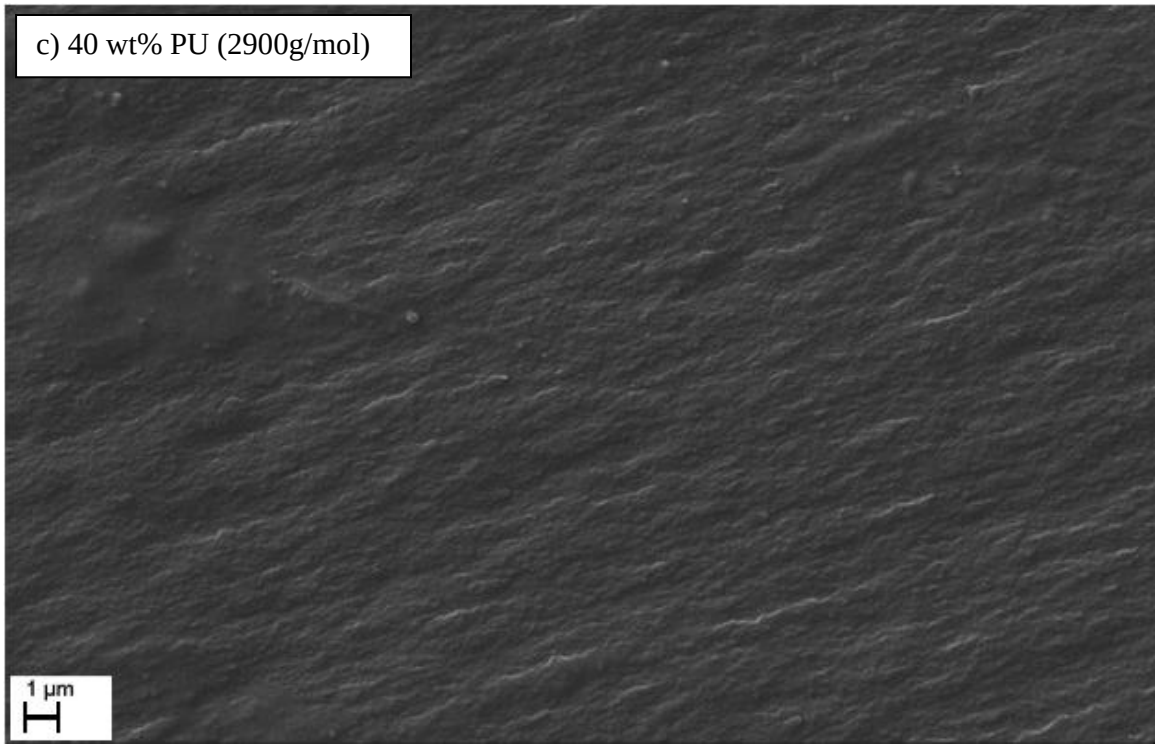

Figure V-15. SEM photos of 50:50 (TRI-EDMA:BisGMA) with 2900g/mol PTMG and a) 5 wt%, b) 15 wt%, and c) 40 wt% PU

Despite the difference in magnification between the SEM photos of samples with a PTMG of 650g/mol and the photos shown in Figure V-15, it was still clear that the surface of the graft-IPNs with PU consisting of a diol with 2900g/mol still had a much rougher topology than those samples with 650g/mol. This was indicative of improvement in the energy dissipation during failure.

Looking at Figure V-15, it also appeared that adding more PU to the graft-IPN system increased the energy dissipation since the surfaces became gradually rougher. When 5 wt% PU was included, ridges during failure were formed. When 15 wt% PU was added, the ridges became more prominent with smaller hair-like ridges forming on the larger ridges, resulting in an

increase in surface area. Finally, when 40 wt% PU was included, the whole surface became much rougher with no evidence of ridges.

The increase in the amount of ridges of ridges suggests that the fracture toughness values steadily increased. Quasi-static fracture tests were conducted to verify these results, which can be seen in Figure V-16.

The abrupt peaks shown in the graph where the P/B fell back down to zero, is indicative of a brittle failure. Adding up to 40 wt% PU may not have been enough to completely avoid this phenomenon. In order to shed better light on the properties of the materials, the fracture toughness can be investigated. The areas under the various curves give the critical-stress intensity factor or the fracture toughness (K_{Ic}) values of the materials. Adding 40 wt% PU, or even just 15 wt% PU, versus 5 wt% PU seemed to show an improvement in the K_{Ic} values. This can be seen by the looking at the differences in the load the samples were able to bear (P/B) and the amount of strain the materials underwent (δ).

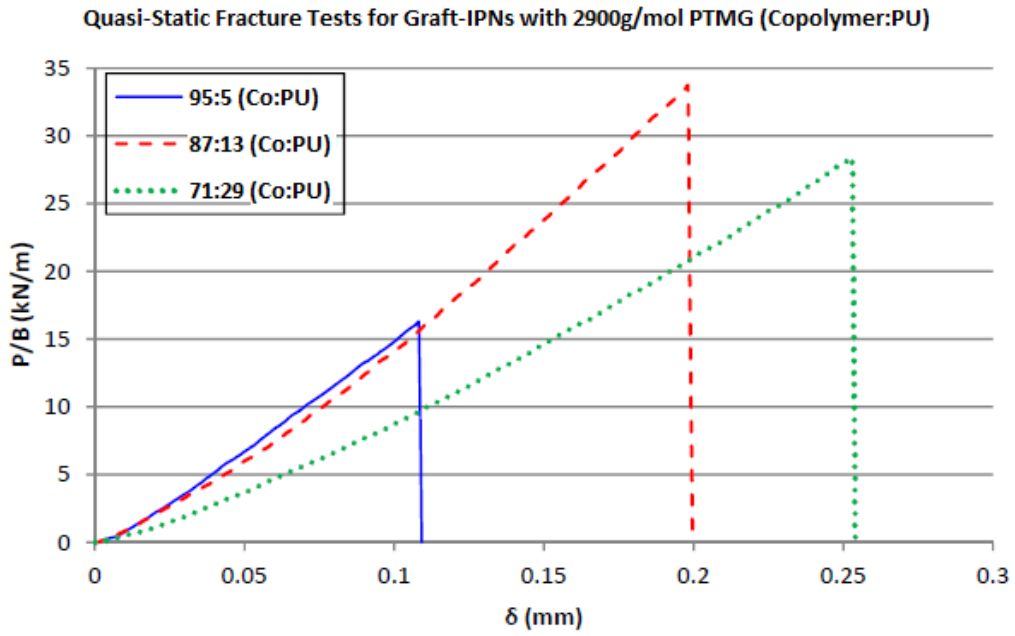

Figure V-16. Quasi-static fracture tests results of graft-IPNs with 2900g/mol PTMG

Shown in Table V-3, a summary of the exact values for the K_{Ic}, along with the T_g and the E' values can be viewed. Although the T_g and E' trends occurred as expected with increasing amounts of PU, the fracture toughness seemed to be negatively affected. With 5 wt% PU, the fracture toughness dropped a considerable degree, and even adding 15 wt% and 40 wt% did not reach the value for when pure copolymer was tested. It is not quite clear why experimental data resulted in this manner. It could still be possible that some slight phase separation did occur for these graft-IPNs, which was undetected by DMA. The phase separation could have contributed to a decrease in the mechanical properties which may have negatively impacted the fracture toughness.

Table V-3. Thermo-mechanical and mechanical properties of graft-IPNs with 2900g/mol

Sample (Copolymer:PU)	**T_g [°C]**	**E' (35°C) [GPa]**	**K_{Ic} [MPa $m^{1/2}$]**
100:0	160.44 ± 1.61	2.40 ± 0.09	0.587
95:5	165.37 ± 4.99	1.80 ± 0.30	0.226
87:13	151.32 ± 2.09	1.68 ± 0.21	0.475
71:29	133.73 ± 4.06	1.09 ± 0.09	0.400

After performing these experiments, it became obvious that simply increasing the molecular weight of the diol in the PU phase would not be a considerable change for the fracture toughness to improve. With this knowledge, a slightly different approach was taken for the next set of experiments.

Graft-IPNs with 1400g/mol PTMG - Optical Properties

Instead of using the ratio of 50:50 (TRI-EDMA:BisGMA) for the studies with 1400g/mol PTMG, the ratio was changed to 90:10 (TRI-EDMA). Based on the previous experiments, it was hypothesized that too many cross-links between the copolymer phase and the PU phase could have decreased the fracture toughness, subtracting from the purpose of these studies. Thus, having a lesser amount of BisGMA and more TRI-EDMA in the copolymer would still maintain the rigidity and transparency required while also lowering the number of reactions that would take place to connect the two different phases.

By increasing the molecular weight of the diol from 650g/mol to 2900g/mol seemed to have a negative impact on the fracture properties of the graft-IPN. Therefore, a molecular weight between these two diols, 1400g/mol, was utilized.

Results from UV-vis analysis for graft-IPN samples with 90:10 (TRI-EDMA:BisGMA) using a 1400g/mol PTMG can be seen in Figure V-17.

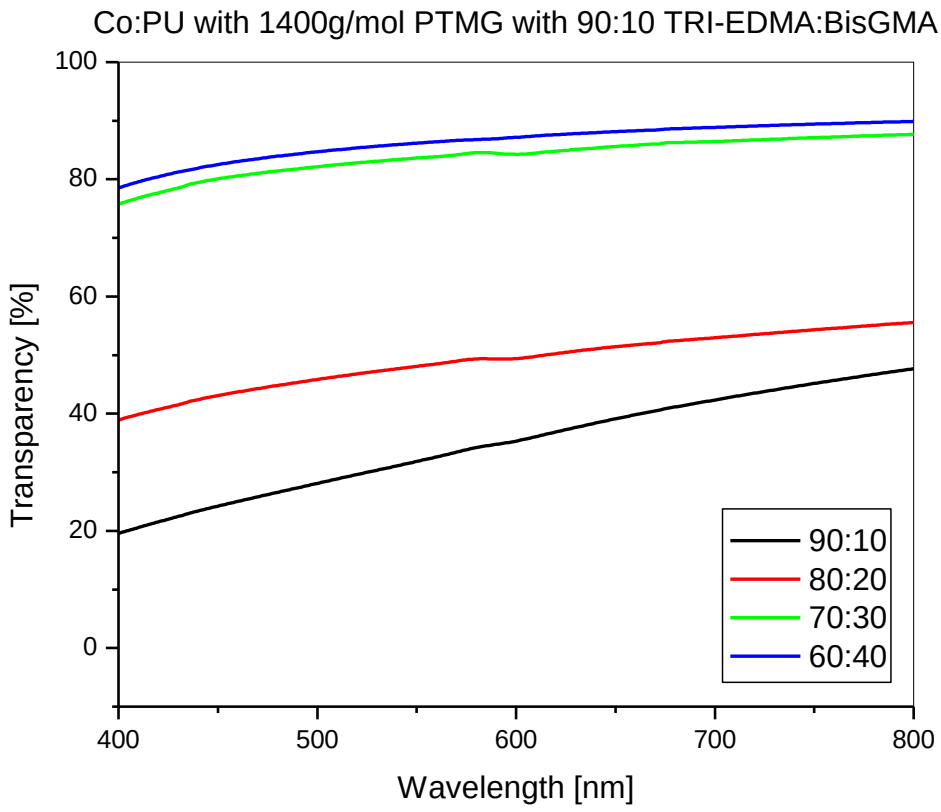

Figure V-17. UV-vis analysis of different copolymer:PU ratios with 1400g/mol PTMG

It is interesting to note that the trend for the transparency reversed from the graft-IPNs with 650g/mol PTMG when the ratio of TRI-EDMA:BisGMA was 50:50. Instead of the materials with the most copolymer and the least amount of PU present being the most transparent, the complete opposite occurred. Samples with more PU present had the highest transparency, while those with the least had the lowest transparency.

This phenomenon may have occurred because of the change in the copolymer ratio. Since increasing the TRI-EDMA and decreasing the BisGMA content should have affected how much the copolymer network could connect with the PU phase, this may have been the root of why the trend in UV-vis analysis switched. When samples with lower amounts of PU were synthesized, perhaps there was not enough of the PU to effectively form a network with accommodate the copolymer and simultaneously create enough cross-links to connect with the BisGMA. As more PU was included in the graft-IPN precursor, a larger PU network would have permitted the network to swell with the copolymer phase and allowed more cross-links with BisGMA. Consequently, phase separation decreased with more PU present in the graft-IPN materials and transparency gradually increased.

In order to confirm these results, swelling tests and calculations for the cross-link density and molecular weight between cross-links were performed so that the morphology of these graft-IPNs could be investigated.

Graft-IPNs with 1400g/mol PTMG - Morphology

Following the procedure outlined for swelling experiments, the results of these tests for graft-IPNs with 1400g/mol PTMG can be seen in Figure V-18. Studying this graph, it appeared that samples with the most PU present were able to swell much more than those with more copolymer present. A couple, or even a combination, of factors could explain why samples such as 60:40 and 70:30 (copolymer:PU) swelled to a lesser degree than the other samples. First, perhaps the copolymer phase is not as favorable to swelling in the THF solvent as PU is known to be. Accordingly, have more of the copolymer phase present would restrict the amount the

graft-IPN would be able to swell. Second, perhaps the copolymer phase was able to form a denser cross-linked network than the PU phase. Having a much higher cross-linked network would further restrict how much the graft-IPNs could swell. Graft-IPNs with more PU present may have had the ability to swell more due to a favorable swelling solvent, a lower cross-linked network, or perhaps for both reasons.

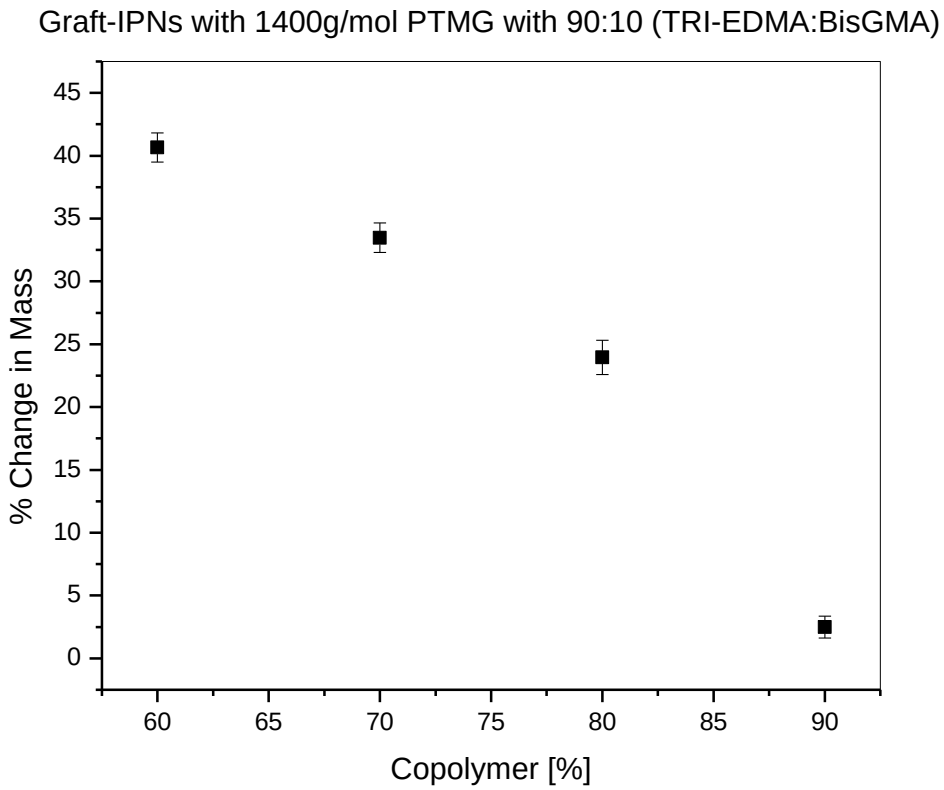

Figure V-18. Swelling results for graft-IPNs with 1400g/mol PTMG

Based on these swelling results, the cross-linked density and the molecular weight between cross-links were calculated, and these results can be seen in Figure V-19. Materials with higher degrees of the copolymer phase exhibited a higher cross-link density and consequently, lower

molecular weight between cross-links. On the other hand, samples with more PU present had a higher molecular weight between cross-links, thus making the cross-link density lower.

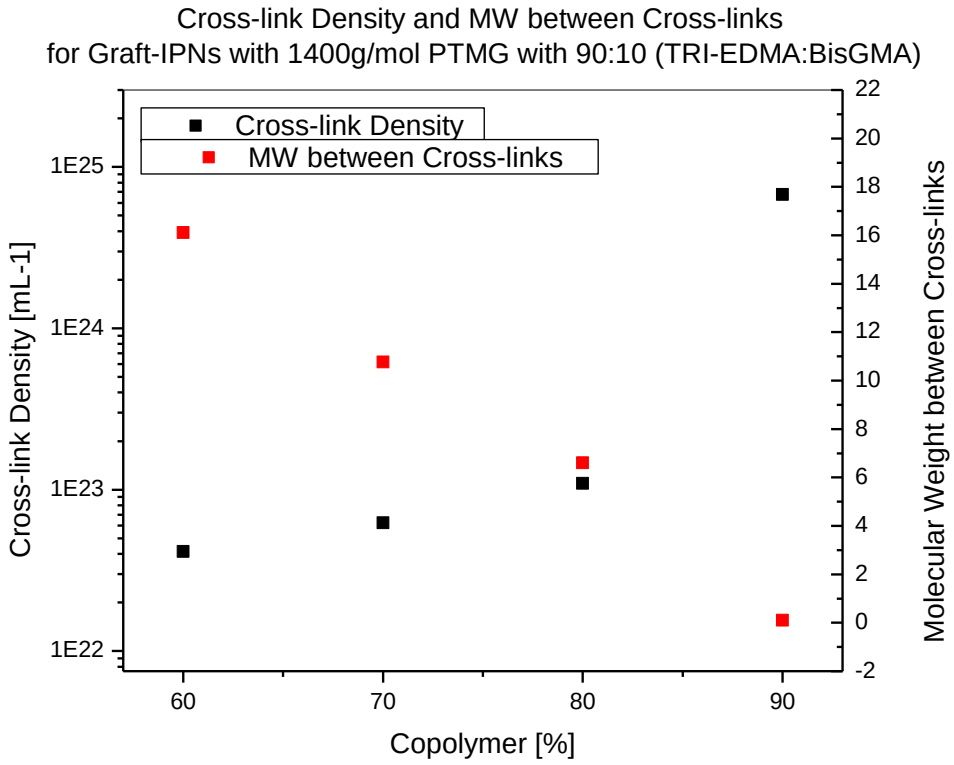

Figure V-19. Cross-link density and molecular weight between cross-links for graft-IPNs with 1400g/mol PTMG

Analysis on how the cross-link density would affect the thermo-mechanical properties was investigated, and these results can be viewed in the next section.

Graft-IPNs with 1400g/mol PTMG - Thermo-mechanical Properties

Graft-IPNs with 1400g/mol PTMG and pure copolymer, all with 90:10 (TRI-EDMA:BisGMA) can be seen in Figure V-20. The graft-IPN with 90:10 (copolymer:PU) failed after reaching approximately 110°C, and this may have been due to the existence of some phase separation, which was discussed earlier. However, the modulus at ambient temperatures can still be observed in the graph.

The materials with the highest storage modulus are the samples with the least amounts of PU present. This trend has been seen many times in this research; when more of the soft, rubbery phase is present, the E' values tend to decrease.

The trends observed in Figure V-20 could also confirm that the cross-link density was higher for the materials with more copolymer present. When there is a high cross-link density present, this means a more rigid network has formed, which in turn translates into a stiffer graft-IPN.

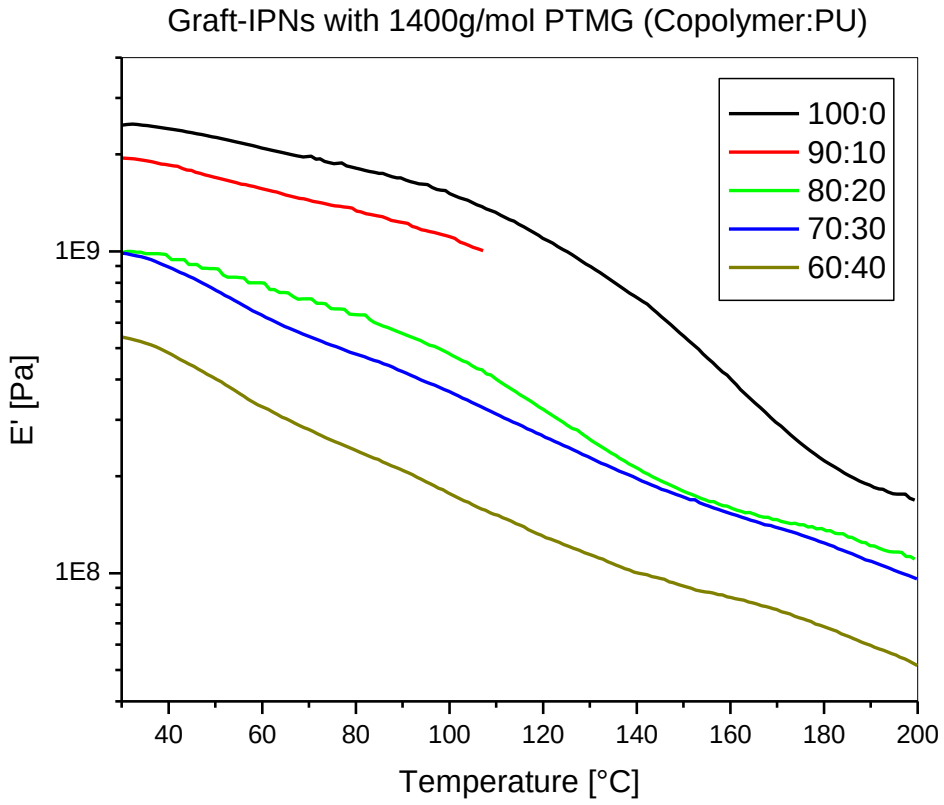

Figure V-20. E' values of graft-IPNs with 1400g/mol PTMG and pure copolymer with 90:10 (TRI-EDMA:BisGMA)

The corresponding tan delta curves to the graph above can be seen in Figure V-21. Note that the tan delta peak could not be observed for the 90:10 (copolymer:PU) sample since failure occurred before the glass transition phase could be reached.

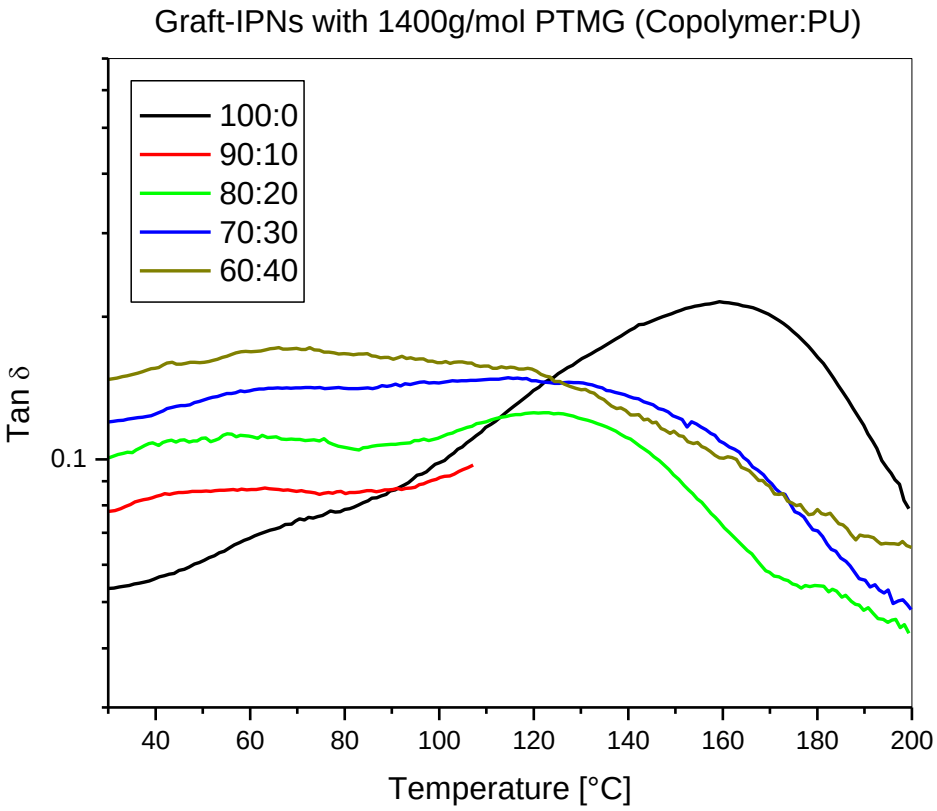

Figure V-21. Tan δ values of graft-IPNs with 1400g/mol PTMG and pure copolymer with 90:10 (TRI-EDMA:BisGMA)

Although the 90:10 (copolymer:PU) sample failed, the dramatic difference in the tan delta peak, or the T_g, between the pure copolymer and the graft-IPNs was still observable. Like the pure copolymer sample which consisted of 50:50 (TRI-EDMA:BisGMA) in Figure V-14-a, a very large peak was seen at high temperatures with a very slight peak at lower temperatures. The peak at lower temperatures is not as prominent as the peak in Figure V-14-a, and this could correlate to the less amount of BisGMA present to create this peak.

The two prominent peaks in the graft-IPN consisting of 80:20 (copolymer:PU) was possibly associated to slight phase separation. This would mean that the 90:10 (copolymer:PU) sample would have exhibited even more phase separation, which would have contributed to its failure during 3-point bending tests.

As more PU was included in the graft-IPNs, the tan delta peak shifted more to the left to lower temperatures and became increasingly broader. This was probably due to increased phase compatibility of the two networks, as mentioned before. Therefore, the formation of one broad tan delta peak was created. Sung and Lin saw similar trends for their samples with PDMS/epoxy graft-IPNs. The T_g of the PDMS phase seemed to merge with the T_g of the epoxy phase and a broad transition region was formed for the damping area. This was associated with partial compatibility between the PDMS phase and the epoxy resin's soft segments [116].

Conclusions

Graft-IPNs with a copolymer phase, consisting of TRI-EDMA and BisGMA, along with a PU phase were synthesized with various molecular weight diols in the PU phase and different TRI-EDMA:BisGMA ratios. Samples with the 650g/mol PTMG and 50:50 (TRI-EDMA:BisGMA) did show some improvement in the fracture toughness compared to the pure copolymer system, but the change was too small to garner enough interest to further pursue studies with these samples. Therefore, a higher molecular weight PTMG was used in the hopes that a more flexible network would increase the fracture toughness even more. However, the fracture toughness

decreased, which was attributed to the increase in the phase separation between the two polymeric phases.

The latest experiments included a slightly different approach. First, the TRI-EDMA:BisGMA ratio was changed from 50:50 to 90:10 so that less cross-linking would occur between the copolymer phase and the PU phase, but would still be sufficient enough to link the two networks to form a graft-IPN and support phase compatibility. Second, the molecular weight of the diol was 1400g/mol. These samples with high amounts of PU content showed high transparency and good phase compatibility. The fracture toughness did improve with the 1400g/mol PTMG in the PU phase.

CHAPTER VI

CONCLUSIONS

The need for transparent, impact-resistant materials is imperative for many applications in both civil and military situations. Conventional materials, such as laminated and tempered glass, have been successfully employed, but these materials have limitations to where they can only be used a certain number of times before they are rendered inadequate and ineffective. The introduction of polymeric, impact-resistant materials, such as Plexiglas® and polycarbonate, have also exhibited enhanced material properties which are required for high impact scenarios while simultaneously offering transparency. Still, these devices are insufficient for everyday situations against weaponry that is constantly being developed. While many other research groups have begun investigating alternatives to these materials, such as in transparent ceramic composites, this research has proposed combining polymeric materials into one synergistic system.

The combination of polymers can be difficult based on several factors, such as differences in thermodynamic and kinetic properties. Even structural dissimilarities can promote phase separation among polymeric components. A widely-studied method of bringing polymers together in close proximity in a macromolecular mixture is through the use of interpenetrating polymer networks (IPNs).

IPNs have just recently been discovered in the last century, but fervent studies on this subject have generated increased interest and research. Individuals have used IPNs for many different applications, but for this particular study, the emphasis was placed on synthesizing a molecular composite material capable of being transparent while offering high fracture toughness comparable or exceeding what is currently available in today's market.

The two types of materials that were utilized in making such a device for this research project included methacrylate-based polymers and polyurethane (PU). Plexiglas®, which is essentially poly(methyl methacrylate) (PMMA), is known to offer exceptional transparent qualities as well as high stiffness and rigidity. PU is a popular polymer among researchers since it can be synthesized into many different forms based on the reactants used as well as the reaction conditions. Due to the many different parameters that can be adjusted, PU is a versatile material that can be tailored to meet specific needs and applications. Accordingly, most of the focus of this research was dedicated to exploring how to manipulate the PU phase to be more compatible with PMMA so that the material properties could ultimately be improved upon.

For the initial part of this research, the goal was to successfully synthesize IPNs while studying different parameters, such as the type of isocyanate included in the PU phase (aliphatic versus aromatic), the effect of using a methyl methacrylate monomer with or without an inhibitor in the PMMA phase (in other words, the effect of having a sequential or a simultaneous polymerization), the curing profile, and the effects of using different ratios of PMMA to PU. Several IPNs with various formulations were created which set the foundation for the other studies in this research.

In the first experiments for this study, it was found that when IPNs consisted of an isocyanate with an aromatic ring in the PU phase, a yellow discoloration formed. On the other hand, when an aliphatic isocyanate was included, transparency could be achieved. Additionally, discoloration formed when post-curing was included in the heat treatment of the IPNs. Since the material properties only slightly increased, IPNs synthesized following this discovery did not have post-curing.

One key aspect that determined the compatibility of the PU and PMMA phases was the curing sequence for synthesizing the IPNs. Having both phases synthesize at the same time created kinetic and thermodynamic differences too great to allow successful interlocking of the two networks. Instead, the phases rejected each other while synthesizing, thus creating two separate networks completely independent of each other with no penetration. Based on this knowledge, all other IPNs created afterwards were synthesized in a sequential fashion where phase separation was minimal.

The following studies focused on manipulating the PU network to further enhance the material properties as well as the compatibility between the PU and PMMA phases. One method of changing the PU network was through the use of different molecular weight diols. By changing the length of the diol, the network morphology of the PU phase altered, which ultimately affected the material properties. Increasing the length also increased the molecular weight between cross-links as well as the cross-link density, which affected how well the PU and PMMA phases coexisted. It was discovered that increasing the chain length did improve the fracture toughness of the material to some degree, while transparency was maintained, but an

upper limit was reached where phase separation became imminent, and fracture toughness began to decrease.

Another method used for altering the PU network was through changing the ratio of diol to triol; that is, changing the ratio of the linear chain to the cross-linking agent in the PU phase. Having more diol present in the PU phase created more open network structures that generated different morphologies that also affected final material properties. Changes in the diol:triol ratio did not have a profound effect on the storage modulus (E') and the glass transition temperature (T_g), as was the case for changing the molecular weight of the diol, thus narrowing the possibilities of improving the impact-resistance with this method.

The last part of this research was based on a slightly different approach; instead of creating a full-IPN as before, where both polymer networks were independent of each other except for physical entanglements, a graft-IPN was explored. For graft-IPNs, not only are there physical entanglements present, but at certain points there are cross-links that connect the two networks together. The idea behind this part of the research was to further enhance the compatibility of the phases by locking the soft, rubbery phase with the rigid phase through physical cross-links in addition to chemical cross-links.

In order to accomplish this, the PMMA phase was replaced by a methacrylate-based copolymer with the capability of cross-linking with the PU phase. Bisphenol A glycidyl methacrylate (BisGMA) and triethylene glycol dimethacrylate (TRI-EDMA) were used together, where the BisGMA had hydroxyl (-OH) groups capable of reacting with the isocyanate groups (-NCO) in

the PU network. Employing this method of creating an IPN did improve the compatibility between the two networks, which can be observed through the smooth, brittle failure the materials underwent. Had the components rejected each other, phase separation would have ensued, and a rougher surface would have resulted. Although smooth surfaces are not necessarily desirable for fracture toughness, this did allude to the improvement of compatibility between the polymer components.

The first attempts in synthesizing graft-IPNs produced somewhat brittle materials, but changing the molecular weight of the diol in the PU phase as well as the ratio of TRI-EDMA:BisGMA produced promising results that could generate future studies that will further improve the fracture toughness in the systems.

This research has demonstrated an alternate route for producing transparent and tough materials that could one day be used in real-world applications. Despite some IPNs not completely fulfilling the requirements needed for high-impact situations, this research project has shown that there are many ways to change the morphology of the IPN network and its component networks, which could eventually lead to a superior material, comparable to what is commercially available.

Other factors can be taken into consideration with the development of IPNs manufactured for use as transparent, safety devices. Mechanical reinforcement with fillers, such as with silica nanoparticles, can be possible through the careful selection of materials with functionalities capable of reacting with the PU phase, so that phase compatibility is still maintained. Even

chemical resistance may be enhanced with other components that can also synthesize with the PU and PMMA phases. Perhaps UV-stabilizers could improve materials which are constantly exposed to sunlight. Coatings could possibly be constructed to the surface of a material through the synthesis of a gradient-IPN. The options for creating a transparent, impact-resistant material are numerous, which is why IPNs are excellent candidates for protective materials.

REFERENCES

1. Furr, A.K., *CRC Handbook of Laboratory Safety*. 5 ed. 2000: CRC Press LLC.

2. Duffy, J.E. and R. Scharff, *Auto Body Repair Technology*. 4 ed. 2004: Delmar Learning.

3. Carraher, C.E., *Introduction to Polymer Chemistry*. 3 ed. 2013: Taylor & Francis Group, LLC.

4. Lunny, D., *Shoplifting, Security, Curtailing Crime - Inside and Out*. 2013: Productive Publications.

5. Houpt, S., *Museum of the Missing: A History of Art Theft*. 2006: Sterling Publishing Co, Inc.

6. Raum, E., *The Declaration of Independence*. 2013: Capstone Global Library, LLC.

7. *The Charters of Liberty: The Declaration of Independence, the United States Constitution, and the Bill of Rights*. 2010: American Liberty Press, LLC.

8. Holden, H., *To Be a U.S. Secret Service Agent*. 2006: Zenith Press.

9. Jarrett, D.N., *Cockpit Engineering*. 2005: Ashgate Publishing Limited.

10. Clugston, M. and R. Flemming, *Advanced Chemistry*. 2000: Oxford University Press.

11. *Active NIJ Standards and Comparative Test Methods*. 2012 [cited 2013; Available from: http://www.nij.gov/topics/technology/standards-testing/active.htm.

12. Macfarlane, A. and G. Martin, *Glass: A World History*. 2002: The University of Chicago Press.

13. Singh, M., et al., *Global Roadmap for Ceramic and Glass Technology*, ed. S. Freiman. 2007: Wiley-American Ceramic Society.

14. Bertino, A.J., *Forensic Science Fundamentals & Investigations*. 2009.

15. Girard, J.E., *Criminalistics: forensic science, crime, and terrorism*. 2 ed. 2011: Jones & Bartlett Learning. 3.

16. McLendon, C., et al., *Shields for Sky Fighters*, in *Popular Science*. 1944.

17. Varasdi, J.A., *Myth Information*. 1989, New York: Ballantine Books.

18. Binggeli, C., *Materials for Interior Environments*. 2008: John Wiley & Sons, Inc.

19. Amstock, J.S., *Handbook of Glass in Construction*. 1997.

20. Basu, B. and K. Balani, *Advanced Structural Ceramics*. 2011, Hoboken: John Wiley & Sons, Inc.

21. Patel, P.J., et al., *Transparent Armor.* The AMPTIAC Newsletter, 2000. **4**(3): p. 1-15.

22. Patel, P.J., et al., *Transparent ceramics for armor and EM window applications*, in *Inorganic Optical Materials II*, E.G.A. Alexander J. Marker III, Editor. 2000. p. 1-14.

23. Morris, P., *Polymer Pioneers*. 1990: Beckman Center for the History of Chemistry.

24. Painter, P.C. and M.M. Coleman, *Essentials of Polymer Science and Engineering*. 2009, Lancaster: DEStech Publications, Inc.

25. Krauthammer, T., et al., *Structural Design for Physical Security: State of the Practice*. 1999: American Society of Civil Engineers.

26. Park, S.-J. and M.-K. Seo, *Interface Science and Composites*. Vol. 18. 2011: Academic Press.

27. Nagyszalanczy, S., *Jigs and Fixtures*, ed. P. Anthony. 2006: The Taunton Press, Inc.

28. *LEXAN Turns 50*, in *Popular Mechanics*. 2003, The Hearst Corporation. p. 22.

29. Ashby, M. and K. Johnson, *Materials and Design: The Art and Science of Material Selection in Product Design*. 2 ed. 2010: Elsevier Ltd.

30. Sun, Y., et al., *Continuous flow polymerase chain reaction using a hybrid PMMA-PC microchip with improved heat tolerance.* Sensors and Actuators B: Chemical, 2008. **130**(2): p. 836-841.

31. Narins, R.S. and R.A. Kazin, *Acrylic Particle-Based Fillers: ArteFill*, in *Office-Based Cosmetic Procedures and Techniques*, S. Eremia, Editor. 2010, Cambridge University Press. p. 84.

32. Cohen, S.R. and M.G. Rubin, *ArteFill*, in *Augmentation Fillers*, N.S. Sadick, Editor. 2010, Cambridge University Press. p. 54.

33. Burrows, A., et al., *Chemistry: Introducing Inorganic, Organic and Physical Chemistry*. 2 ed. 2013: Oxford University Press.

34. Sastri, V.R., *Plastics in Medical Devices: Properties, Requirements and Applications*. 2010: Elsevier Inc.

35. Bernini, U., et al., *Ultra-tough synthetic glasses made by reactive blending of PMMA and EVA rubbers: opto-thermal characterization.* Journal of Materials Processing Technology, 1995. **55**(3â€“4): p. 224-228.

36. Cangialosi, D., et al., *Electron beam induced polymerisation of MMA in the presence of rubber: a novel process to produce tough materials.* Radiation Physics and Chemistry, 2002. **63**(1): p. 63-68.

37. Guo, S., A. Ait-Kadi, and M. Bousmina, *A modified model predictions and experimental results of weld-line strength in injection molded PS/PMMA blends.* Polymer, 2004. **45**(9): p. 2911-2920.

38. Giancola, G., R.L. Lehman, and J.D. Idol, *Melt processing and domain morphology of PMMA/HDPE polymer blends prepared from powder precursors.* Powder Technology. **218**(0): p. 18-22.

39. Vijayalakshmi Rao, R., P.V. Ashokan, and M.H. Shridhar, *Study of cellulose acetate hydrogen phthalate(CAP)-poly methyl methacrylate (PMMA) blends by thermogravimetric analysis.* Polymer Degradation and Stability, 2000. **70**(1): p. 11-16.

40. Sasaki, H., et al., *Miscibility of PVDF/PMMA blends examined by crystallization dynamics.* Polymer, 1995. **36**(25): p. 4805-4810.

41. Schneider, S., et al., *Impact of nucleating agents of PVDF on the crystallization of PVDF/PMMA blends.* Polymer, 2001. **42**(21): p. 8799-8806.

42. Moon, E.J., et al., *Gas transport and thermodynamic properties of PMMA/PVME blends containing PS-b-PMMA as a compatibilizer.* Journal of Membrane Science, 2002. **204**(1â€“2): p. 283-294.

43. Plunkett, J.W., *Plunkett's Chemicals, Coatings, & Plastics Industry Almanac*. 2005, Houston: Plunkett Research Ltd.

44. *Polymer Data Handbook*, J.E. Mark, Editor. 1999, Oxford University Press, Inc.

45. Meckel, W., et al., *Thermoplastic Polyurethane Elastomers*, in *Thermoplastic Elastomers*, G. Holden, H.R. Kricheldorf, and R.P. Quirk, Editors. 2004, Hanser Gardner Publications, Inc. p. 15-17.

46. Petrovic, Z.S., *Polyurethanes*, in *Handbook of Polymer Synthesis*, H.R. Kricheldorf, O. Nuyken, and G. Swift, Editors. 2005, Marcel Dekker. p. 503-504.

47. Luo, S.-G., et al., *Catalytic mechanisms of triphenyl bismuth, dibutyltin dilaurate, and their combination in polyurethane-forming reaction.* Journal of Applied Polymer Science, 1997. **65**(6): p. 1217-1225.

48. Robeson, L., *Polymer Blends: 'A Comprehensive Review*, ed. L.M. Robeson. 2007: Hanser Gardner Publications, Inc.

49. Sperling, L.H. and V. Mishra, *The Current Status of Interpenetrating Polymer Networks.* Polymers for Advanced Technologies, 1996. **7**: p. 197-208.

50. Utracki, L.A., *Polymer Blends Handbook*, ed. L.A. Utracki. Vol. 1. 2002: Kluwer Academic Publishers.

51. Sperling, L.H., *Interpentrating Polymer Networks: An Overview*, in *Interpenetrating Polymer Networks*. 1994, American Chemical Society: Washington, DC. p. 3-38.

52. Ebewele, R.O., *Polymer Science and Technology*. 2000: CRC Press LLC.

53. Calleja, F.B. and Z. Roslaniec, *Block Copolymers*. 2000: Marcel Dekker, Inc.

54. Albores-Velasco, M., R.I. Gascon, and O.A. Rodriguez, *Compatibilizers, Polymeric*, in *Concise Polymeric Materials Encyclopedia*, J.C. Salamone, Editor. 1999, CRC Press LLC. p. 272-273.

55. Porte, R.J.L., *Hydrophilic Polymer Coatings for Medical Devices: Structure/Properties, Development, Manufacture and Applications*. 1997: CRC Press LLC.

56. Alger, M.S.M., *Polymer Science Dictionary*. 2 ed. 1997: Chapman & Hall

57. Allcock, H.R., *Introduction to Materials Chemistry*. 2008, Hoboken: John Wiley & Son, Inc.

58. Frisch, H.L., K.C. Frisch, and D. Klempner, *Interpenetrating Polymer Networks*, in *Chemistry and Properties of Crosslinked Polymers*, S.S. Labana, Editor. 1977, Academic Press, Inc. p. 207.

59. Sperling, L.H., *History and Development of Polymer Blends and IPNs*, in *Applied Polymer Science: 21st Century*, C. Craver and C. Carraher, Editors. 2000, Elsevier Science Ltd. p. 345.

60. Sperling, L.H., *Introduction to Physical Polymer Science*. 4th ed. 2006, Hoboken: John Wiley & Sons, Inc.

61. Klempner, D. and K.C. Frisch, in *Advances in Interpenetrating Polymer Networks*, D. Klempner and K.C. Frisch, Editors. 1994, CRC Press: Lancaster.

62. Thomas, D.A. and L.H. Sperling, *Interpenetrating Polymer Networks*, in *Polymer Blends*, D.R. Paul and S. Newman, Editors. 1978, Academic Press, Inc. p. 26.

63. George, S.C. and S. Thomas, *Manufacturing of Multiphase Polymeric Systems*, in *Handbook of Multiphase Polymer Systems*, A. Boudenne, et al., Editors. 2011, John Wiley & Sons Ltd. p. 153.

64. Ali, S.A.M. and D.J. Hourston, *Thermoplastic Interpenetrating Polymer Networks*. Advances in Interpenetrating Polymer Networks, ed. D. Klempner and K.C. Frisch. Vol. 4. 1994, Lancaster: Technomic Publishing Company, Inc.

65. Roland, C.M., *Viscoelastic Behavior of Rubbery Materials*. 2011: Oxford University Press. 141.

66. Mita, I. and S. Akiyama, *Molecular Design of Network Polymers*, in *Macromolecular Design of Polymeric Materials*, K. Hatada, T. Kitayama, and O. Vogl, Editors. 1997, Marcel Dekker, Inc. p. 400.

67. Huang, Y., et al., *Mechanisms of Toughening Thermoset Resins*, in *Toughened Plastics I*, C.K. Riew and A.J. Kinloch, Editors. 1993, American Chemical Society. p. 1-35.

68. Kinloch, A.J. and F.J. Guild, *Predictive Modeling of the Properties and Toughness of Rubber-Toughened Epoxies*, in *Toughened Plastics II*, C.K. Riew and A.J. Kinloch, Editors. 1996, Ameican Chemical Society. p. 1-25.

69. Verchère, D., et al., *Rubber-Modified Epoxies*, in *Toughened Plastics I*, C.K. Riew and A.J. Kinloch, Editors. 1993, American Chemical Society. p. 335-363.

70. Kim, S.C., D. Klempner, and K.C. Frisch, *Polyurethane Interpenetrating Polymer Netoworks. V. Engineering Properties of Polyurethane-Poly(methyl Methacrylate) IPN's.* Journal of Applied Polymer Science, 1977. **21**: p. 1289-1295.

71. Kim, S.C., et al., *Polyurethane Interpenetrating Polymer Networks. II. Density and Glass Transition Behavior of Polyurethane-Poly(methyl methacrylate) and Polyurethane-Polystyrene IPNs.* Macromolecules, 1976. **9**(2): p. 263-266.

72. Kim, S.C., et al., *Polyurethane Interpenetrating Polymer Networks. 3. Viscoelastic Properties of Polyurethane-Poly(methyl methacrylate) Interpenetrating Polymer Networks.* Macromolecules, 1977. **10**(6): p. 1187-1191.

73. Kim, S.C., et al., *Polyurethane Interpenetrating Polymer Networks 4. Volume Resistivity Behavior of Polyurethane-Poly(methyl methacrylate) Interpenetrating Polymer Networks.* Macromolecules, 1977. **10**(6): p. 1191-1193.

74. Kim, S.C., et al., *Polyurethane-Polystyrene Interpenetrating Polymer Networks.* Polymer Engineering and Science, 1975. **15**(5): p. 339-342.

75. Kim, S.C., et al., *Polyurethane Interpenetrating Polymer Networks. I. Synthesis and Morphology of Polyurethane-Poly(methyl methacrylate) Interpenetrating Polymer Networks.* Macromolecules, 1976. **9**(2): p. 258-263.

76. Lee, D.S. and S.C. Kim, *Polyurethane Interpenetrating Polymer Networks (IPN's) Synthesized under High Pressure. 1. Morphology and T_g Behavior of Polyurethane-Poly(methyl methacrylate) IPN's.* Macromolecules, 1984. **17**: p. 268-272.

77. Allen, G., et al., *Composites formed by interstitial polymerization of vinyl monomers in polyurethane elastomers: 1. Preparation and mechanical properties of methyl methacrylate based composites.* Polymer, 1973. **14**: p. 597-603.

78. Mazurek, M., *Silicone Copolymer Networks and Interpenetrating Polymer Networks*, in *Silicon-Containing Polymers: The Science and Technology of Their Synthesis and Applications*, R.G. Jones, A. Wataru, and J. Chojnowski, Editors. 2000, Kluwer Academic Publishers. p. 117.

79. Anslyn, E.V. and D.A. Dougherty, *Modern Physical Organic Chemistry*. 2006: University Science Books.

80. Harabagiu, V., et al., *Macromolecular and Supramolecular Architectures Based on Cellulose and Cyclodextrins*, in *New Trends in Natural And Synthetic Polymer Science*, G.E.Z. Cornelia Vasile, Editor. 2006, Nova Science Publishers, Inc. p. 61.

81. Sperling, L.H., *Interpenetrating Polymer Networks and Related Materials.* Journal of Applied Polymer Science: Macromolecular Reviews, 1977. **12**(1): p. 141-180.

82. Miyata, T., *Gels and Interpenetrating Polymer Networks*, in *Supramolecular Design for Biological Applications*, N. Yui, Editor. 2002, CRC Press LLC. p. 127.

83. Obeng, Y.S., et al., *Mechanistic Aspects of the Relationship between CMP Consumables and Polishing Characteristics*, in *Chemical Mechanical Planariarization in Integrated Circuit Device Manufacturing*, S. Raghavan, R.L. Opila, and L. Zhang, Editors. 1998, The Electrochemical Society, Inc. p. 256.

84. Allen, G., et al., *Composites formed by interstitial polymerization of vinyl monomers in polyurethane elastomers: 2. Morphology and relaxation processes in methyl methacrylate based composites.* Polymer, 1973. **14**(12): p. 604-616.

85. Sanford, R.J., *Principles of Fracture Mechanics*. 2003, Upper Saddle River: Prentice Hall.

86. Babkina, N.V., et al., *Effect of Spatial Constraints on Phase Separation during Polymerization in Sequential Semi-Interpenetrating Polymer Networks.* Polymer Science Series A, 2008. **50**(7): p. 798-807.

87. Rosu, D., L. Rosu, and C.N. Cascaval, *IR-change and yellowing of polyurethane as a result of UV irradiation.* Polymer Degradation and Stability, 2009. **94**: p. 591-596.

88. Yang, J.H., et al., *Comparison of thermal/mechanical properties and shape memory effect of polyurethane block-copolymers with planar or bent shape of hard segment.* Polymer, 2003. **44**: p. 3251-3258.

89. Mishra, A., V.K. Aswal, and P. Maiti, *Nanostructure to Microstructure Self-Assembly of Aliphatic Polyurethanes: The Effect on Mechanical Properties.* Journal of Polymer Science Part B, 2010. **114**(16): p. 5292-5300.

90. Eceiza, A., et al., *Thermoplastic Polyurethane Elastomers Based on Polycarbonate Diols With Different Soft Segment Molecular Weight and Chemical Structure: Mechanical and Thermal Properties.* Polymer Engineering and Science, 2008: p. 297-306.

91. Rink, H.-P., *Polymeric Engineering for Automotive Coating Applications*, in *Automotive Paints and Coatings*, H.-J. Streitberger and K.-F. Dossel, Editors. 2008, Wiley-VCH Verlag GmbH & Co. p. 232.

92. O'Sickey, M.J., B.D. Lawrey, and G.L. Wilkes, *Structure-Property Relationships of Poly(urethane urea)s with Ultra-low Monol Content Poly(propylene glycol) Soft Segments. I. Influence of Soft Segment Molecular Weight and Hard Segment Content.* Journal of Applied Polymer Science, 2002. **84**: p. 229-243.

93. Li, F., et al., *Crystallinity and Morphology of Segmented Polyurethanes with Different Soft-Segment Length.* Journal of Applied Polymer Science, 1996. **62**: p. 631-638.

94. Panwiriyarat, W., et al., *Effect of the Diisocyanate Structure and the Molecular Weight of Diols on Bio-Based Polyurethanes.* Journal of Applied Polymer Science, 2013.

95. Dadbin, S. and M. Frounchi, *Effects of Polyurethane Soft Segment and Crosslink Density on the Morphology and Mechanical Properties of Polyurethane/Poly(allyl diglycol carbonate) Simultaneous Interpenetrating Polymer Networks.* Journal of Applied Polymer Science, 2003. **89**: p. 1583-1595.

96. Xiao, H.X., K.C. Frisch, and H.L. Frisch, *Interpenetrating Polymer Networks from Polyurethanes and Methacrylate Polymers. I. Effect of Molecular Weight of Polyols and NCO/OH Ratio of Urethane Prepolymers on Properties and Morphology of IPNs.* Journal of Polymer Science Part A: Polymer Chemistry, 1983. **21**: p. 2547-2557.

97. Kim, B.K., et al., *Polyurethane ionomers having shape memory effects.* Polymer, 1998. **39**(13): p. 2803-2808.

98. Lin, J.R. and L.W. Chen, *Study on Shape-Memory Behavior of Polyether-Based Polyurethanes. II. Influence of Soft-Segment Molecular Weight.* Journal of Applied Polymer Science, 1998. **69**: p. 1575-1586.

99. Hiemenz, P.C., *Polymer Chemistry: The Basic Concepts*. 1984: Marcel Dekker, Inc.

100. Amin, M., et al., *Determination of the crosslink density of conductive ternary rubber vulcanizates by solvent penetration.* Materials Letters, 1996. **28**: p. 207-213.

101. Lamba, N.M.K., K.A. Woodhouse, and S.L. Cooper, *Polyurethanes in Biomedical Applications*. 1998: CRC Press LLC.

102. Orwoll, R.A. and P.A. Arnold, *Polymer-Solvent Interaction Parameter X*, in *Physical Properties of Polymers Handbook*, J.E. Mark, Editor. 2007, Springer Science+Business Media, LLC: New York. p. 249.

103. Xiao, H.X., K.C. Frisch, and H.L. Frisch, *Interpenetrating Polymer Networks from Polyurethanes and Methacrylate Polymers. I. Effect of Molecular Weight of Polyols and NCO/OH Ratio of Urethane Prepolymers on Properties and Morphology of IPNs.* Journal of Polymer Science: Part A: Polymer Chemistry, 1983. **21**(8): p. 2547-2557.

104. Brydson, J.A., *Plastics Materials*. 7 ed. 1999: Butterworth-Heinemann.

105. *Poly(tetrahydrofuran) average Mn ~650* 2013; Available from: http://www.sigmaaldrich.com/catalog/product/aldrich/345288?lang=en&region=US.

106. *2-Ethyl-2-(hydroxymethyl)-1,3-propanediol, 98%*. 2013; Available from: http://www.acros.com/DesktopModules/Acros_Search_Results/Acros_Search_Results.aspx?search_type=CatalogSearch&SearchString=77-99-6.

107. Kato, K.J., *Osmium Tetroxide Fixation of Rubber Latices.* Journal of Polymer Science Part B: Polymer Letters, 1966. **4**(1): p. 35-38.

108. Thomas, L.C. and S.J. Schmidt, *Thermal Analysis*, in *Food Analysis*, S.S. Nielsen, Editor. 2010, Springer Science+Business Media, LLC. p. 565.

109. Leng, Y., *Materials Characterization: Introduction to Microscopic and Spectroscopic Methods*. 2008: John Wiley & Sons, Ltd.

110. Menczel, J.D. and R.B. Prime, *Thermal Analysis of Polymers: Fundamentals and Applications*. 2009: John Wiley & Sons, Inc.

111. Scheirs, J., *Compositional and Failure Analysis of Polymers: A Practical Approach*. 2000: John Wiley & Sons, Ltd.

112. Yuri S. Lipatov, T.T.A., *Phase-Separated Interpenetrating Polymer Networks*. 2007: Springer-Verlag Berlin Heidelberg.

113. Ignat, L. and A. Stanciu, *Advanced Polymers: Interpenetrating Networks*, in *Handbook of Polymer Blends and Composites*, A.K. Kulshreshtha and C. Vasile, Editors. 2003, Rapra Technology Limited. p. 296-297.

114. Huang, J. and L. Zhang, *Effects of NCO/OH molar ratio on structure and properties of graft-interpenetrating polymer networks from polyurethane and nitrolignin.* Polymer, 2002. **43**(8): p. 2287-2294.

115. Kostrzewa, M., et al., *Effects of Various Polyurethanes on the Mechanical and Structural Properties of an Epoxy Resin.* Journal of Applied Polymer Science, 2010. **119**: p. 2925-2932.

116. Sung, P.-H. and C.-Y. Lin, *Polysiloxane modified epoxy polymer networks-I. Graft interpenetrating polymeric networks.* European Polymer Journal, 1997. **33**(6): p. 903-906.

117. Sung, P.-H. and C.-Y. Lin, *Polysiloxane modified epoxy polymer network-II. Dynamic mechanical behavior of multicomponent graft-IPNs (Epoxy/Polysiloxane/Polypropylene glycol).* European Polymer Journal, 1997. **33**(3): p. 231-233.

118. Hsieh, K.H., et al., *Graft interpenetrating polymer networks of urethane-modified bismaleimide and epoxy (I) - mechanical behavior and morphology.* Polymer, 2001. **42**: p. 2491-2500.

119. Wang, T., et al., *Damping analysis of polyurethane/epoxy graft interpenetrating polymer network composites filled with short carbon fiber and micro hollow glass bead.* Materials & Design. **31**(8): p. 3810-3815.

120. Lin, S.P., et al., *Composites of UHMWPE fiber reinforced PU/epoxy grafted interpenetrating polymer networks.* European Polymer Journal, 2007. **43**: p. 996-1008.

121. Albers, H.F., *Tooth-Colored Restoratives: Principles and Techniques*. 9 ed. 2002: BC Decker Inc.

122. Sherwood, I.A., *Essentials of Operative Dentistry*. 2010: Jaypee Brothers Medical Publishers Ltd.

123. *Characterization and Failure Analysis of Plastics*. 2003: ASM International.

124. Nishikida, K. and J. Coates, *Infrared and Raman Analysis of Polymers*, in *Handbook of Plastics Analysis*, H. Lobo and J.V. Bonilla, Editors. 2003, Marcel Dekker, Inc. p. 244.

125. *Bisphenol A Glycidyl Methacrylate* [cited 2013; Available from: http://catalog.esstechinc.com/item/resins/bisgma/x-950-0000?forward=1.

126. *Triethyleneglycol Dimethacrylate*. [cited 2013; Available from: http://catalog.esstechinc.com/viewitems/difunctional-monomers/triethyleneglycol-dimethacrylate.

127. Elbert, D.L., *Polymer-Peptide Conjugate Networks: Formation, Swelling and Degradation*, in *Biologically-responsive Hybrid Biomaterials: A Reference for Material Scientists and Bioengineers*, E. Jabbari and A. Khademhosseini, Editors. 2010, World Scientific Publishing Co. Pte. Ltd. p. 68-69.